UNIVERSITY OF SOUTHAMPTON

FACULTY OF NATURAL AND ENVIRONMENTAL SCIENCES

School of Ocean and Earth Sciences

Investigating reasons for the growth and survival of the dinoflagellate genus *Neoceratium* in oligotrophic subtropical gyres

by

David Aldridge

Thesis for the degree of Doctor of Philosophy

June 2014

Abstract

FACULTY OF NATURAL AND ENVIRONMENTAL SCIENCES

Thesis for the degree of Doctor of Philosophy

By David Aldridge

The dinoflagellate *Neoceratium* is frequently observed in oligotrophic subtropical gyres (OSGs) where major inorganic nutrients such as nitrogen and phosphorus are depleted in the surface waters. In Chapter 2, continuous plankton recorder (CPR) data demonstrate that *Neoceratium* inhabit surface waters of the North Atlantic subtropical gyre (NAG) throughout the year. The presence of *Neoceratium* in surface waters contrasts with the fact that nutrients are severely depleted in the surface 100 to 130 m. In Chapter 3, it is shown that *Neoceratium* cannot grow when exposed to low nutrient concentrations comparable to those found in surface waters of OSGs. However, cells are able to survive and re-establish growth after a maximum of >3 weeks of "nutrient starvation", with signs of stress becoming noticeable after 10 days. In Chapter 4, nutrient ratios in large areas of surface waters of OSGs in the Atlantic are shown to be favourable to mixotrophy (86 % of sites in the North and South Atlantic OSGs). It is estimated that 0.01 to 0.44 ciliates per day would need to be ingested for *Neoceratium* to survive in these waters. In Chapter 5, growth was only observed when cells were exposed to a range of irradiances (6 to 60 µmol quanta m^{-2} s^{-1}), above 22 µmol quanta m^{-2} s^{-1}; an irradiance that is typically only found 15 to 22 metres above the nutricline at midday, implying that VM would be required to access the nutricline. A mechanism for VM in OSGs is suggested whereby vertical movement is triggered by phosphate-limitation of cells. In Chapter 6, the thesis concludes with a conceptual model to explain how a number of the above findings likely interact to enable *Neoceratium* to successfully survive and grow in OSGs.

Contents

List of tables

List of figures

List of accompanying materials

Appendix 1: Seasonal abundance patterns of *Neoceratium* (genus) in the North Atlantic Ocean standard CPR zones that were combined into 5 larger zones (Zones 1-5). Below the figure, a table shows the results from a Kruskal-Wallis one-way ANOVA on ranks performed on the standard CPR areas combined into each zone.

Appendix 2: Table showing the differences in experimental design between mixotrophy experiments.

Appendix 3: Details of cultures maintained

Appendix 4: Vertical distributions of *N. tripos* cells at different times of the day, from day 4, 7, 10, 13, 17 and 21. Grey columns represent periods in the dark; white columns represent periods in the light.

Appendix 5: Changes in the sinking rate distributions of immotile *N. tripos* cells with increasing PO_4^{3-} limitation between day 1 and 21.

Appendix 6: Changes in the sinking rate distributions of motile *N. tripos* cells with increasing PO_4^{3-} limitation between day 1 and 21.

DECLARATION OF AUTHORSHIP

I, David Aldridge

declare that the thesis entitled

"Investigating the reasons for the ecological success of the dinoflagellate *Neoceratium* in oligotrophic subtropical gyres"

and the work presented in the thesis are both my own, and have been generated by me as the result of my own original research. I confirm that:

- this work was done wholly or mainly while in candidature for a research degree at this University;
- where any part of this thesis has previously been submitted for a degree or any other qualification at this University or any other institution, this has been clearly stated;
- where I have consulted the published work of others, this is always clearly attributed;
- where I have quoted from the work of others, the source is always given. With the exception of such quotations, this thesis is entirely my own work;
- I have acknowledged all main sources of help;
- where the thesis is based on work done by myself jointly with others, I have made clear exactly what was done by others and what I have contributed myself;
- Parts of this work have been published as: (Aldridge et al. 2014)

Signed: ……..

Date:……

Acknowledgements

I would first and foremost like to thank my supervisors for their guidance and support over the last three and a half years. Specifically, I would like to thank Duncan Purdie for helping me to keep this PhD on track by always making the time to discuss ideas, read over text, or help out with problems no matter how big or small; Mike Zubkov, for asking the tough questions which drove me to become a better researcher, and Adrian Martin for always bringing a fresh perspective to meetings and discussions. I also thank my panel chair, Clive Truman, for his patience in dealing with some "eventful" meetings.

I thank SAHFOS for providing CPR data, specifically David Johns and Darren Stevens who dealt with my data requests. I thank BODC for providing numerous data sets from past AMTs, and also Alex Poulton for providing me with the plankton counts from those AMTs (and Derek Harbour for performing the counts). I also thank the crew from the RRS James Cook and RV Squilla, and the staff from PML who helped with the isolation of *Neoceratium* samples.

I am also indebted to all those people who helped out with various technical aspects throughout the PhD: all lab-mates, past and present, who helped to show me the ropes, but especially Manuela Hartman and Ross Holland; Harriet Cole, whose patience in explaining the infuriating intricacies of Matlab to me was endless; Martha Valiadi, who first helped me with the culturing of *Neoceratium*; John Gittins, Matt O'Shaughnessy and Nik Pratt, for helping me get hold of various lab equipment and materials, and Mark Stinchcombe for performing nutrient analyses. I also thank Per Juel Hansen, who provided *Mesodinium* cultures and whose discussions on the subject of mixotrophy were invaluable.

I would like to thank my office mates (Liz Sargent, Harriet Cole and Helen Smith), and all my friends from NOC: being able to laugh, scream and cry about the frustrations of a PhD with you all has probably saved me thousands of pounds in therapist bills. Thank you also to my friends, from outside NOC, and family for reminding me that there are more important things in life than phytoplankton and academia, and for always putting me back on my feet after particularly stressful periods. I especially thank my parents for their endless

support throughout my studies at university. Finally, I would like to thank my partner and best friend, Glaucia, whose love and encouragement has helped the last year and a half of my PhD run so smoothly; I hope that I can return the favour when it is your turn to finish your PhD.

Definitions and Abbreviations

AMT – Atlantic Meridional Transect

ATP – Adenosine Triphosphate

BCA – Bicinchoninic Acid

CPR – Continuous Plankton Recorder

DCM – Deep Chlorophyll Maxima

DON – Dissolved Organic Nitrogen

DOP – Dissolved Organic Phosphorus

DVM – Diurnal Vertical Migration

EA – Equatorial Atlantic

FRRf Fast Repetition-Rate Fluorometry

F_v/F_m – Maximum Photosystem II Photochemical Efficiency

FISH – Fluoresence In-Situ Hybridisation

HPLC – High Performance Liquid Chromatography

K_s – Half Saturation Constant

LNSW – Low Nutrient Seawater

NAG – North Atlantic Subtropical Gyre

NAGSW – North Atlantic Gyre Seawater

NUSW – Nutricline Seawater

NPSG – North Pacific Subtropical Gyre

OSG – Oligotrophic Subtropical Gyre

PAR – Photosynthetically Active Radiation

PC – Polycarbonate

PCR – Polymerase Chain Reaction

PFA – Paraformaldehyde

RSW – Nutrient Replete Seawater

SAG – South Atlantic Subtropical Gyre

TON – Total Oxidised Nitrogen (nitrate + nitrite)

VM – Vertical Migration

1. Introduction

1.1 *Neoceratium* Background and Biogeography

Of the dinoflagellates, the thecate (armoured) genus of *Ceratium* Schrank is probably the most recognisable and iconic. Their large size and easily recognisable shape (Fig. 1.1) makes identification incredibly simple. For this reason, the first descriptions of this genus date all the way back to the late 18th century (Müller, 1786). Since then, there have been a vast number of studies on these organisms: over 450 studies mention this genus since 1950 (Tunin-Ley and Lemée 2013). Recently, it has been suggested that the marine and freshwater species should be split into separate genera based on morphological evidence: the name of *Neoceratium* has been proposed for marine species, whilst *Ceratium* is suggested solely for freshwater species (Gomez et al. 2010).

The ease with which *Neoceratium* can be identified, combined with their worldwide distribution (from equatorial to polar regions), has led to this genus becoming one of the preferred model organisms for studies on dinoflagellate eco-physiology (Tunin-Ley and Lemée 2013). However, the high morphological diversity within the genus (and even within single species) can make the identification of individual species problematic. It is estimated that there are 120 species of *Neoceratium* in total, not including approximately 85 species whose identity remains in doubt (Dodge and Marshall 1994).

Temperature is thought to be the main environmental factor influencing the distribution of species (Graham 1941; Dodge and Marshall 1994; Tunin-Ley et al. 2007), and has been proposed as a major factor influencing the morphological variability seen within the genus, via its effects on water viscosity (Sournia 1967). Species can be broadly classed as tropical, subpolar, or cosmopolitan (Graham 1941). Tropical species can be further split into three

more groups based on tolerance to lower temperatures: intolerant, slightly tolerant, and very tolerant (Graham 1941). This narrow tolerance of certain species to specific water temperatures has already proved useful for studying water masses and current regimes (Ochoa and Gómez 1987; Raine et al. 2002). More recently, this narrow tolerance, in combination with ease of collection/identification and a wealth of studies on their eco-physiology, has led to the suggestion that these organisms would be well-suited as ecological indicators for monitoring ocean warming resulting from climate change (Edwards et al. 2006; Tunin-Ley and Lemée 2013).

1.2 Morphology and Life Cycle

Neoceratium cells (and their freshwater relatives, *Ceratium*) are markedly asymmetric, with one apical horn and 2-3 long antapical horns (Fig. 1.1) filled with cytoplasm. The girdle divides the cell into two approximately equal, but dissimilar halves: the epicone and the hypocone, which are divided into a number of thecal plates. Like other dinoflagellates, *Neoceratium* possess two flagella: a longitudinal flagellum that projects out from the cell, and a wave-like transverse flagellum that is closely appressed to the girdle (Dodge and Crawford 1970).

Fig. 1.1. *Neoceratium horridum* micrograph. The apical horn and 2 antapical horns are clearly visible. Image magnification = x60.

Dinoflagellates are known to be homothallic, if sexual reproduction can occur within a clone, or heterothallic, if more than one clone needs to be present for sexual reproduction (Pfiester 1984). Heterothallism has been documented in the freshwater *Ceratium* species *C. cornutum* (Von Stosch 1964), and in the absence of evidence to the contrary this would appear to be the common reproductive strategy of this genus. However, both homothallic and heterothallic strains are found in a number dinoflagellate species (Zingmark 1970; Hayhome et al. 1987; Montresor et al. 2003; Figueroa et al. 2010) and therefore it may be that different species (possibly even strains) of *Neoceratium* utilise homothally instead of heterothally.

Gamete formation has been confirmed in a number of *Neoceratium* species (Von Stosch 1972; Weiler and Eppley 1979; Montresor and Tomas 1988). Von Stosch (1972) described the life cycle of *N. horridum*, a life cycle that is similar to other dinoflagellates. The male gamete's ventral side attaches to the ventral side of the female gamete. Subsequently, the cell wall of the male breaks down into its individual thecal plates, which are taken up by the female cytoplasm, at which point the naked male gamete fuses with the female gamete to produce a zygote (planozygote) which remains motile through the following steps. The planocyte grows for several days, forming a large cell with unusually long horns and a thick cell wall. Meiosis commences approximately 12 hours after nuclear cycloses (movement), which is preceded by nuclear enlargement. The first meiotic division halves the chromosome number, resulting in one flagellate with normally-sized apical and abnormally long antapical horns, and a 2nd flagellate with abnormally long apical and normally-sized antapical horns. After 2-3 days the 2nd meiotic division occurs to yield haploid vegetative cells. This division process usually takes place at night or in the early morning (Lebour 1925).

It is worth noting that under unfavourable environmental conditions (low nutrient concentrations and high temperatures) *Neoceratium* species have been shown to transform into the sexual phase of their life history (von Stosch 1972), accompanied by an increase in the abundance of male gametes (Von Stosch 1964, 1972; Weiler and Eppley 1979) known as microswarmers. Microswarmers have reduced cell (and nucleus) size, pigmentation, and cell

wall thickness (von Stosch 1964). One possible explanation for this may be provided by Myers (1978), who speculated that poor environmental conditions should lead to the production of the energetically cheaper sex, allowing for the number of offspring produced to be maximised.

1.3 Movement and Swimming

Dinoflagellates are relatively fast swimmers and can achieve rates of movement of 200-500 μm s^{-1} (Graham & Wilcox 2000). These organisms are capable of directed swimming behaviour in response to chemical stimuli, light, and gravity. It is suggested that this enables dinoflagellates to position themselves in the water column to take full advantage of available light and nutrients.

Swimming is achieved using both the longitudinal and transverse flagella (Fig. 1.2). The ribbon-like transverse flagellum moves helically in a semi-circular groove on the body surface, propagating waves from the attached to the free end (base to tip) which propels the cell forward as well as causing rotation; a single line of long fine hairs aids in forward motion of the cell (Leadbeater and Dodge 1967; Miyasaka et al. 2004). The longitudinal flagellum extends beyond the cell body and accounts for approximately half of the forward swimming speed as well as acting as a rudder (Graham and Wilcox 2000). In *Neoceratium* the plane of the waveform that results from the beating of the longitudinal flagellum is parallel to the cell body, in contrast to other dinoflagellates where it is perpendicular (Graham & Wilcox 2000).

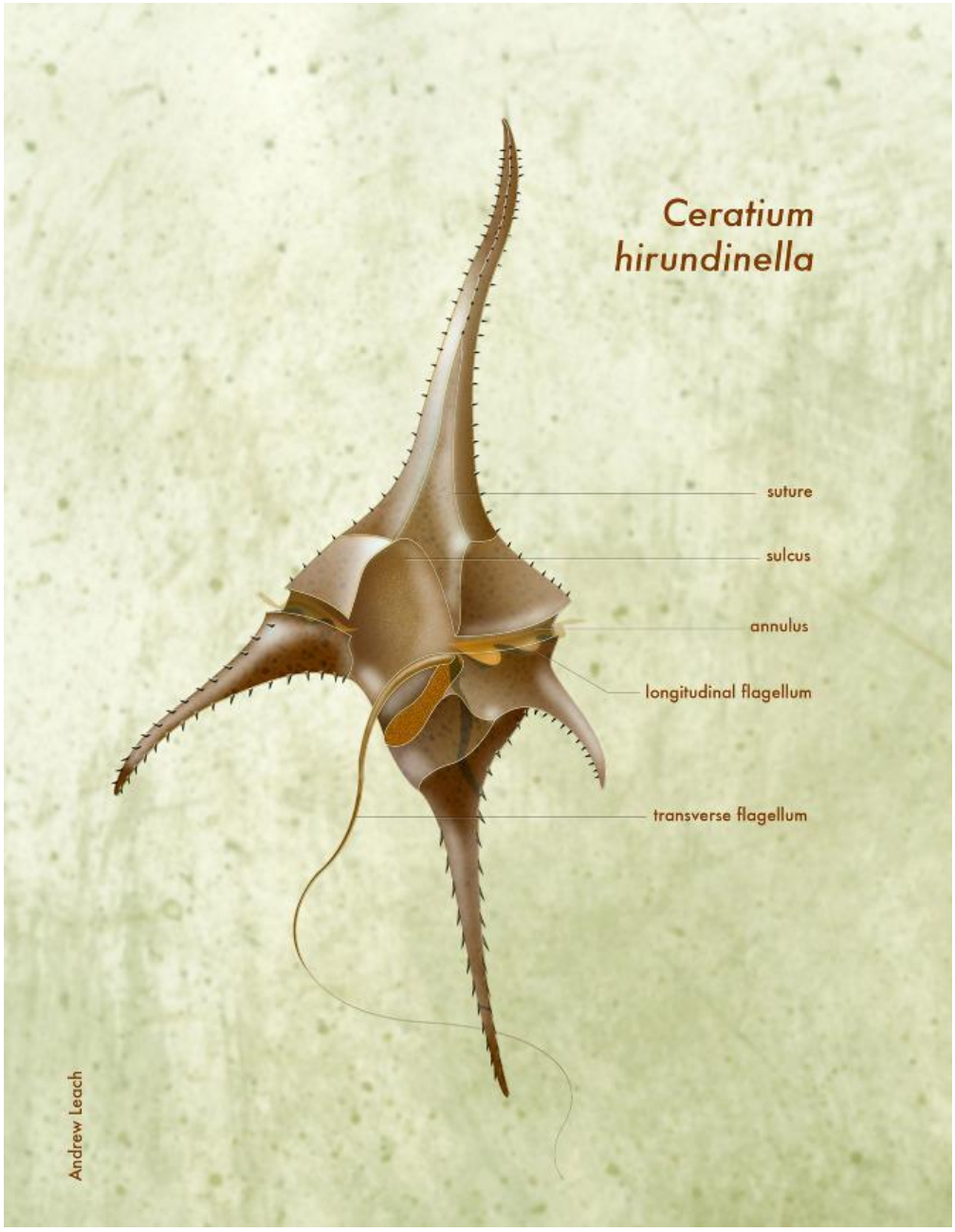

Fig. 1.2. Diagram of *Ceratium hirundinella* showing the position of the longitudinal and transverse flagella. Image courtesy of Andrew Leach.

Dinoflagellates can stop or reverse their swimming direction by changing the position of the longitudinal flagellum. In *Neoceratium* the longitudinal flagellum retracts when mechanically stimulated; it is folded from the tip to the base, and is stored in the sulcus on the ventral side of the cell body (Maruyama 1981). This folding is achieved through the contraction of the R-fibre (Maruyama 1981). The R-Fibre, unique to *Neoceratium*, runs parallel to the

axoneme (the flagella's inner core or 'skeleton') and is composed of contractile but non-actin filaments (Maruyama 1982).

1.4 Oligotrophic subtropical gyres

Oligotrophic subtropical gyres (OSGs) cover approximately 30 % of the Earth's surface. Here, strong thermal vertical stratification reduces the supply of nutrients to surface waters from below the thermocline. Consequently, nitrogen and/or phosphorus are frequently severely depleted in surface waters of OSGs, typically in sub-micro to nanomolar concentrations (Maranon et al. 2000; Wu et al. 2000; Zubkov et al. 2007; Moore et al. 2013). Phytoplankton biomass and productivity are primarily limited by low nitrogen concentrations (Reviewed by Moore et al. 2013; Fig. 1.3), with phosphate being co-limiting in some areas, such as the North Atlantic subtropical gyre (NAG). This leads to low phytoplankton productivity and biomass (McClain et al. 2004; Morel et al. 2010). However, because these areas cover over 60 % of the surface of the ocean, they still account for over 30 % of total marine primary production (Longhurst et al. 1995). It is important, therefore, to understand how phytoplankton function at the low nutrient concentrations found in these environments.

The dominant autotrophs (in terms of numbers and biomass) in the OSGs are small organisms: cyanobacteria and small flagellates are estimated to contribute somewhere between 70-90 % of phytoplankton biomass (Marañón et al. 2000). The photosynthetic cyanobacteria genus *Prochlorococcus* is the dominant autotroph, followed by the eukaryotic picophytoplankton (size range, 0.2 to 2 μM) (Zubkov et al. 1998, 2000); a group that includes the Prymnesiophyceae, Chrysophyceae, Prasinophyceae and Pelagophyceae (Lepère et al. 2009; Cuvelier et al. 2010). The reason that the dominant autotrophs in OSGs are small is that reduced size is associated with low sinking velocities and with increased nutrient uptake rates, which have been shown to scale with cell surface area to volume ratios (Finkel et al. 2009).

Larger phytoplankton species, such as diatoms, coccolithophores and dinoflagellates are less abundant, although still persistent members of OSG phytoplankton communities (Venrick 1982): in terms of their average contributions to phytoplankton biomass, Marañón et al. (2000) estimate that diatoms contribute <2 %, coccolithophores contribute 2-10 % and dinoflagellates contribute approximately 4 %. *Neoceratium* is one genera of dinoflagellate commonly found in OSGs. Although there is no direct published value for its contribution towards dinoflagellate biomass in OSGs, one study estimates that in terms of cell volume contributions, in Hawaiian subtropical waters, *Neoceratium* species constitute approximately 8 % towards the total dinoflagellate value (Takahashi and Bienfang 1983), making them a significant component of the dinoflagellate population. Understanding how this genus is adapted to life in OSGs is not only intrinsically interesting, but also important for understanding how dinoflagellates (and perhaps other large phytoplankton) are adapted to this environment.

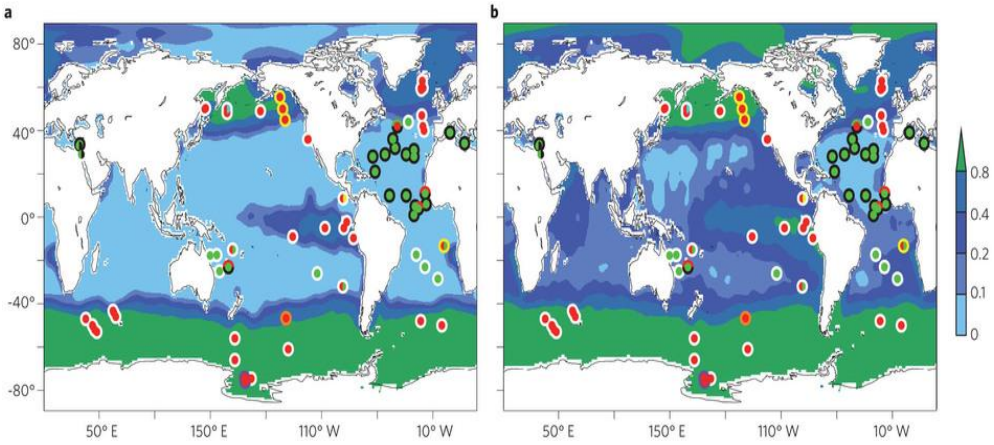

Fig. 1.3. Nutrient limitation in the world's oceans. Backgrounds indicate annual average surface concentrations of nitrate (a) and phosphate (b) in µmol kg^{-1}. To assist comparison, nitrate is scaled by the mean N:P ratio of organic matter (that is, divided by 16). Symbols indicate the primary (central circles) and secondary (outer circles) limiting nutrients as inferred from chlorophyll and/or primary productivity increases following artificial amendment of: N (green), P (black), Fe (red), Si (orange), Co (yellow), Zn (cyan) and vitamin B12 (purple). Divided circles indicate potentially co-limiting elements. White outer circles indicate that no secondary limiting nutrient was identified, which in many cases will be because of the lack of a test. After Moore et al. (2013).

1.5 *Neoceratium* in Oligotrophic Environments

Neoceratium is generally more common in warmer tropical waters, demonstrated by the fact that less than 10 species are found in the North Atlantic, compared to > 20 species in warmer more southerly waters (Graham and Bronikovsky 1944). In coastal regions, blooms have been observed throughout the world (Graham 1941; Graham and Bronikovsky 1944; Chang and Carpenter 1994; Smalley et al. 1999, Baek et al. 2008a) and appear to follow the onset of stratification. Baek et al (2008a) linked bloom development of *N. fusus* and *N. furca* in Japanese coastal waters to low wind speed and low nutrient concentrations. They suggest that motility, low tolerance to turbulence and an ability to take up nutrients at low concentrations may be the reasons for this.

The abundance of *Neoceratium* cells encountered in oligotrophic surface waters is significantly lower than in coastal waters, e.g. in the North Pacific central gyre, where *Neoceratium* is estimated to contribute <1 % of total phytoplankton carbon, concentrations range from 0.8-3 cells L^{-1} (Weiler 1980; Matrai 1986), compared to cell concentrations of ~22 cells L^{-1} in the California Current (Matrai 1986). Curiously, however, doubling times of *Neoceratium* in the oligotrophic waters of the pacific central gyre are estimated to be relatively high: 5.2-7.5 days, or 26-38 % of the maximum rates observed for this genus (Wieler 1980). These relatively high division rates may reflect, in addition to optimal positioning in the water column for nutrients and light, a physiological adaptation to low nutrient concentrations, an ability to supplement growth via phagotrophy, or a combination of all three. Weiler (1980) suggested that the low standing stocks of *Neoceratium*, coupled with the high division rates, may result from an equilibrium whereby growth is balanced by mortality (predominantly through grazing pressure).

1.6 Potential adaptations of *Neoceratium* to Oligotrophic Environments

1.6.1 Physiological adaptations

Neoceratium, similar to some other phytoplankton, has shade-adapted forms which become more abundant between the surface and 100 m depth. These shade forms tend to be found in oligotrophic waters where upper layers are limited with respect to phosphate and nitrate (Sournia 1982). These organisms are adapted to low light conditions through increased cellular surface area, achieved via expansion of their cell body and/or horns; these extensions also tend to be packed with chloroplasts. Shade forms have an advantage in these environments as they can utilise available nitrogen and phosphate at depth but can still receive enough light to keep their photosynthetic rate above their respiratory rate.

Two species of *Neoceratium*, *N. furca* and *N.fusus*, are known to have low phosphate (0.03-0.17 µM) and nitrate (0.32-0.49 µM) half saturation constants (K_s) (Qasim et al. 1973; Baek et al. 2008a): the lower the value for K_s the greater the rate of uptake of nutrients at low concentrations. These values are significantly lower than the K_s values of other dinoflagellates, e.g. *Alexandrium tamarense* and *Prorocentrum minimum* have reported K_s values for phosphate of 0.4 µM and 1.96 µM respectively (Cembella et al. 1984; Leong and Taguchi 2004). It is also likely that the presence of cytoplasmic vacuoles (Smalley et al. 1999) allow for the luxury uptake and subsequent storage of inorganic nutrients. Furthermore, the production of the enzyme alkaline phosphatase, which has been found to be active in *Neoceratium* cells from the North Pacific (Mackey et al. 2012; Girault et al. 2012), may allow for the exploitation of dissolved organic phosphorus (DOP) pools. Additionally, it has been suggested that dinoflagellates may be able to make use of some of the more labile forms of dissolved organic nitrogen (DON), such as urea, dissolved free amino acids, and nucleic acids (Bronk et al. 2007) Baek et al. (2008a) demonstrated that

urea and ammonia concentrations up to 20 µM supported *N. furca* growth in cultures where inorganic nutrient concentrations were otherwise limiting; higher concentrations of urea and ammonia were shown to inhibit growth.

1.6.2 The potential role of ephemeral nutrient upwelling

Ephemeral physical processes can introduce nutrients into surface waters, and may contribute to the survival of *Neoceratium* in OSGs. Karl (1999) identified at least four physical mechanisms that can increase phytoplankton productivity by introducing nutrients into surface waters of the subtropical Pacific gyres: internal waves and tides, cyclonic mesoscale eddies, wind-driven Ekman pumping, and atmospheric storms.

In deep ocean environments internal waves are thought to be a common occurrence, propagating horizontally along the density gradients associated with isopycnal surfaces and entraining nutrients into the euphotic zone (Garrett and Munk 1972). McGowan and Hayward (1978) observed a deep mixing event, attributed to enhanced internal wave activity, which subsequently doubled primary production in the area. More recently Karl et al. (1996) found nitrate concentrations an order of magnitude greater than expected in the North Pacific subtropical gyre (NPSG) that they attributed to internal wave activity based on changes in depth profiles of potential density.

Mesoscale eddies are ubiquitous features in subtropical seas throughout most of the year. Cyclonic eddies have been shown to “lift” nutrient replete isopycnals into the euphotic zone (Fig. 1.4) (Falkowski et al. 1991; McGillicuddy and Robinson 1997; McGillicuddy et al. 1998; Siegel et al. 1999), a process referred to as “eddy pumping”. Accordingly, eddies are an important source of nutrients into surface waters in OSGs. The effects of this nutrient addition have been shown to increase primary production. Falkowski et al. (1991) showed that primary production was enhanced by about 20 % by the process of eddy pumping, and Allen et al. (1996) showed that photosynthetic

rates near the edge and at the centre of the eddy were 31% and 66% higher, respectively, than outside the eddy.

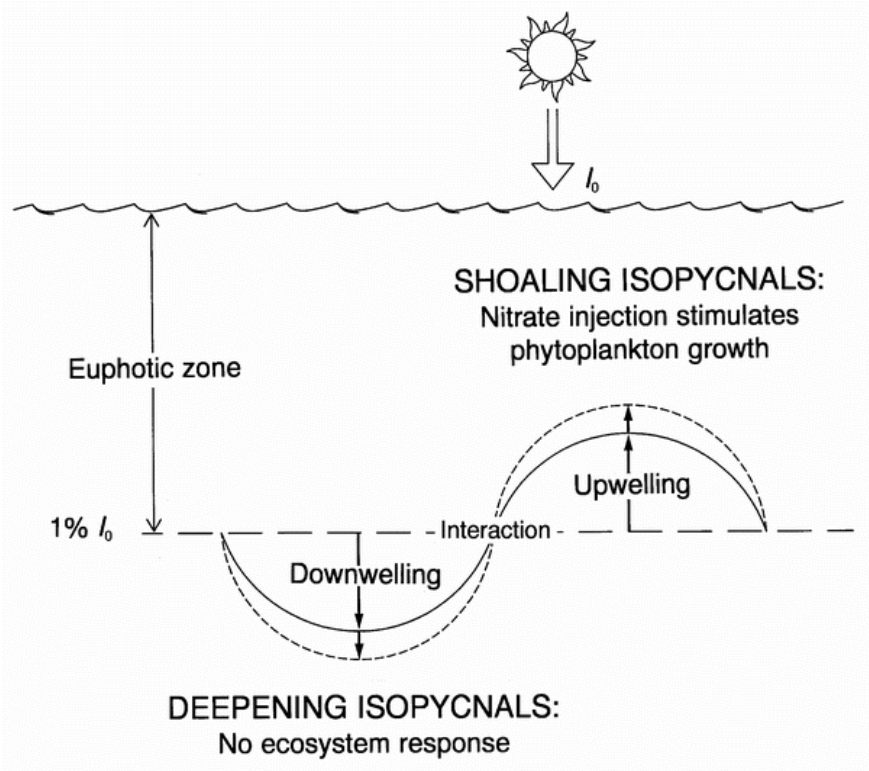

Fig. 1.4. The effect of mesoscale eddies on isopycnals. Anti-cyclonic eddies result in downwelling of nutrients with no effect on primary productivity. Cyclonic eddies inject nutrients into the euphotic zone, stimulating phytoplankton growth. After McGillicuddy et al. 1998).

Sea-surface divergence from local wind forcing can cause upwelling as a result of Ekman pumping, similar to that caused by mesoscale eddies.
Williams and Follows (1998) showed the vertical Ekman supply of nitrate to be a significant source of nutrients to the euphotic zone throughout the NAG; the potential for these events to cause short-term peaks in productivity was demonstrated by Letelier et al. (2000), where it was shown that strong winds, in combination with the passage of a cyclonic eddy, led to a large upwelling event resulting in increases in primary productivity.

Storm events also appear to enhance nutrient supply to the euphotic zone; the mechanism for this appears to be due to wet deposition (via precipitation) of nitrate rather than upwards vertical mixing (DiTullio and Laws 1991). In the NPSG, increases in primary production were shown to follow a low pressure disturbance (DiTullio and Laws 1991). Furthermore, high performance liquid chromatography (HPLC) pigment analysis showed that all phytoplankton groups except cyanobacteria increased immediately after the disturbance.

1.6.3 The potential role of water column position and diurnal vertical migration (DVM) in oligotrophic environments

In the oligotrophic Pacific Ocean a persistent chlorophyll maximum often occurs between 90 and 135 m, just above the nutricline, where irradiances are typically <1% of surface values (Venrick et al. 1973; Venrick 1979); a similar deep chlorophyll maxima has been observed in the Atlantic between 67 and 126 m (Perez et al. 2006). Cells in this environment are alive but light-limited. This phenomenon does not represent a phytoplankton-biomass or primary productivity maxima but is thought to result primarily from increased cellular chlorophyll concentrations, which are an adaptation to low light levels (Kiefer et al. 1976; Perez et al. 2006). Venrick (1982) showed that in the same environment a two-layered phytoplankton distribution exists: an upper 'association', where most of the primary production occurs, that receives sufficient light but is dependent on regenerated nutrients; and a lower 'association' where light intensities are suboptimal (generally <1.5 %), but nutrient concentrations are higher.

The motility of *Neoceratium* most likely allows individuals in low turbidity, stratified environments to change their vertical position in the water column in order to seek favourable conditions with regard to the level of irradiance and nutrient concentrations – an ability that is of little use in well-mixed water columns where motile and non-motile species are dispersed by turbulence. At night, downward migration would allow for the exploitation of N and P rich waters, followed by upwards migration in the day to take advantage of high

irradiances: a pattern of migration that is common in dinoflagellates, including *Neoceratium* (Eppley et al. 1968; Cullen & Horrigan 1981; Heaney & Eppley 1981; Taylor et al. 1988; Watanabe et al. 1988; James et al. 1992; Whittington et al. 2000) and allows dinoflagellates to change their position in the water column by 5-10 m per day (Eppley et al. 1968; Blasco 1978). Whilst this behaviour in motile protists has been hypothesised to be energetically expensive via increased metabolic requirements (Epp & Lewis 1984; Crawford 1992), recent evidence suggests that the energetic cost of motility may be via a reduced capacity to effectively use higher light irradiances (Striebel et al. 2009).

Diurnal vertical migration (DVM) has been well studied in *Neoceratium*. For example, in the freshwater species *C. hirundinella* a number of studies have shown that this species exploits optimal nutrient (phosphate) concentrations and irradiance levels according to the pattern of migration described above (Taylor et al. 1988; James et al. 1992; Whittington et al. 2000), although cells in a stationary growth phase showed a pattern of DVM that coincided with the light regime more closely (Heaney and Furnass 1980). The significance of this behaviour in mitigating nutrient limitation was demonstrated by the finding that when DVM was restricted, due to anoxia, cellular phosphate concentrations were reduced and alkaline phosphatase activity increased, suggesting that P-limitaion of *Neoceratium* occurred (James et al. 1992).

A large number of studies indicate that *Neoceratium* undergoes cell division at depth around dawn (e.g. Weiler & Chisholm 1976; Weiler & Eppley 1979; Baek et al. 2009), advantageous as nutrient concentrations are higher, and turbulence is reduced – dividing cells tend to be damaged by physical forces (Baek et al. 2009). Following this, upwards migration before the transition from dark to light typically occurs (followed by downwards migration before dusk). It has been suggested that this DVM pattern may be dependent on the cell division cycle, which is possibly under the control of an endogenous rhythm (Baek et al. 2009). Support for some kind of endogenous rhythm comes from experiments where *N. furca* continued DVM patterns in complete darkness over 6 days (Weiler and Karl 1979).

In laboratory studies by Heaney and Eppley (1981) on the primarily coastal *Neoceratium furca*, increased nitrate depletion resulted in progressively earlier

downward migration before the end of the light period, an advantage as these cells are more likely to reach the nitracline while light is still available (uptake rates of nitrate are higher in the presence of light). In the same study a cessation of upwards migration was also observed once nitrate and phosphate had been exhausted from the medium, possibly resulting from insufficient adenosine triphosphate (ATP) being produced under low phosphate concentrations.

It should be pointed out that this pattern of DVM has not been observed in all species of *Neoceratium* studied: one study in Danish coastal waters found that DVM only occurred in *N. fusus*. *N. furca* and *N. tripos* were consistently found concentrated at the surface, with an additional peak in the pycnocline found for *N. tripos* (Nielsen 1991).

1.6.4 The potential role of feeding and mixotrophy

Marine dinoflagellates are recognised as having three major trophic modes: autotrophic, heterotrophic, and mixotrophic (although in reality a continuum of nutritional strategies exists: from fully autotrophic to fully heterotrophic). Many mixotrophic species have only been recognised in the last two decades having previously been thought to be exclusively autotrophic (see reviews by Stoecker 1999; Hansen 2011). it is widely accepted that dinoflagellates originally obtained their photosynthetic pigments from prey plastids (Bhattacharya et al. 2004). Mixotrophy, therefore, is probably a major force behind dinoflagellate evolution and its persistence in extant species should not come as a surprise. This behaviour would confer an advantage to *Neoceratium* in oligotrophic subtropical gyres (OSGs) as it would provide a major source of inorganic nutrients in a concentrated form.

Dinoflagellate prey species include heterotrophic protists (including nanoflagellates and ciliates), cryptophytes, other algae, cyanobacteria (*Synechococcus*), and heterotrophic bacteria (Bockstahler & Coats 1993; Li et al. 1996; Stoecker et al. 1997; Li et al. 1999; Li et al. 2000; Jeong, et al. 2005b; Jeong et al. 2005c; Seong et al. 2006; Shim et al. 2011). Cells have also been

shown to ingest fluorescent microbeads (Zhang et al. 2011), a prey-substitute which can be useful for specific purposes. For example, Smalley et al. (1999) fed beads to dinoflagellates, but only once they had first been fed to ciliate prey. This allowed the ciliates to easily be detected inside the dinoflagellate cells, but avoided well-known issues of protists potentially not eating inert surrogate prey (Stoecker 1988).

All mixotrophic species show a growth response to irradiance similar to fully autotrophic algae. However, some species cannot grow for prolonged periods in the light in the presence of only inorganic nutrients, they need prey to sustain growth (photosynthesis is used only to survive periods of starvation). Conversely, only a few species are capable of growing in the dark if supplied with prey: they are primarily autotrophic, using phagotrophy to supplement inorganic nutrient acquisition (Hansen 2011). In fact there are currently 6 different types of mixotrophy that are recognised (Table 1.1).

Mixotrophy has been reported in a number of *Neoceratium* species (Bockstahler and Coats 1993b; Chang and Carpenter 1994; Li et al. 1996; Smalley et al. 1999, 2003, 2012; Smalley and Coats 2002). In *Neoceratium*, as with most dinoflagellates, feeding occurs via direct engulfment of prey (Bockstahler and Coats 1993b) through the sulcus at the posterior end of the cell. Although the freshwater species *C. hirundinella* is reported to be capable of extracellularly digesting prey using pseudopods (Hofender 1930), this observation has never been confirmed and has been questioned due to the likely presence of artefacts (Hansen and Calado 1999).

Neoceratium furca is known to prey on *Choreotrich* ciliates and the photosynthetic ciliate *Mesodinium rubrum* (Bockstahler and Coats 1993b; Smalley et al. 1999, 2003, 2012; Smalley and Coats 2002). In this species feeding is proposed to be strongly influenced by nutrient concentrations, a phenomenon that has been observed in other dinoflagellates (e.g. Stoecker et al. 1997). Smalley et al. (2003) showed, using cultures, that in *N. furca* feeding on ciliates did not occur in nutrient replete conditions, only when nutrients were limited: feeding increased as cellular C:N:P ratios deviated from those found under optimum growth conditions and this was also accompanied by a reduction in photosynthetic rate, possibly as nitrate and phosphate were

redirected towards the synthesis of morphological structures and enzymes required for ingestion and digestion.

It has been suggested that the retractile nature of the longitudinal flagellum in *Neoceratium* may also play an important role in prey capture. The contraction-relaxation cycle of the various structures has been proposed to trap food particles between the folds of the flagellar membrane, which would be subsequently carried into the flagellar pocket (about 6 µm in diameter) and then towards the mouthpart, or cytostome (Cachon et al. 1991; Cachon et al. 1992).

Table. 1.1. The 6 general types of mixotrophy that occur in phytoplankton, as proposed by Stoecker (1998).

Type of Mixotrophy	Description
Type I	**Species that grow equally well as phototrophs or heterotrophs**
Type II	**Primarily phototrophic organisms that are capable of phagotrophy under certain conditions**
A	*Feed in response to limiting dissolved inorganic nutrients*
B	*Feed in order to obtain a limiting trace organic growth factor*
C	*Feed in order to obtain carbon when light is limiting*
Type III	**Primarily phagotrophic**
A	*Use their 'own' plastids*
B	*Use algal symbionts or sequestered algal plastids*

1.7 Thesis structure, aims and objectives

1.7.1 Thesis structure

The overall aim of this thesis is to answer how *Neoceratium* obtain nutrients for survival and growth in OSGs. This is addressed according to the thesis structure below (Fig. 1.5). Firstly, the temporal and spatial distribution of this species in the Atlantic OSGs is examined in relation to factors controlling growth. This provides the platform for the following chapters, where the specific strategies that *Neoceratium* may use are investigated.

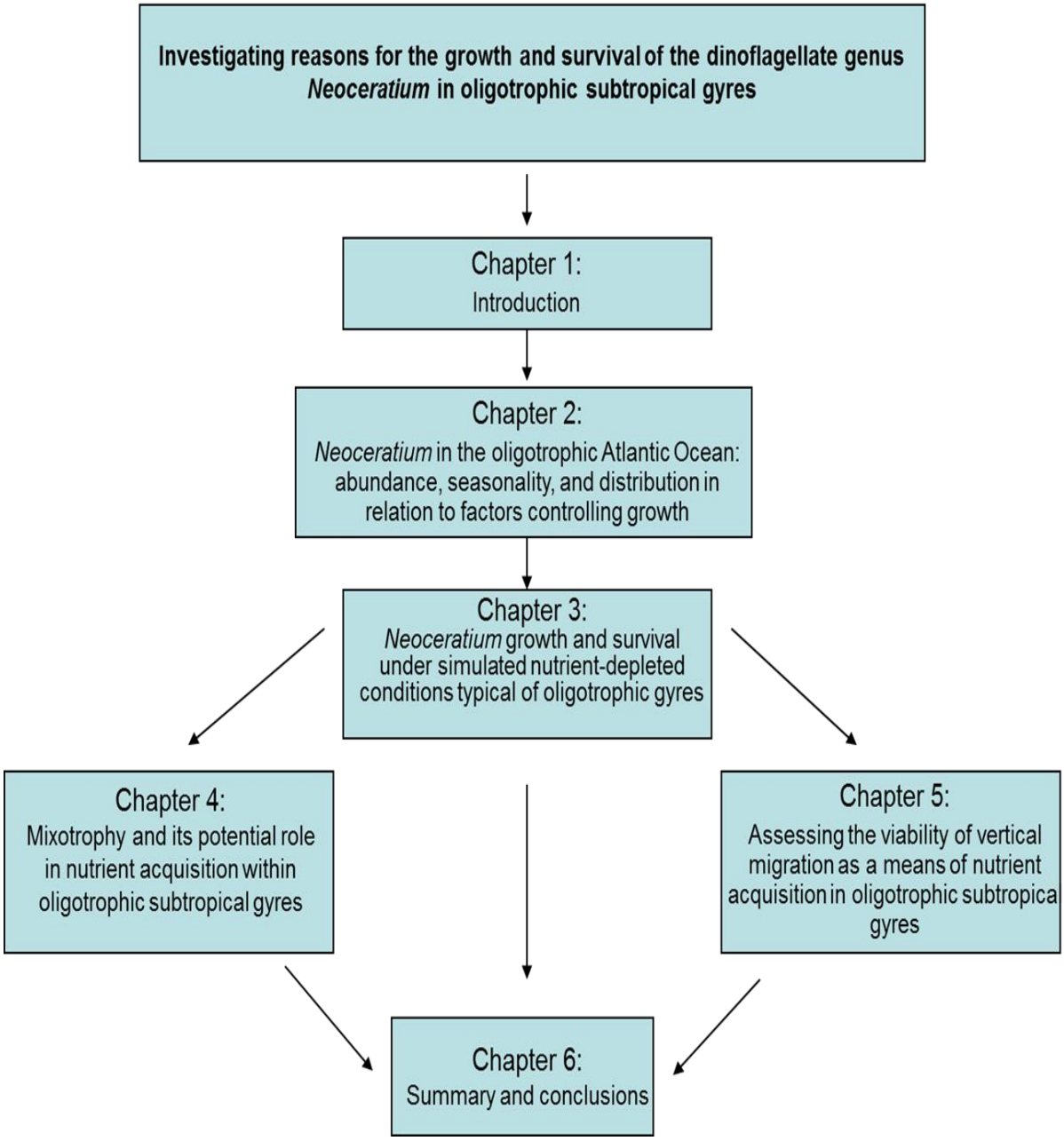

Fig. 1.5. Thesis structure. Chapter 3 has been published in a shorter form in *The Journal of Plankton Research* under the title *"Growth and survival of Neoceratium hexacanthum and Neoceratium candelabrum under simulated nutrient-depleted conditions"*, with co-authors D.A Purdie and M.V Zubkov. Data from chapters 2, 4 and 5 is being prepared for publication in *Marine Ecology Progress Series* with the title *"Explanations for Neoceratium survival and growth in the oligotrophic subtropical gyres"*, with co-authors D.A Purdie and M.V Zubkov.

1.7.2 Objectives

Chapter 2: *Neoceratium* in the oligotrophic Atlantic Ocean: abundance, seasonality, and distribution in relation to factors controlling growth

1) To determine the *in situ* abundance of *Neoceratium* within surface waters of the oligotrophic gyres of the North and South Atlantic using data from vertical net tows and the continuous plankton recorder (CPR).
2) To determine the seasonal variations of *Neoceratium* in the subtropical North Atlantic, and compare this to the rest of the North Atlantic Ocean.
3) To examine the vertical distribution of factors that control *Neoceratium* growth and survival (nutrients, light and ciliate prey concentrations).

Chapter 3: *Neoceratium* growth and survival under simulated nutrient-depleted conditions typical of oligotrophic gyres

1) To determine whether *Neoceratium* can grow at low nutrient concentrations found in surface waters of oligotrophic gyres, by monitoring various indicators of "health" (cell numbers, cell division, protein per cell and *Fv/Fm*) in laboratory-grown cultures.
2) To determine the survival time of *Neoceratium* under nutrient-depleted conditions by monitoring cell growth properties (survival time, viability, time-lag of growth response and growth rate) in cells exposed to low nutrient conditions for increasing periods of time before the addition of nutrients.

Chapter 4: Mixotrophy and its potential role in nutrient acquisition within oligotrophic subtropical gyres

1) To test the ability of *Neoceratium* to feed via direct engulfment and via contraction of the flagellar into the flagellar pocket, using a number of different prey organisms.

2) To visually examine samples collected from the North and South Atlantic subtropical gyres during Atlantic Meridional Transect (AMT) for signs of mixotrophy.
3) To determine whether mixotrophy is a feasible mechanism for obtaining inorganic nutrients in OSGs, based on nutrient ratios within OSGs, likely prey ingestion rates and prey concentrations in OSG seawater.

Chapter 5: Assessing the viability of vertical migration as a means of nutrient acquisition in oligotrophic subtropical gyres

1) To determine the growth response of *Neoceratium* cells under nutrient conditions representative of the nutricline in oligotrophic environments by monitoring various indicators of "health" (cell numbers, cell division, protein per cell and *Fv/Fm*) in laboratory-grown cultures.
2) To investigate whether *Neoceratium* cells can grow under low light conditions found close to the nutricline in oligotrophic environments by monitoring cell growth and division at a range of low light intensities.
3) To investigate the survival time of *Neoceratium* under very low light conditions by monitoring cell growth properties (survival time, viability, time-lag of growth response and growth rate) in cells exposed to low light conditions for increasing periods of time before transference into the light.
3) To determine whether *Neoceratium* undergo diurnal migration and whether this changes as cells become phosphate limited by monitoring the diurnal vertical distribution of cells exposed to a 12:12 light/dark cycle.
4) To determine whether phosphate depletion leads to buoyancy changes caused by changes in motility, by comparing the sinking rates of live and dead *N.tripos* cells exposed to increasingly phosphate-depleted conditions.

Thesis chapters have been written in the style of stand-alone papers, leading to some unavoidable repetition of core information. Every effort has been made to keep repetition to a minimum.

2. *Neoceratium* in the oligotrophic Atlantic Ocean: abundance, seasonality, and vertical distribution in relation to factors controlling growth.

2.1 Abstract

Neoceratium are present in the oligotrophic Atlantic Ocean, but little is known about their abundance, seasonality or their vertical distribution in relation to factors controlling growth. Here, *in situ* cell counts, from vertical net tows, show that average *Neoceratium* abundances in the North Atlantic subtropical gyre (NAG) during late autumn are significantly different from abundances in the South Atlantic subtropical gyre during late spring (0.48 compared to 1 cell L^{-1}; P = <0.05). Continuous plankton recorder (CPR) data from 1958 to 2010 demonstrates that *Neoceratium* abundances begin to increase in March, peaking in June. Using *Neoceratium* counts from Niskin bottle samples in the NAG and South Atlantic subtropical gyre (SAG), it is shown that *Neoceratium* is present from the surface down to about 160 metres. However, nutrient concentrations that likely support growth are not present in the surface 100 to 130 m. Below this depth, irradiances are low (<2 to 21 µmol quanta m^{-2} s^{-1}). However, Ciliates – potential prey for *Neoceratium* – are abundant (393 to 3045 cells L^{-1}) in the surface 160 metres of the NAG and SAG.

2.2 Introduction

The general global seasonal cycle of phytoplankton has predominantly been studied using remote sensing of surface chlorophyll *a* concentrations. Based on these observations the subtropical "bloom" (peak phytoplankton abundances in the subtropical regions of the ocean) is considered to begin in autumn or winter throughout the North Atlantic as the mixed layer begins to deepen and nutrients become available in the euphotic zone. The "bloom" progresses northward, commencing in May in sub-polar regions (Henson et al. 2009) – a transition zone, experiencing considerable inter-annual variability separates the two zones. This "transition" zone may experience either, or both, nutrient and light limitation. The patterns that have been observed through remote-sensing, in the subtropical Atlantic, contrast with previous *in situ* observations by Beers et al. (1982). In their study, seasonal microplankton (organisms < 200 μM) biomass changes in the North Pacific central gyre were monitored. It was suggested that although there is little change in biomass throughout the year (less than two-fold), the peak occurs in spring.

Little is known about the seasonal cycle of *Neoceratium* abundance within subtropical gyres. The seasonal abundance of *Neoceratium fusus* (a commonly occurring species in the North Atlantic), between 40°N and ~60°N throughout the North Atlantic (Colebrook 1982), generally follows the seasonal pattern expected of dinoflagellates from the North Atlantic (McQuatters-Gollop et al. 2007): increases in abundance occur in spring, peaking in summer, often with a secondary peak in late summer/autumn, before cell numbers decline to very low numbers over the winter (the onset of these events occurs earlier at lower latitudes). However, at the most southern latitudes studied (~40°N) in the eastern North Atlantic – just south of Nova Scotia – high abundances persist into December, suggesting that *Neoceratium* in oligotrophic subtropical gyres (OSGs) may follow the seasonal cycle suggested by Henson et al. (2009).

In the North Atlantic Ocean, water temperature has a large influence on species distributions and species diversity of *Neoceratium*: many species are only able to survive within a fairly narrow temperature range, and although abundances

decrease towards lower latitudes, species diversity increases (Graham and Bronikovsky 1944; Dodge and Marshall 1994). The low abundances of *Neoceratium* at low latitudes make accurate enumeration difficult, as a large quantity of seawater must be analysed to obtain accurate estimates. In the North Pacific subtropical gyre (NPSG) *Neoceratium* abundances are relatively low during autumn and spring, ranging from 0.2 to 2.4 cells L^{-1} (Weiler 1980; Matrai 1986), and it is likely that abundances in the Atlantic oligotrophic subtropical gyres (OSGs) are similar.

Even these low abundances of *Neoceratium* in OSGs are mysterious, however, as in the euphotic zone nutrient concentrations (particularly nitrate, but often phosphate) limit primary production (Moore et al. 2013), and large phytoplankton, such as *Neoceratium*, should be at a disadvantage when it comes to accessing the small quantities of nutrients available, due to their low nutrient affinities (Aksnes and Egge 1991). In addition to passive advection to the nutricline, and/or ephemeral upwelling of nutrient-rich waters (Karl 1999; Gonzalez et al. 2001; Gregg et al. 2003; Falkowski et al. 2004; Jochum et al. 2004), vertical migration (Weiler and Karl 1979; Heaney and Furnass 1980; Taylor et al. 1988; Baek et al. 2009) and/or phagotrophy on ciliates (Bockstahler and Coats 1993b; Li et al. 1996; Smalley et al. 1999, 2003, 2012; Smalley and Coats 2002) may allow *Neoceratium* to access sufficient nutrients for growth in OSGs. However, there is no information on how depth distributions of *Neoceratium* compare to factors that influence their growth, such as nutrients, light, and prey concentrations.

Here, monthly *Neoceratium* abundance averages from 8 zones in the North Atlantic Ocean were obtained from Continuous Plankton Recorder (CPR) data between 1958 and 2010, and are used to examine seasonal abundance changes throughout the North Atlantic Ocean. Data from vertical net tows (100 m to surface), performed in the North Atlantic subtropical gyre (NAG), South Atlantic subtropical gyre (SAG) and Equatorial Atlantic (EA) from October/November 2010 allow for the determination of *Neoceratium* abundances during autumn/spring in the North and South Atlantic OSGs. Finally, using phytoplankton counts from Niskin bottle samples between 1995 and 2000, the vertical distribution of *Neoceratium* – from equatorial to

subtropical latitudes – is compared to vertical distributions of nutrients, light and potential prey (ciliates), in order to gain an insight into how nutrients may be obtained in OSGs.

2.3 Methods

2.3.1 Continuous Plankton Recorder (CPR) survey data

The CPR is a self-contained automatic plankton recorder (Fig. 2.1), towed behind ships of opportunity, which collects plankton continuously from approximately 6-7 metres (Richardson et al. 2006). Water passes through a moving filter band of silk with a mesh size of 270 µM. Once back in the laboratory, the roll of silk is unwound and cut into sections corresponding to 10 n miles, or approximately 3 m^3 of filtered seawater (Hays and Warner 1993) – this equates to one "sample". The method is considered to be semi-quantitative, with a tendency to under-sample true abundances – especially smaller species. Regardless, data between tows are considered to be comparable as the sampling methodology has remained largely unchanged since 1958. Consequently, patterns in the data collected are believed to reflect real changes in abundances, distributions and community composition (Hays and Warner 1993; Batten et al. 2003).

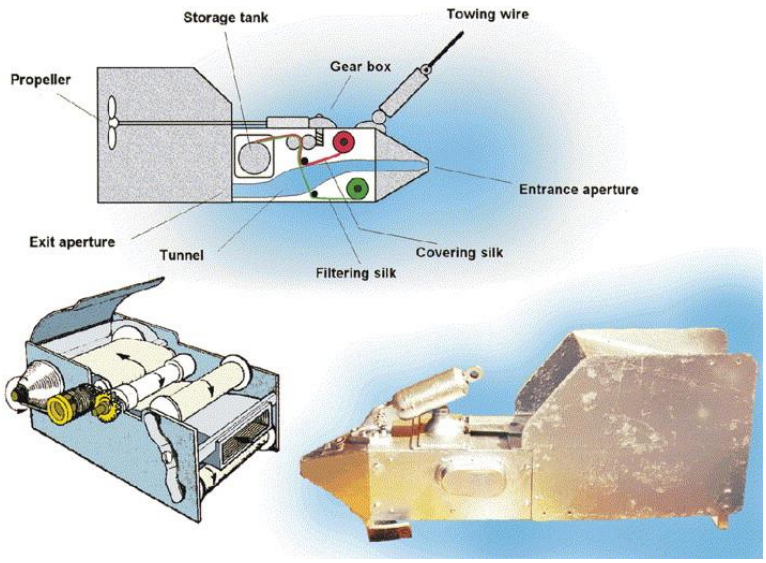

Fig. 2.1. A cross-section of the CPR, its internal mechanism and CPR body (After Richardson et al. 2006).

The robustness of dinoflagellates makes them a good target species for using CPR data. To cover much of the fine-scale variability associated with plankton counts, CPR data are commonly averaged both spatially by geographic areas of interest, and temporally as monthly or annual means. The most common relatively large areas used are the CPR standard zones (Fig. 2.2). These standard zones were combined into 5 larger zones here (Zones 1-5) (Fig. 2.2), based on the zones suggested by Dodge and Marshall (1994). The statistical similarity of l *Neoceratium* (genus only) abundance patterns within these zones was first checked, and in all but one case there was no statistically significant difference between the standard areas that were grouped into each of these 5 zones (Appendix 1). The three standard CPR zones in Zone 4, however, were significantly different from each other (Kruskal-Wallis one-way ANOVA on ranks: D.F. = 2, $P < 0.05$), and further pairwise comparisons showed that this was due to the difference between Zones F8 and D8 (Tukey test: $P < 0.05$). As moving either of these standard areas into a neighbouring zone led to significant differences it was decided to keep to leave Zone 4 as originally suggested by Dodge and Marshall (1994). Additionally, CPR data from south of the standard zones was obtained (between 30 and 40 ^{o}N) and combined into three "subtropical" zones (Zones 6-8) (Fig. 2.2). All CPR data was temporally averaged, by month, from 1958 to 2010, providing a monthly average based on 52 years of CPR data. The number of samples from which the monthly averages were calculated, for each zone, are shown in Table 2.1. Although monthly averages are presented as cells per L, it is prudent not to view these as accurate estimates of absolute abundance, but as a means of comparing relative abundances, both temporally and between different geographic regions (Richardson et al. 2006).

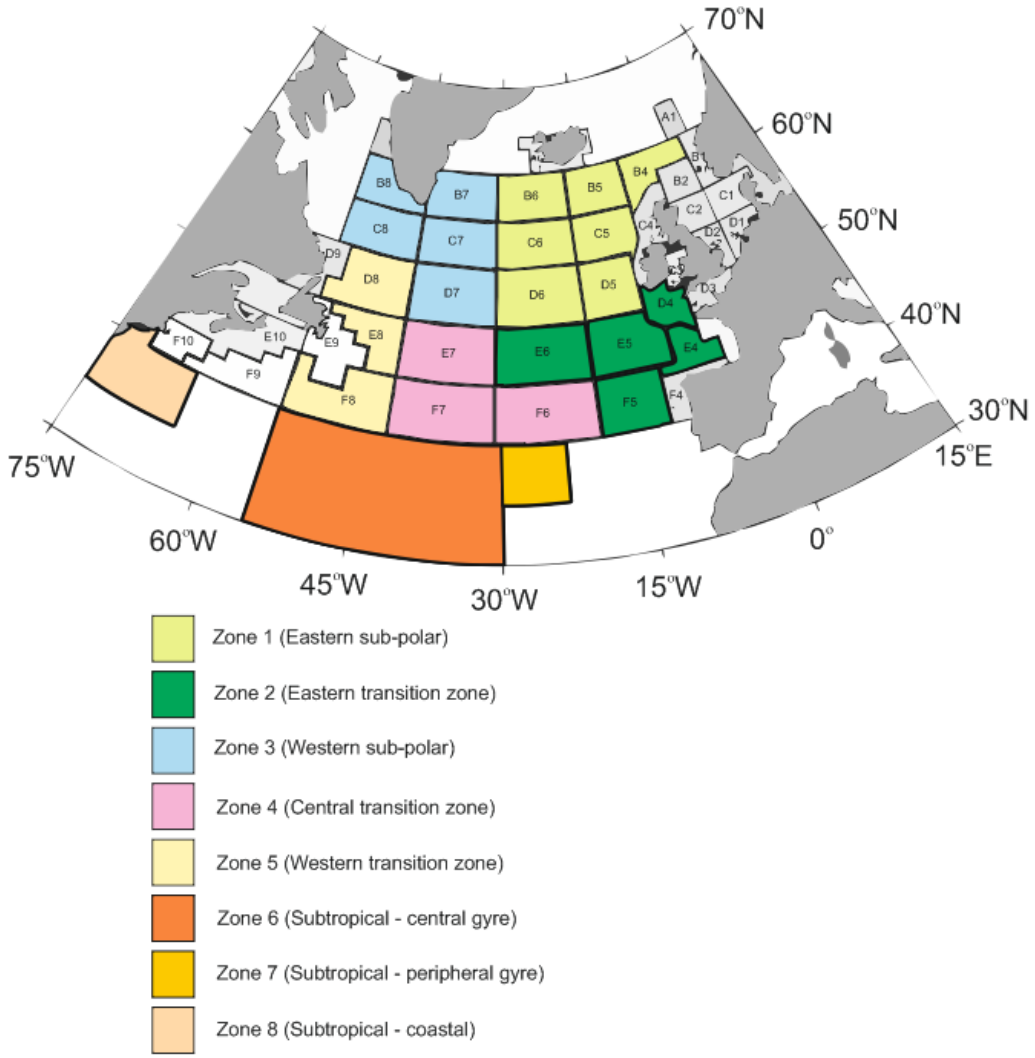

Fig. 2.2. CPR standard zones (A1 to F10) and the eight areas used to compare CPR abundance data of *Neoceratium* in the North Atlantic Ocean.

Table. 2.1. Number of samples (10 n mile tows, approximately 3 m^3) from each of the designated CPR zones from which monthly averages of *Neoceratium* abundances were based.

	Area ID							
Month	Zone 1	Zone 2	Zone 3	Zone 4	Zone 5	Zone 6	Zone 7	Zone 8
J	3264	1918	951	876	618	382	90	130
F	3258	2397	954	698	646	353	41	104
M	4396	2496	1448	926	712	254	28	131
A	4216	2638	1346	897	684	375	31	108
M	4138	2527	1497	877	525	227	22	111
J	4062	2393	1452	961	505	236	52	125
J	4302	2556	1652	984	583	163	16	90
A	4089	2362	1802	1021	671	280	29	112
S	4058	2339	1869	1059	504	280	36	112
O	4080	2116	1501	962	481	326	77	112
N	4070	2048	1446	930	389	266	60	101
D	3377	1879	1225	1065	380	246	60	113

2.3.2 Atlantic Meridional Transect (AMT) data

The Atlantic Meridional Transect (AMT) is an ocean observation programme that undertakes biological, chemical and physical oceanographic research over a latitudinal transect of the Atlantic Ocean from nearly 50˚ N to 50˚ S. *In situ* abundance data on *Neoceratium*, from microplankton vertical net tows, analysed with a FlowCAM, were obtained during AMT 20. Data from the North, South and Equatorial Atlantic Ocean, at a number of different depths, was obtained from Alex Poulton (cell abundances of *Neoceratium* and ciliates) and The British Oceanographic data Centre (BODC, http://www.amt-uk.org/data.aspx) (nitrate, phosphate, and irradiance).

2.3.3 *Neoceratium* cell counts from FlowCAM on AMT 20

During AMT 20, between October 18th and November 15th 2010, samples were collected using an 11m size-fractionating microzooplankton net, with an opening of 18 cm (diameter), at various locations in the Atlantic Ocean (Fig. 2.3). The net was deployed vertically to 100 metres in the water column and then slowly raised to the surface at approximately 10 m minute^{-1}, filtering approximately 2835 L of seawater. Size fractions collected were ≤20 um, ≤40 um, and ≤100 um. 49 ml of each size fraction sample collected from the net was passed through a FlowCAM for 7 minutes at a rate of 7 ml minute^{-1} in order to calculate *Neoceratium* abundances. This method has previously been shown to be a highly quick and effective method for determining abundances of microplankton in seawater (Sieracki et al. 1998). Abundances of *Neoceratium* (genus) per L were calculated by following the recommendations of the manufacturer, and also by taking into account: the size of the net opening, the amount of water the net travelled through, and the volume of water in the sample collection bottles.

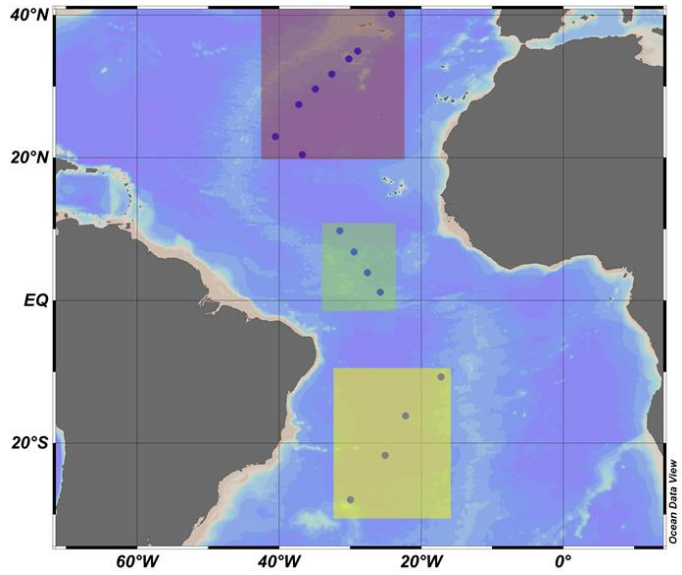

Fig. 2.3. Location of microzooplankton net samples taken during AMT 20, from the NAG (red), SAG (yellow) and EA (green), from which *Neoceratium* abundances were derived.

2.3.4 Cell counts from Niskin bottles – *Neoceratium* and ciliates

Phytoplankton count data had previously been collected on AMTs 1, 2, 3, 4, 5, 7, 8 and 10 between 1995 and 2000. Even-numbered cruises took place in spring (commencing in April/May); odd-numbered cruises took place in autumn (commencing in September). Phytoplankton data were sampled using a rosette fitted with 12 10-l General Oceanics water bottles. 100 ml samples from the NAG, SAG and EA (Fig. 2.4A) were taken, at a number of different depths (Fig. 2.4B); Table 2.2 shows how much water was sampled for each depth within each ocean region. Samples were preserved with 2 % acidic lugol's iodine solution and *Neoceratium* species and ciliates (small, medium, large aloricate ciliates, and loricate *tintinnid* spp.) were identified and counted following the Uthermol's sedimentation technique (using 100 ml Hydrobios settling chambers) under an inverted microscope. Average abundances, at a number of different depth ranges (0-10 m, 11-40 m, 41-70 m, 71- 100 m and 101-160 m), for all *Neoceratium* species and ciliates were calculated for the North, South and Equatorial Atlantic Ocean, providing a depth distribution of

Neoceratium and ciliates in these regions. A number of zeros were present in the *Neoceratium* data set, most likely due to the relatively low volume of water sampled. Zero values were dealt with by substituting in ln(CV) (where CV is the coefficient of variation). This value was calculated for each sample depth in each oceanographic region. This approach was used as it is preferential to leaving the zero values in the data, ignoring them, or choosing an arbitrary zero value (Wolda and Marek 1994).

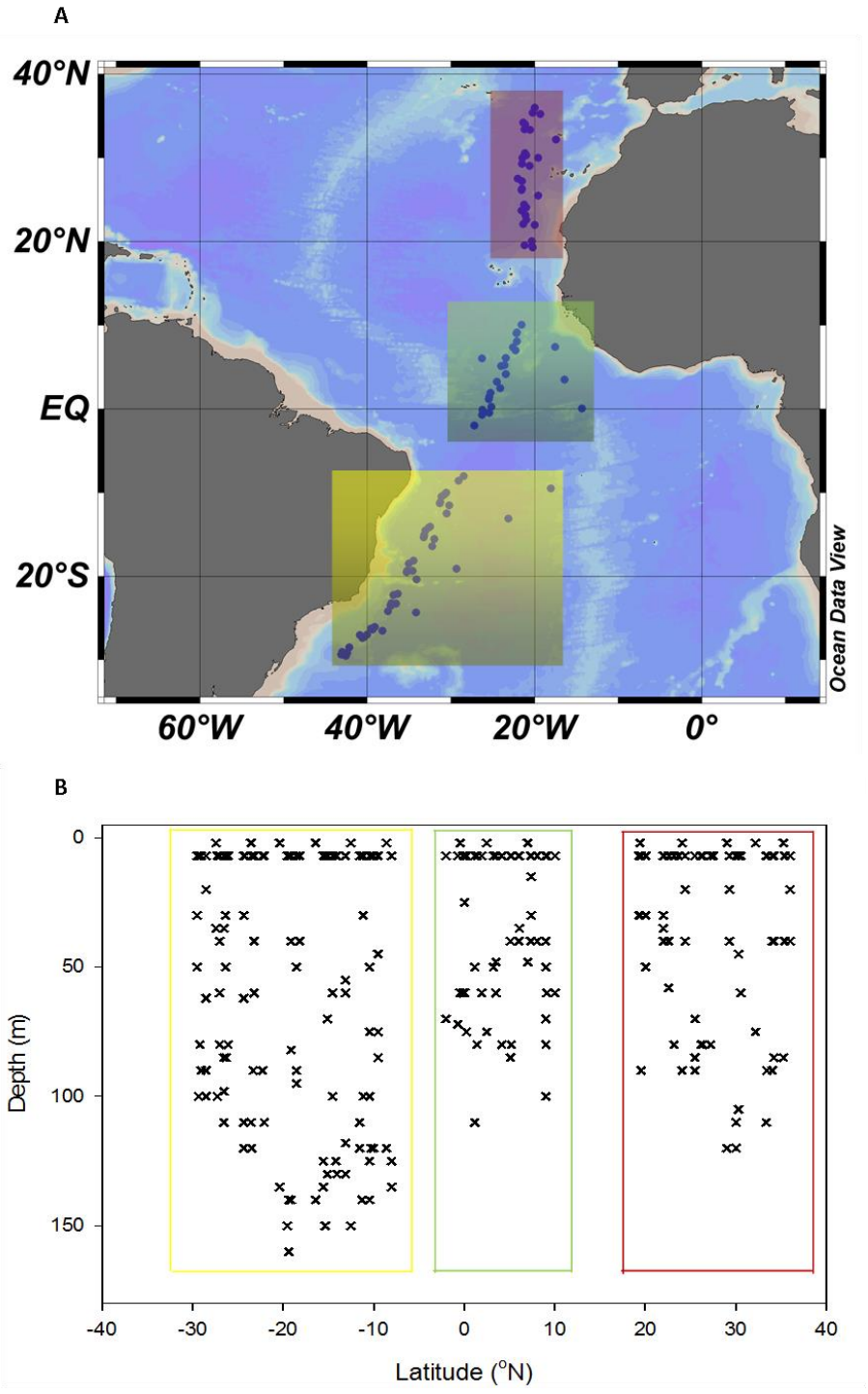

Fig. 2.4. Location of Niskin bottle samples (for analysis of *Neoceratium* and ciliate abundances) from the NAG (red), SAG (yellow) and EA (green) (A). The depth at which each sample was taken is also shown (B). Samples were taken between 1995 and 2000 on-board AMTs 1, 2, 3, 4, 5, 7, 8 and 10 (even numbers, spring; odd numbers, autumn).

Table 2.2. Total volume of seawater sampled from Niskin bottles at each depth (individual samples were 0.1 L), within the NAG, SAG and EA, from which *Neoceratium* and ciliate depth distributions were based.

Depth range (m)	Total volume of water sampled (L)		
	NAG	EA	SAG
0 to 10	2.9	2.3	4.8
11 to 40	1.2	0.8	1.1
41 to 70	0.4	1.1	1.3
71 to 100	1	0.7	2.4
101 to 160	0.6	0.1	3.1

2.3.5 Nitrate and Phosphate concentrations

Nitrate and phosphate data were obtained from AMTs 1, 2, 3, 4, 5 and 10. Water samples were taken from the CTD system at a number of different stations (Fig. 2.5) to a depth of 200 m, and subsampled into clean Nalgene bottles. The analysis of the samples was completed within 3 h of sampling. Nutrients were analysed with a 5-channel Technicon AAII, segmented flow autoanalyser, using standard methodologies for nitrate (Brewer and Riley 1965) and phosphate (Kirkwood 1989).

Nitrate and phosphate measurements, from each oceanographic region, were averaged according to depth (0-10m, 11-20 m, 21-30 m, 31-40m m, 41-50 m, 51-60 m, 61-70 m, 71-80 m, 81-90 m, 91-100 m, 101-130 m, 131-160 m, and 161-200 m). Individual data values that were more than two standard

deviations from the mean measurement for each depth were excluded from the final analysis.

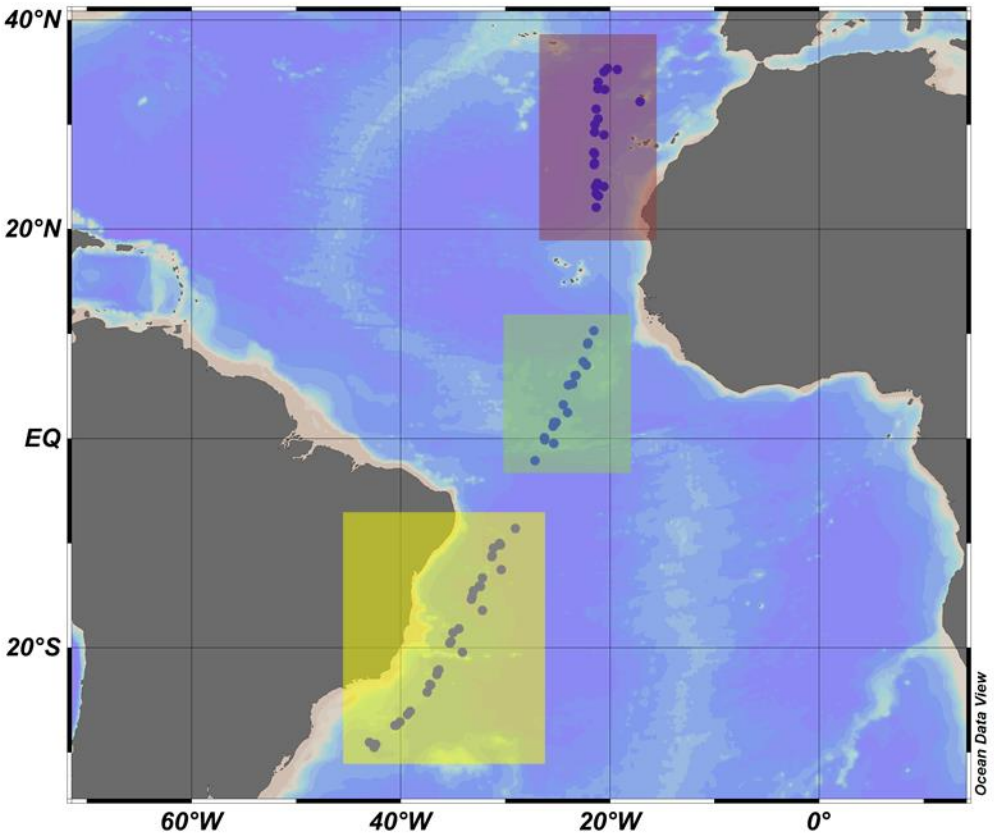

Fig. 2.5. Location of nutrient samples taken in the NAG (red), SAG (yellow) and EA (green) between 1995 and 2000 on-board AMTs 1, 2, 3, 4, 5 and 10.

2.3.6 Irradiance

Irradiance data throughout the water column (every 1 m) was obtained from AMTs 5, 7, and 10 at a range of different locations (Fig. 2.6). Station irradiance data were measured shortly after noon by the SeaWIFS Square Underwater Reference Frame (SeaSURF), composed of: an in water irradiance sensor, the SeaWIFS Buoyant Optical Surface Sensor (SeaBOSS), and a Photosynthetically Active Radiation (PAR) sensor (with deck cell) integrated into the CTD system.

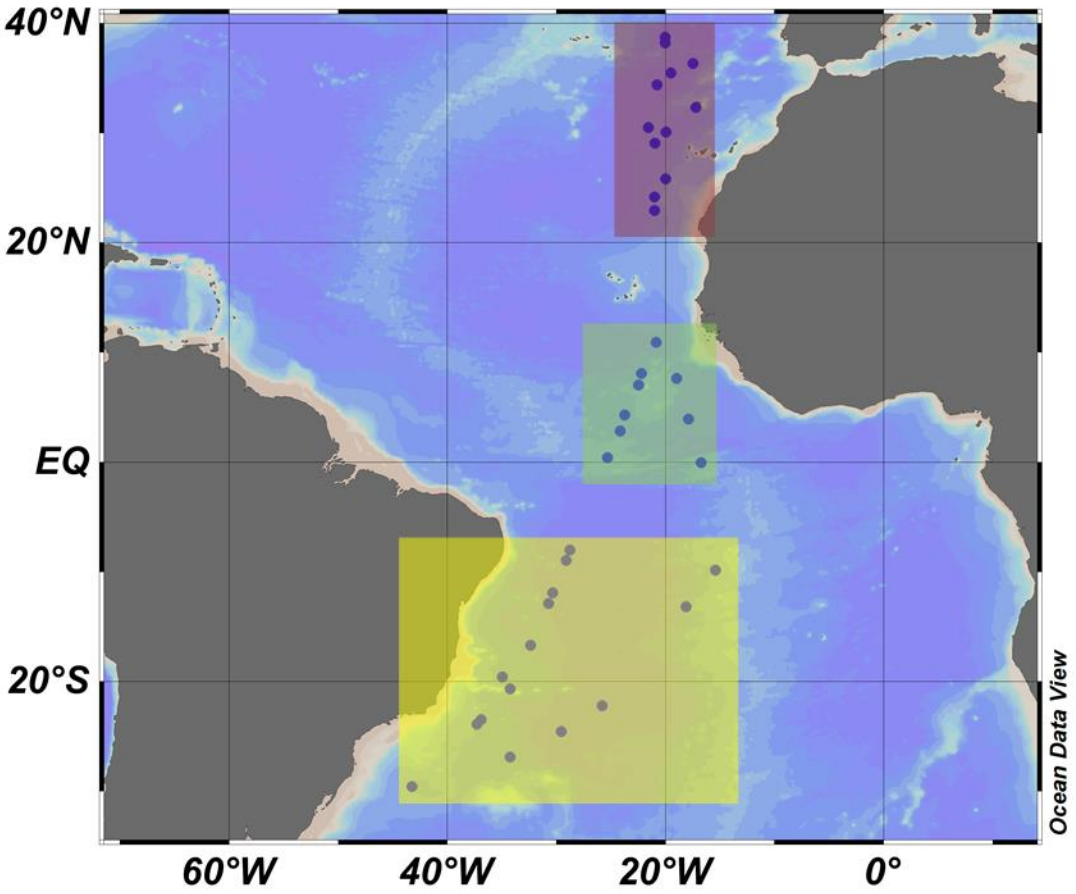

Fig. 2.6. Location of irradiance samples taken in the NAG (red), SAG (yellow) and EA (green), between 1997 and 2000 on-board AMTs 5, 7 and 10.

2.4 Results

2.4.1 *Neoceratium* abundances in the NAG, SAG and Equatorial Atlantic, determined from microplankton net tows

Neoceratium abundances determined from microzooplankton vertical net tows (Fig. 2.7) show that in the NAG, during late autumn (October) in the Northern Hemisphere, concentrations of *Neoceratium* were between 0.17 and 0.55 cells L^{-1}, with a mean of 0.48 cells L^{-1} (standard deviation = 0.21). In the SAG, during late spring (November) in the Southern Hemisphere, concentrations of *Neoceratium* were higher than in the NAG: between 0.66 and 1.84 cells L^{-1}, with a mean of 1.0 cell L^{-1} (standard deviation = 0.57). The difference between the mean cell abundances in the NAG and SAG were statistically significant (t-test: D.F. = 10; $P < 0.05$). Abundances were similarly high in the EA: between 0.41 and 1.58 cells L^{-1}, with a mean of 0.85 cells L^{-1} (standard deviation = 0.26).

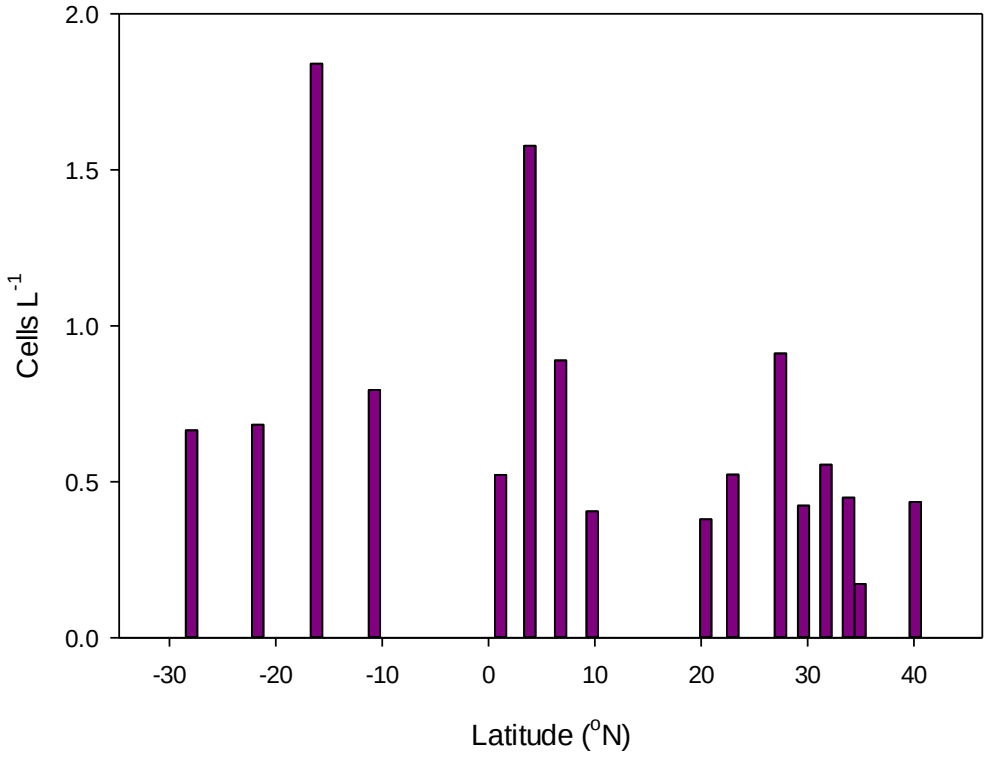

Fig. 2.7. *Neoceratium* abundances between 40°N and 28°S in the Atlantic Ocean, determined from microplankton vertical net tows (0 to 100 m) that were analysed using FlowCAM during AMT 20.

2.4.2 *Neoceratium* seasonality in the North Atlantic Ocean

The same general seasonal trend in cell abundances is seen throughout almost the entire North Atlantic Ocean, from 30 to >60°N and from 0 to 75°W (Fig. 2.8): cell abundances begin to increase in spring (between March and May), peaking in early to late summer (between May and August). The variations in the timings of these abundance increases/peaks appears to be latitude and longitude dependent, with abundance increases/peaks occurring later at more northerly latitudes – at the most northerly latitudes, abundance increases/peaks occur later in the east. For example, in the most southerly subtropical regions, cell abundances begin to increase in March and peak in

June/July; in the most northerly regions (Zones 1 and 3) cell abundances begin to increase in April (Zone 1, Eastern sub-polar region) and May (Zone 3, Western sub-polar region), and peak in July (Zone 1, Eastern sub-polar region) and August (Zone 3, Western sub-polar region). The exception to this trend is Zone 4 (central transition zone), where a second peak in cell abundances occurs in December.

The highest peak abundances coincide with the most northerly latitudes on the eastern side of the Atlantic. In the Eastern sub-polar region (Zone 1), for example, abundances peak at 418 cells L^{-1}, which is considerably higher than the peak seen in the Western sub-polar region (Zone 3, 68 cells L^{-1}). Peak abundances decrease southwards, and reach their lowest values at subtropical latitudes, within the central gyre (2.2 cells L^{-1}, Fig. 2.9). In all regions *Neoceratium* are present year round, albeit often at extremely low concentrations (lowest concentrations from all zones, 0.1 to 9 cells L^{-1}).

At subtropical latitudes, similar species compositions are seen inside and outside of the gyre (Fig. 2.9). Within the gyre *N. fusus* is dominant – consistently over 50 % of the community. Other species found include *N. macroceros*, *N. tripos*, *N. lineatum*, *N. horridum*, *N. furca* and *N. candelabrum*. The major difference outside the gyre is that *N. tripos* is commonly the dominant species (especially in spring/ early summer), and *N. articum is* occasionally present early in the year (from March to June).

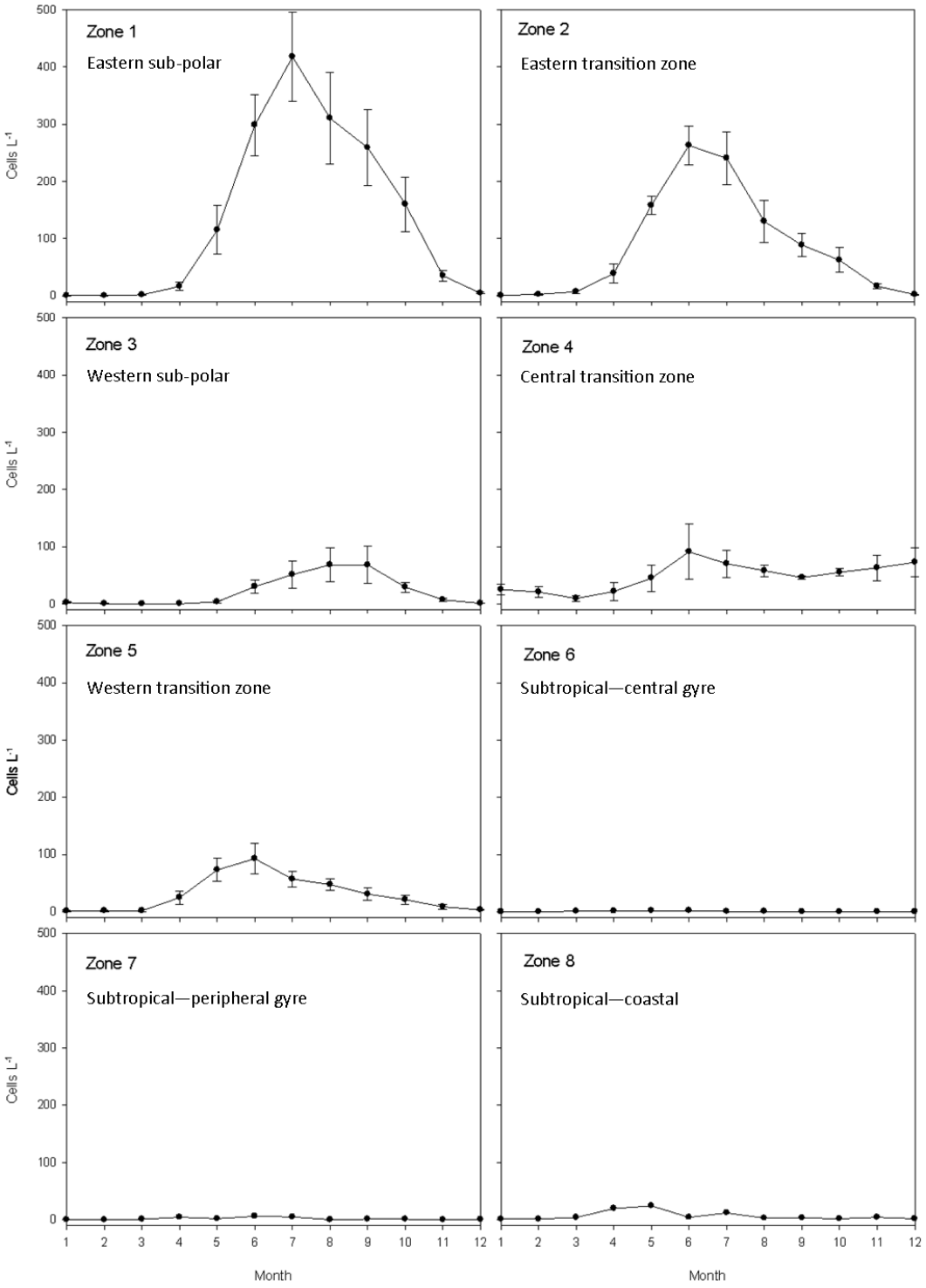

Fig. 2.8. *Neoceratium* seasonal abundances in the North Atlantic Ocean, averaged from 1958 to 2010. Based on CPR data. See Fig. 2.2 for zones. Error bars for zones 1 to 5 represent the standard errors of the CPR standard zones that were combined for each of these zones (See Appendix 1). The seasonal abundance patterns of Zones 6-8 can be seen in more detail in Fig. 2.9.

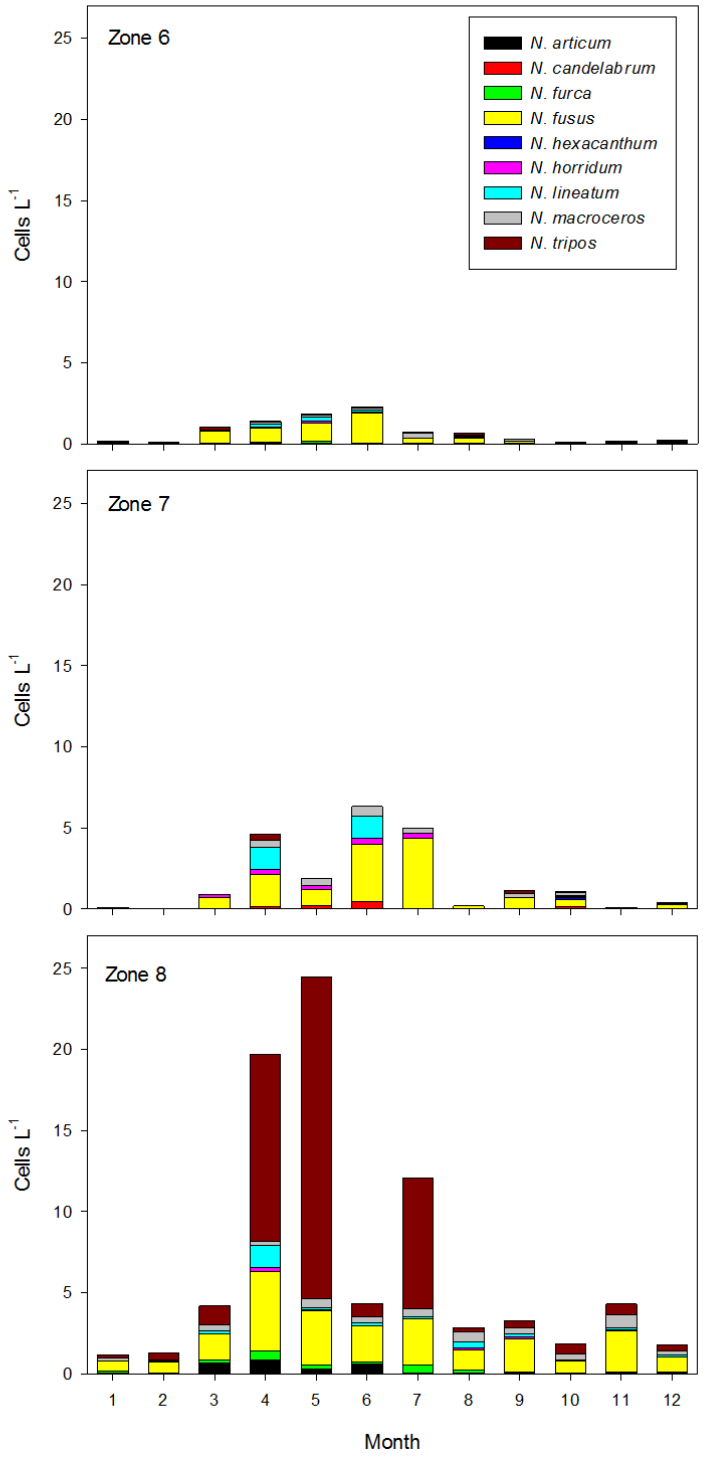

Fig. 2.9. *Neoceratium* seasonal abundances, and species composition, at subtropical latitudes in the North Atlantic Ocean, averaged from 1958 to 2010. Based on CPR data.

2.4.3 *Neoceratium* vertical distributions in the NAG, SAG and EA

Neoceratium abundances determined from Niskin bottle counts show that average *Neoceratium* abundances were greater in the NAG than the SAG (50 compared to 14 cells L^{-1}) (Fig. 2.10). In the NAG, EA and SAG, peak *Neoceratium* abundances were found in the surface 40 m (118, 77 and 31 cells L^{-1} respectively). In the NAG and EA, cell abundances decrease with increasing depth down to 18 cells L^{-1} between 101 and 160m in the NAG, and down to 18 cells L^{-1} between 70 and 100 m in the EQ (Fig.2.10A, B). In the SAG, however, abundances remain roughly similar between 11 and 160 m, between 11 and 20 cells L^{-1} (Fig. 2.10C).

In all 3 regions a wide variety of *Neoceratium* species are found (Fig. 2.10) at all depths. Species that appear to be commonly found at the deepest depths include: *N. boehmi*, *N. declinatum*, *N. fusus*, *N. pentagonum*, *N. teres* and *N azoricum*. Species that are abundant in surface waters are not necessarily abundant at depth. For example, one of the most dominant species in surface waters of the NAG (13- 15 % of the *Neoceratium* population), *N. lineatum*, is less dominant below 70 m (just 5 % of the population).

Comparing the surface community from the NAG Niskin bottle samples (0 to 10 m) to the surface community from the most relevant CPR zone (zone 7, Fig. 2.9) from spring and autumn, it is evident that two of the species that dominate the community from the CPR data (*N. fusus* and *N. lineatum*) are also prevalent in the Niskin bottle samples. But other species that are prevalent in the Niskin bottle samples are absent from the CPR data (notably *N. boehmii* and *N. teres*).

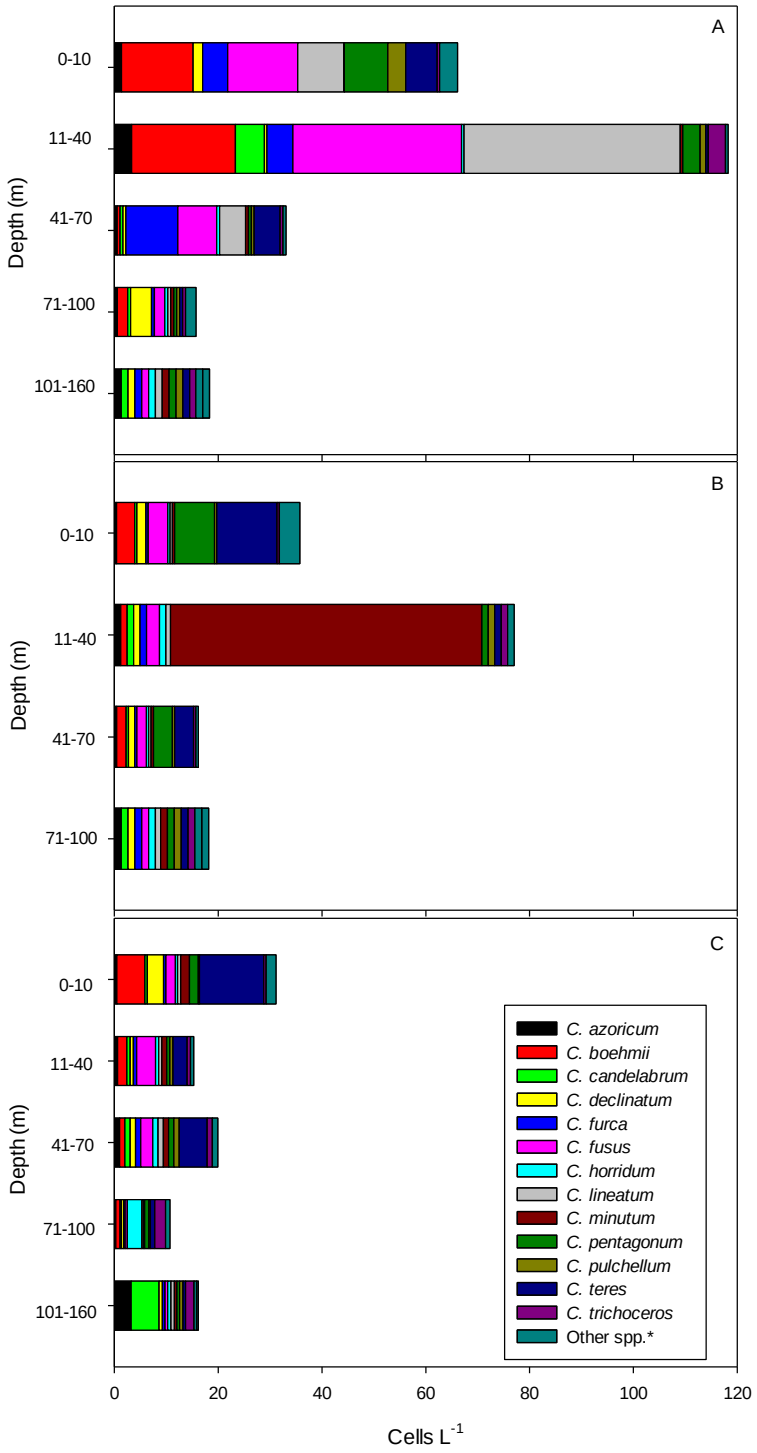

Fig. 2.10. Comparison of *Neoceratium* depth distributions, and species compositions, between the NAG, SAG and EA, based on Niskin bottle samples (1995 to 2000). Other spp.*: *N. carrense*, *N. extensum*, *N. geniculatum*, *N. gibberum*, *N. hexacanthum*, *N. inflatum*, *N. limulus*, *N. longipes*, *N. macroceros*, *N. platycorne*, *N. symmetricum*, *N. tripos*, *N. vulture*.

2.4.4 Vertical distributions of nutrients in the NAG, SAG and EA

In the NAG, average nitrate concentrations are undetectable (< 0.02 μM) between the surface and 50 m (Fig. 2.11A). Concentrations rise a little between 51 and 100 m (up to approximately 0.5 μM). Beyond 101 meters nitrate concentrations rise rapidly to 2.3 μM between 101 and 130 m, 5.01 between 131 and 160 m, and 6.07 between 161 and 200 m. Phosphate concentrations are undetectable (< 0.02 μM) between the surface and 30 m (Fig. 2.11B). Between 31 and 100 m concentrations are generally a little higher (0.03 to 0.08 μM). Beyond 101 meters phosphate concentrations rise rapidly to 0.20 μM between 101 and 130 m, 0.36 μM between 131 and 160 m, and 0.33 μM between 161 and 200 m.

In the EA, average nitrate concentrations are undetectable (< 0.02 μM) between the surface and 40 m (Fig. 2.12A). Concentrations rise a little between 41 and 50 m (up to 0.93 μM). Beyond 51 meters nitrate concentrations are always greater than 1.36 μM, reaching a peak concentration of 19.40 μM between 161 and 200 m. Phosphate concentrations are undetectable (< 0.02 μM) between the surface and 40 m (Fig. 2.12B) and then rise sharply beyond this: from 0.16 μM, between 41 and 50 m, to 1.38μM between 161 and 200 m.

In the SAG, average nitrate concentrations are undetectable (< 0.02 μM) between the surface and 90 m (Fig. 2.13A). Concentrations rise a little between 91 and 130 m (up to 0.16 μM). Beyond 131 meters nitrate concentrations rise rapidly to 3.18 μM between 161 and 200 m. Phosphate concentrations range between 0.035 and 0.055 μM between the surface and 100 m (Fig. 2.13B). Between 101 and 130 m concentrations rise a little to 0.098 μM. Beyond 131 meters phosphate concentrations rise rapidly to 0.18μM between 131 and 160 m, and 0.36 between 161 and 200 m.

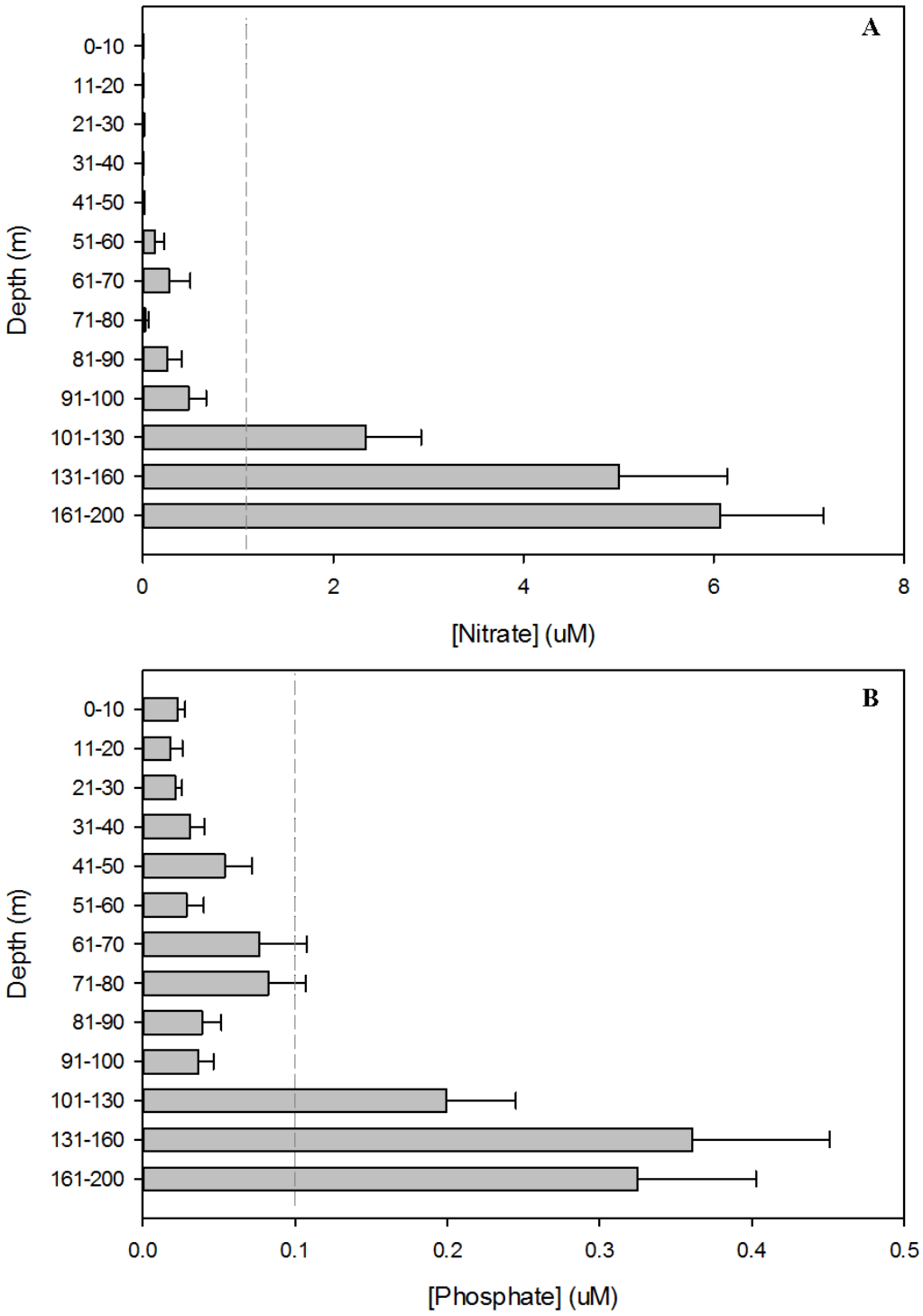

Fig. 2.11. Variations in average nutrient concentrations (A, nitrate; B, phosphate) with depth in the NAG. The dotted line represents the lowest concentration of nutrients at which *Neoceratium* have previously been shown to grow (Baek et al. 2008a). Error bars represent the standard error of all the measurements taken at that depth from AMTs 1, 2, 3, 4, 5 and 10.

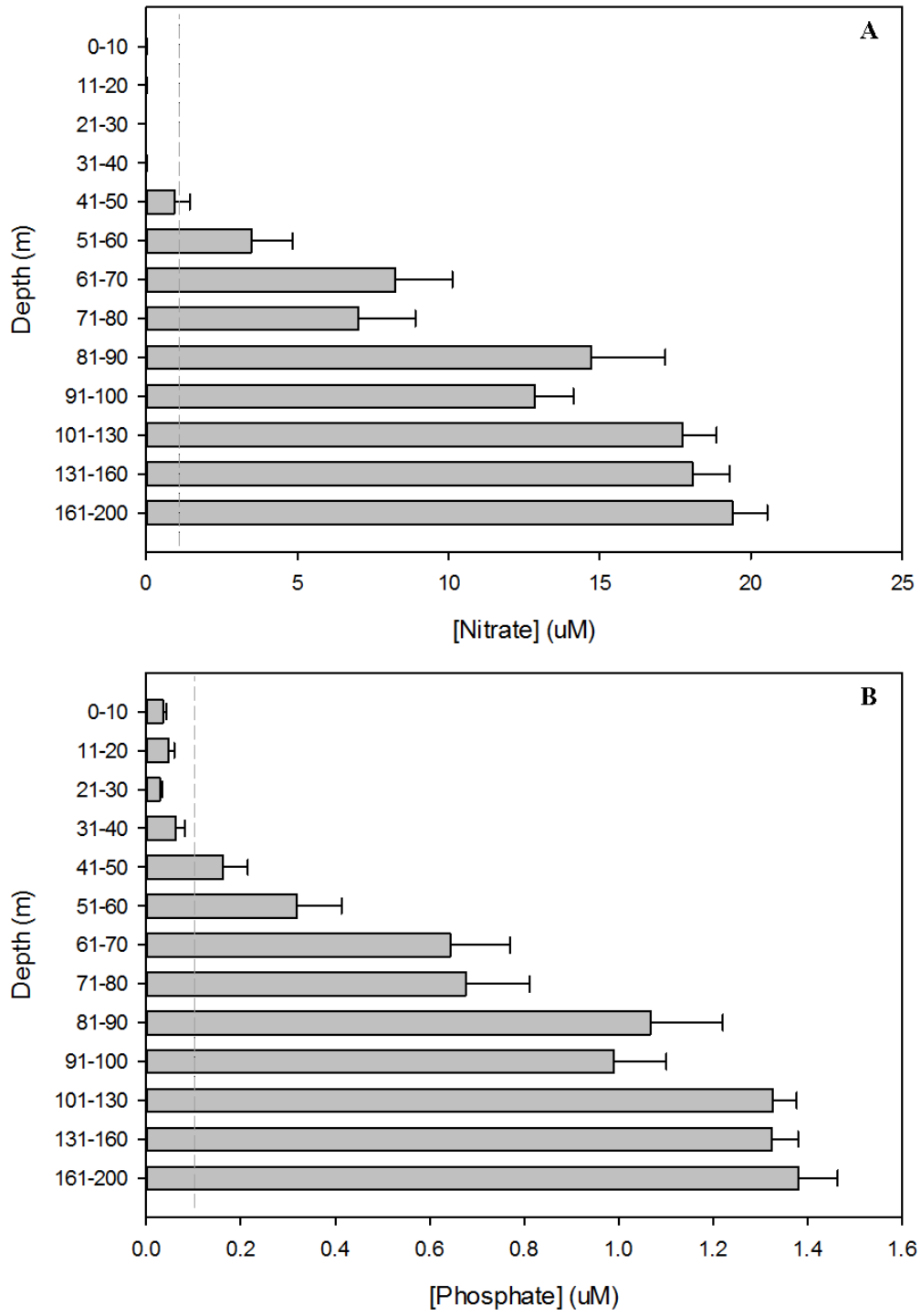

Fig. 2.12. Variations in average nutrient concentrations (A, nitrate; B, phosphate) with depth in the EA. The dotted line represents the lowest concentration of nutrients at which *Neoceratium* have previously been shown to grow (Baek et al. 2008a). Error bars represent the standard error of all the measurements taken at that depth from AMTs 1, 2, 3, 4, 5 and 10.

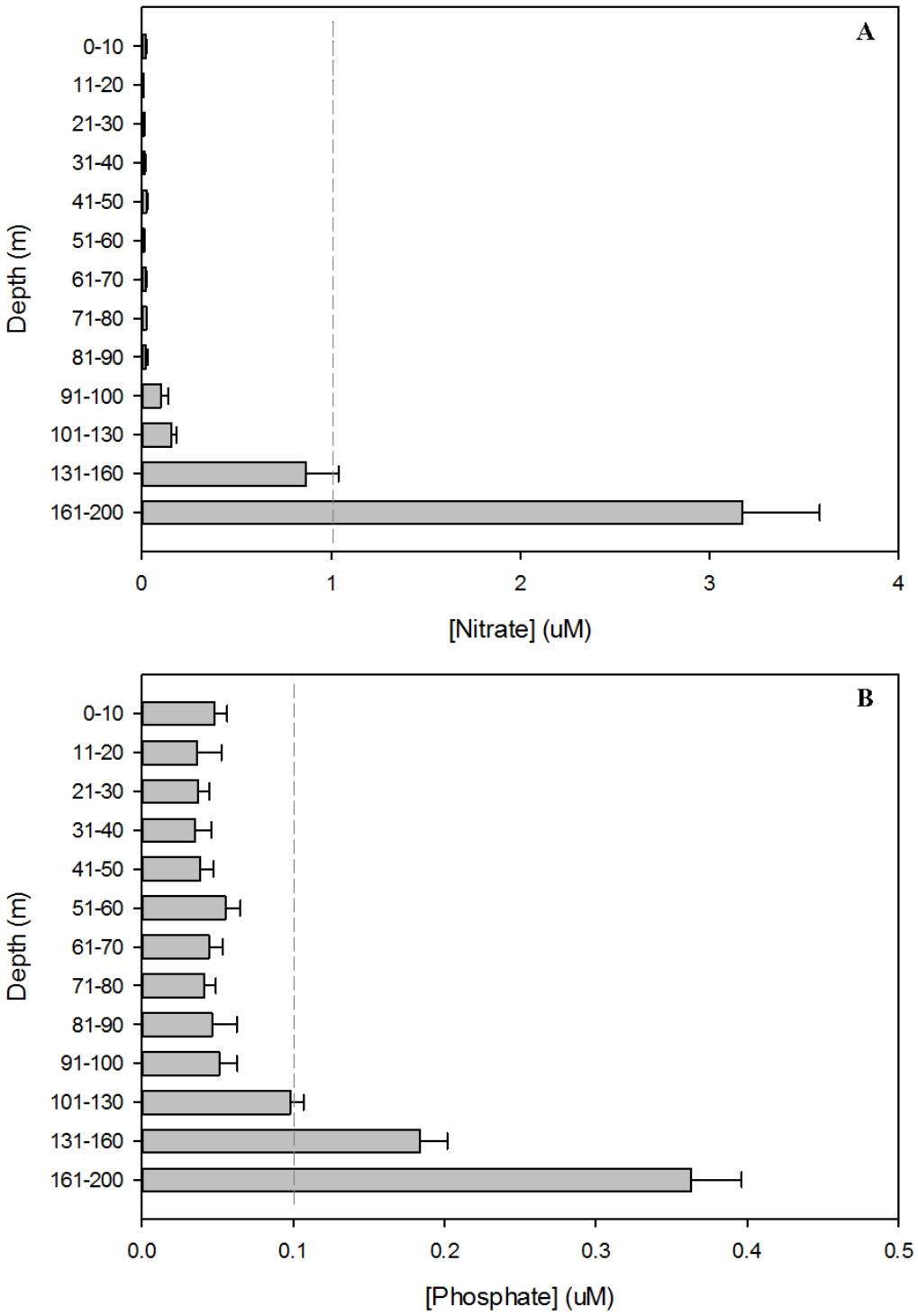

Fig. 2.13. Variations in average nutrient concentrations (A, nitrate; B, phosphate) with depth in the SAG. The dotted line represents the lowest concentration of nutrients at which *Neoceratium* have previously been shown to grow (Baek et al. 2008a). Error bars represent the standard error of all the measurements taken at that depth from AMTs 1, 2, 3, 4, 5 and 10.

2.4.5 Vertical distributions of irradiance in the NAG, SAG and EA

In the NAG, between the surface and 40 m, irradiances range from 40 to 2291 µmol quanta m^{-2} s^{-1} during midday (Fig. 2.14A), with a mean of 215 to 1275 µmol quanta m^{-2} s^{-1} (Fig. 2.14B). Between 41 and 70 m irradiances range from 3 to 363 µmol quanta m^{-2} s^{-1}, with a mean of 50 to 207 µmol quanta m^{-2} s^{-1}. Between 71 and 100 m the range of irradiances is 4 to 98 µmol quanta m^{-2} s^{-1}, with a mean of 9 to 49 µmol quanta m^{-2} s^{-1}. Between 101 and 160 m irradiances are between <2 and 20 µmol quanta m^{-2} s^{-1}, with a mean of <2 to 9 µmol quanta m^{-2} s^{-1}.

In the EA, between the surface and 40 m, irradiances range from 62 to 2293 µmol quanta m^{-2} s^{-1} (Fig. 2.14C), with a mean of 146 to 1728 µmol quanta m^{-2} s^{-1} (Fig. 2.14D). Between 41 and 70 m irradiances range from 4 to 217 µmol quanta m^{-2} s^{-1}, with a mean of 20 to 132 µmol quanta m^{-2} s^{-1}. Between 71 and 100 m the range of irradiances is <2 to 37 µmol quanta m^{-2} s^{-1}, with a mean of <2 to 19 µmol quanta m^{-2} s^{-1}. Between 101 and 160 irradiances are between <2 and 7.9 µmol quanta m^{-2} s^{-1}, with a mean of <2 µmol quanta m^{-2} s^{-1}.

In the SAG, between the surface and 40 m, irradiances range from 93 to 2293 µmol quanta m^{-2} s^{-1} (Fig. 2.14E), with a mean of 235 to 1434 µmol quanta m^{-2} s^{-1} (Fig. 2.14F). Between 41 and 70 m irradiances range from 42 to 436 µmol quanta m^{-2} s^{-1}, with a mean of 88 to 233 µmol quanta m^{-2} s^{-1}. Between 71 and 100 m the range of irradiances is 41 to 165 µmol quanta m^{-2} s^{-1}, with a mean of 31 to 86 µmol quanta m^{-2} s^{-1}. Between 101 and 160 m irradiances are between <2 and 56 µmol quanta m^{-2} s^{-1}, with a mean of <6 to 30 µmol quanta m^{-2} s^{-1}. Deeper than 160 m irradiances are between <2 and 5 µmol quanta m^{-2} s^{-1}.

2.4.6 Ciliate vertical distributions in the NAG, SAG and EA

Similar abundances and distributions of ciliates are observed throughout the water column in the NAG, SAG and EA (Fig. 2.15). Average ciliate concentrations range from 593 to 3045 cells L^{-1}, with a subsurface peak occurring between 11 and 70 m (>2000 cells L^{-1} in all regions). Small aloricate

ciliates are almost always dominant (making up 43 to 91 % of the ciliate community), followed by medium aloricate ciliates (6 to 52 %), loricate *tintinnids* (2 to 12 %) and large aloricate ciliates (0 to 1 %).

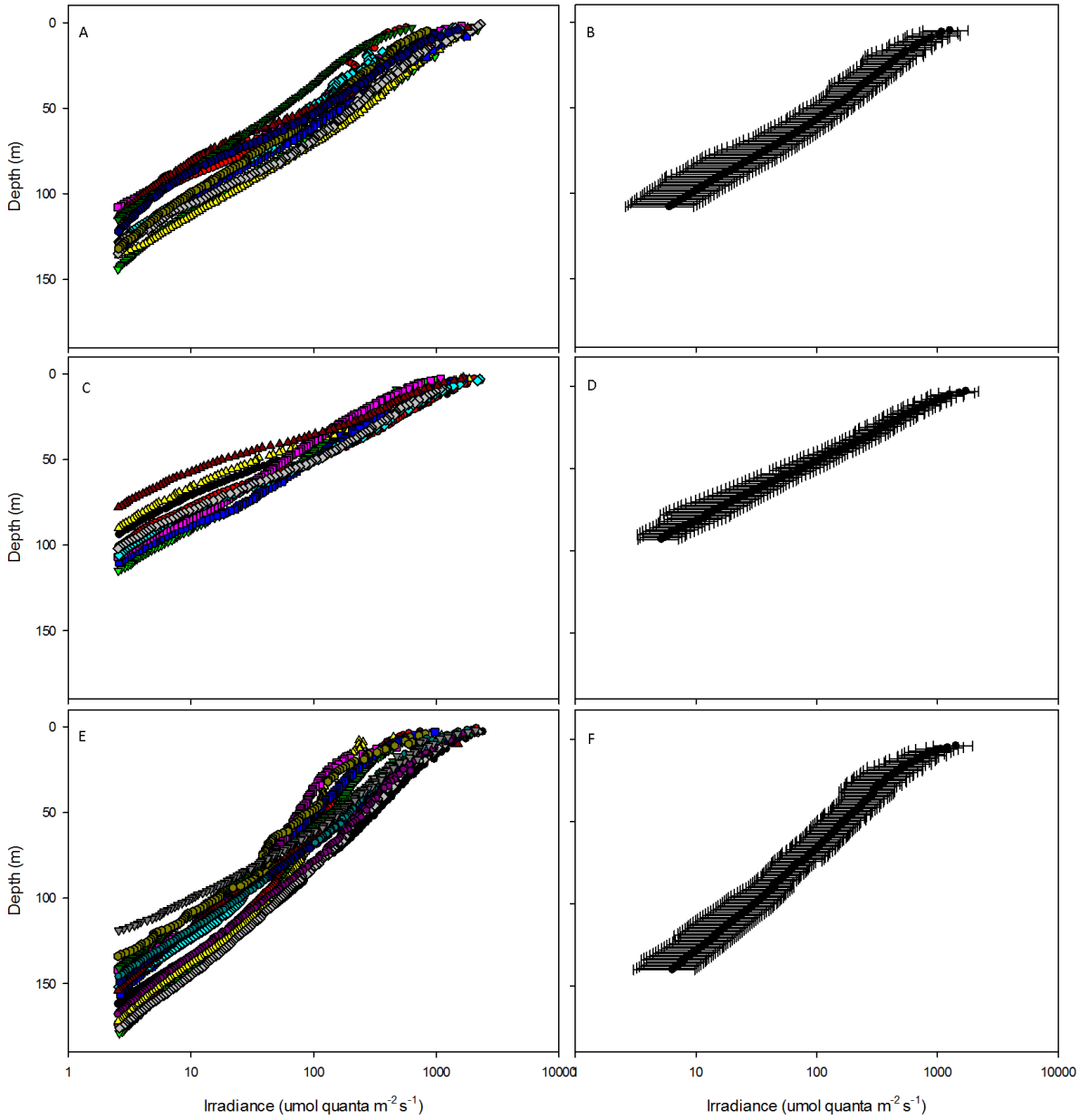

Fig. 2.14. Variations and means in irradiance with depth shortly after noon in the NAG (A, B), EA (C, D) and SAG (E, F). Error bars in B, D and F represent the standard errors of measurements made at each depth shown in A, C and E.

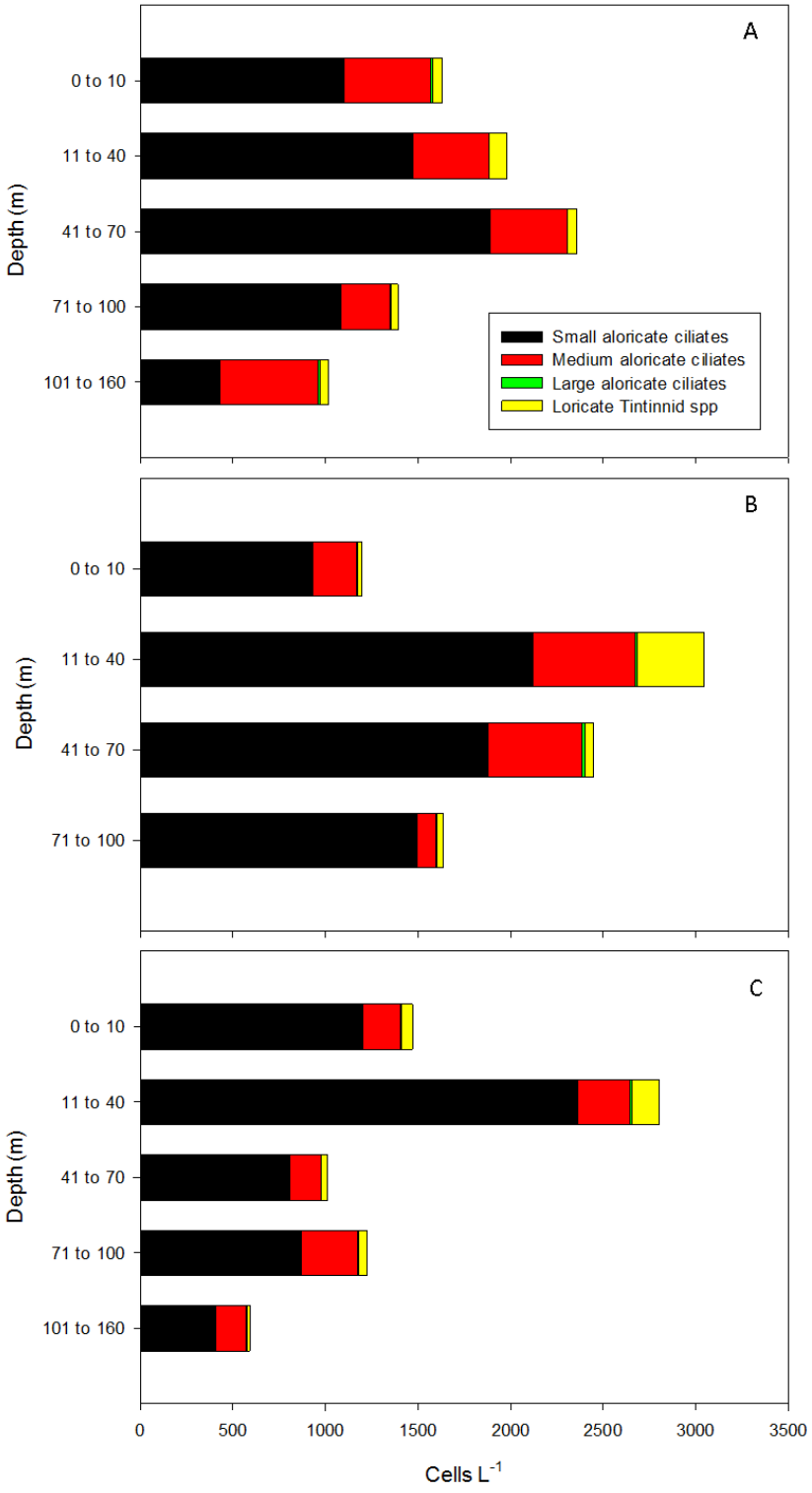

Fig. 2.15. Comparison of ciliate depth distributions between the NAG, SAG and EA.

2.5 Discussion

2.5.1 Seasonality of *Neoceratium* in OSGs

CPR data demonstrated that in the central North Atlantic subtropical gyre (NAG) *Neoceratium* is present year-round, in surface waters, at concentrations that range between 0.1 and 2.2 cells L^{-1}. Average abundances from net tows onboard AMT 20 in the NAG (late autumn) and SAG (late spring) were 0.48 and 1.0 cells L^{-1} respectively. It is well established that CPR data under-samples true plankton abundances due to its relatively large mesh size (270 µM). However, *Neoceratium* abundances from CPR data compared well to abundance estimates from net tows using a much smaller net-mesh size of 20 µM. The average *Neoceratium* abundances in the central NAG estimated from CPR data between September and December (from 1958 to 2010) were compared to average abundances from net samples taken in late October 2010. Average abundances from CPR data (~6 to 7 m; 0.21 cells L^{-1-}) were significantly lower than net sample abundances (100 m to surface; 0.48 cells L^{-1}) (t-test: D.F. = 10; $P < 0.05$). However, the CPR only appears to have underestimated the net-sample abundances by about half. This is perhaps not too surprising given the fact that *Neoceratium* abundances were shown to decrease with depth — consequently, the CPR, which only operates in the surface 6-7 m, samples where abundances are at their highest. Also, the relatively large size of *Neoceratium* cells may be a factor: Weiler (1980) showed that, for a range of different species, body size (girdle diameter) ranged from 23 to 93 µm and horn length varied from 10 to over 500 µm. Both of the abundance estimates discussed above are comparable to *Neoceratium* abundances in the NPSG, which were also estimated using vertical net tows with similar sized meshes. Using vertical net tows (mesh size 25 µm) Weiler (1980) estimated abundances to be between 0.2 and 2.4 cells L^{-1} during cruises that took place in June, July and September; Matrai (1986) found abundances to be < 1.6 cells L^{-1} based on vertical net tows (mesh size 35 µm) performed in January.

Cell abundances follow the same seasonal abundance pattern expected of dinoflagellates from further north in the North Atlantic (McQuatters-Gollop et al. 2007). Increases in abundance occur in spring (March), peaking in early summer (June) – this general pattern was common throughout the entire North Atlantic Ocean, but the onset occurred later at higher latitudes, as would be expected due to the later onset of stratification at higher latitudes. This observation is consistent with *in situ* microplankton biomass measurements, in the Pacific Ocean central gyre, that suggest a peak in abundance during spring (Beers et al. 1982), and not with remote sensing measurements of chlorophyll which suggest phytoplankton begin to bloom in autumn, peaking within two months of the winter solstice (usually in January). The reason for the discrepancy between CPR counts of (surface) *Neoceratium* abundances and remote sensing of (surface) chlorophyll may be due to the fact that *Neoceratium* are not representative of the phytoplankton community as a whole – either in terms of their seasonal abundance patterns, or in terms of their depth distribution. Alternatively (or additionally), the fact that chlorophyll is not necessarily a perfect proxy for phytoplankton concentrations may help to explain the discrepancy: peaks in chlorophyll may represent an increase in chlorophyll per cell or reduced mortality (Wilson and Qiu 2008), and therefore may represent an increase in cellular biomass, or an adaptation to reduced light intensities in winter. It has already been demonstrated that in the North Pacific Gyre algae undergo a photo-acclimation response, resulting in an increase in chlorophyll per cell (Winn et al. 1995).

It was also shown that species compositions within the gyre are similar to those outside the gyre at similar latitudes (water temperatures). This suggests that species within OSGs are selected according to their temperature preference (e.g. Graham & Bronikovsky 1944; Graham 1941; Dodge & Marshall 1994) and not special adaptations for survival at low nutrient concentrations.

2.5.2 Comparison of *Neoceratium* depth distributions with the distributions factors influencing growth

In the NAG, SAG and EA *Neoceratium* were found from the surface to greater than 100 m. In all three regions *Neoceratium* was most abundant in surface waters (from the 0 – 40 m), but especially in the NAG and EA; in the SAG, *Neoceratium* were more evenly distributed throughout the water column. However, these abundances are an order of magnitude greater than the CPR abundances (from spring/autumn) from the zone (zone 7) closest to the area where Niskin bottle samples were taken on the AMT cruises. They are also considerably higher than the abundances recorded using the vertically-towed plankton net on AMT 20 — although these samples were taken further towards the centre of the gyre. In surface waters average abundances from Niskin bottle samples in the NAG were 50 cells L^{-1}, compared to a maximum of ~1 cell L^{-1} from CPR samples, and 0.55 cells L^{-1} from the vertical net samples, at approximately the same time of year. Likely explanations for this discrepancy are under-sampling by the CPR and vertically-towed net; they both probably have a tendency to miss smaller cells, but this would be especially true for the CPR, which has a much larger mesh size (270 µM compared to 20 µM). Losses due to cells adhering to the meshes of these nets may also have caused under-sampling as may the fact that the sample area for the Niskin bottle samples was further towards the edge of the NAG than the sample areas for the CPR and vertical net. The depth distributions that are observed are inconsistent with other observations. Graham (1941) looked at the depth distributions of 29 *Neoceratium* species from data collected during extensive cruises in the Atlantic and Pacific Ocean and found that 20 of these species showed an increase in frequency between 0 and 100 meters. Cregeen et al. (in prep) used a closing-plankton net in surface waters and close to the deep chlorophyll maxima (DCM), in the NAG and SAG, and showed that *Neoceratium* are more abundant close to the DCM.

The lowest nutrient concentrations that have been shown to facilitate growth of *Neoceratium* are 1 µM nitrate and 0.1 µM phosphate (Baek et al. 2008). Average nutrient concentrations in the NAG are below these values between the surface and 100 metres (nitrate, <0.5 µM; phosphate, <0.08 µM). In the

SAG average nitrate concentrations are significantly lower than this between the surface and 130 metres (< 0.16 µM), and phosphate concentrations are significantly lower than this above 100 metres (<0.05 µM). The importance of this is that there are *Neoceratium* cells present at depths where there are not sufficient (inorganic) nutrients available for growth. It is possible that cells may be able to grow, or at least survive for a long time, at the nutrient concentrations that are observed in surface waters. Alternatively, nutrients may be accessed periodically via vertical advection of cells (Denman and Gargett 1983), ephemeral upwelling of nutrients (Falkowski et al. 1991; Karl 1999; Gonzalez et al. 2001), vertical migration (Weiler and Chisholm 1976; Weiler and Karl 1979; Baek et al. 2009) or phagotrophy on ciliates (Bockstahler and Coats 1993b; Li et al. 1996; Smalley et al. 1999, 2003, 2012; Smalley and Coats 2002). Ciliates were shown to be abundant throughout the water column in the NAG and SAG and are present at concentrations approximately two orders of magnitude greater than *Neoceratium*.

Neoceratium are present in the NAG and SAG at depths (below 100 to 130 meters) where nutrient concentrations are high enough to support growth and survival. Here, the problem for cells is potentially low light levels (<2 to 21 µmol quanta m^{-2} s^{-1}), and it is important to know if *Neoceratium* can grow at these low irradiances; if they cannot grow, it would be instructive to know how long they might be able to survive under these conditions. It has been shown that in *N. furca* and *N. fusus* potential growth rates decrease gradually with increasing exposure to zero-light conditions (Baek et al., 2008), and became negative after 10 days of continuous dark exposure. It is not known, however, how cells react when exposed to the very low light levels that are present at the nutricline.

2.6 Conclusion

It has been shown that *Neoceratium* abundances in the NAG and SAG are comparable to abundances in the North Pacific subtropical gyre, and that in the NAG *Neoceratium* follow a seasonal pattern common to dinoflagellates at more northerly latitudes – cell numbers increase in spring and peak in summer. *Neoceratium* are present from the surface to 160 metres depth in the NAG and SAG. However, nutrient concentrations appear to be too low for growth to occur in the surface 100 to 130 metres. This suggests that nutrients may be accessed from deep periodically or via feeding on ciliates, which were shown to be two orders of magnitude more abundant than *Neoceratium*. Before considering these potential means of obtaining nutrients, it is first necessary to determine if the nutrient concentrations found in the surface 100 to 130 meters of the NAG and SAG can support the growth of *Neoceratium*. This is the subject of the next chapter of this thesis.

3. *Neoceratium* growth and survival under simulated nutrient-depleted conditions typical of oligotrophic subtropical gyres

3.1 Abstract

The dinoflagellate *Neoceratium* is commonly observed in oceanic waters, depleted in major inorganic nutrients such as nitrogen and phosphorus. Using culture isolates, it was investigated whether two *Neoceratium* species (*N. hexacanthum* and *N. candelabrum*) can grow phototrophically at low nutrient concentrations found in surface waters of oligotrophic subtropical gyres (OSGs). No phototrophic growth (indicated by changes in cell numbers, the presence of dividing cells, or cellular protein increase) was observed when *N. hexacanthum* and *N. candelabrum* were grown in low nutrient seawater (nitrate = 0.58 µM; phosphate = 0.04 µM). In separate experiments, to determine survival time under oligotrophic nutrient conditions, 68 % of *N. hexacanthum* cells were able to re-establish growth after spending 1-10 days in North Atlantic gyre seawater (NAGSW: nitrate <0.02 µM; phosphate < 0.02 µM); 40 % recovered after 11-20 days and only 3 % recovered after 21-30 days. The longest period any single cell survived, and then went on to divide, was 26 days. These findings demonstrate that *Neoceratium* cells could remain viable for >3 weeks in surface waters of oligotrophic subtropical gyres, but to sustain their growth nutrients must be obtained periodically from an alternative source: via the uptake of dissolved organic nutrients, ephemeral upwelling of nutrient-rich waters, phagotrophy, and/or movement to and from the nutricline.

3.2 Introduction

In oligotrophic subtropical gyres (OSGs), globally important ecosystems that cover over 30% of the surface of the Earth, primary productivity is limited by low standing stocks of nutrients, usually nitrogen (Moore et al. 2013). The low nutrient concentrations found here are predominantly sustained via microbial regeneration in the surface mixed layer, rather than by inputs from below the nutricline (Karl 2002). Organisms that have low sinking velocities and high nutrient uptake rates are better able to cope with low nutrient conditions, compared to larger cells, (Fuhrman et al. 1989; Zubkov et al. 2007), which explains why these environments are typically dominated by prokaryotes and small eukaryotic algae (Cho and Azam 1988; Zubkov et al. 2000; Zubkov and Tarran 2008; Hartmann et al. 2012).

Dinoflagellates in the genus *Neoceratium* (cell volume: 49,000 to 331,000 μm^3 $cell^{-1}$, Takahashi and Bienfang 1983) are commonly found, although not dominant, in OSGs (Graham 1941; Graham and Bronikovsky 1944; Weiler 1980). In the North Pacific central gyre, for example, where *Neoceratium* is estimated to contribute <1% of total phytoplankton carbon, concentrations range from 0.8 to 3 cells L^{-1} (Weiler, 1980; Matrai, 1986). Although cell concentrations are significantly lower in the central gyre than in coastal waters of the Pacific Ocean (typically 4-14 %) (Weiler, 1980; Matrai, 1986), growth rates (based on frequency of dividing cells) are relatively high based on one *in situ* study in the North Pacific subtropical gyre (NPSG): 26-38 % of the maximum rates observed for this genus (Weiler, 1980). This is curious, as large cells, with low surface area to volume ratios, should be at a disadvantage due to their relatively low nutrient affinities (Aksnes and Egge 1991).

The presence of *Neoceratium* in OSGs may reflect an ability of cells to optimally position themselves in the water column for nutrients and light (Weiler and Karl 1979; Heaney and Furnass 1980; Taylor et al. 1988; Baek et al. 2009), or supplement their nutrient demand via phagotrophy (Bockstahler and Coats 1993b; Li et al. 1996; Smalley et al. 1999, 2003, 2012; Smalley and Coats 2002). However, it is also possible that *Neoceratium* do not require an alternative source of nutrients: cells may be able to survive and grow at the low

nutrient concentrations typically found in OSGs. Physiological adaptations to low nutrient concentrations may allow cells to survive and grow in nutrient impoverished surface waters of OSGs. For example, low half saturation constants for nitrogen and phosphorus and specific characteristics for nutrient uptake – such as luxury consumption – have been suggested to give *Neoceratium* an advantage over other algal species growing at low nutrient concentrations (Baek et al. 2008a), and the production of the enzyme alkaline phosphatase may allow for the exploitation of dissolved organic phosphorus pools (Mackey et al. 2012; Girault et al. 2012). These adaptations may account for the previous observation of *Neoceratium fusus* growing in low nutrient culture medium (Baek et al., 2007, Baek et al. 2008a); Nitrate ≤1.0 µM and Phosphate ≤0.1 µM).

Here two cultures of *Neoceratium* spp. (*N. hexacanthum,* and *N. candelabrum*) commonly found in OSGs are used to determine if (and for how long) cells can survive and grow at nutrient concentrations typically found in surface waters of these environments. Cell growth, under these conditions, is investigated by monitoring changes in cell numbers, dividing cells, protein per cell and *Fv/Fm* in low nutrient seawater (LNSW) compared to nutrient replete seawater (RSW). In a separate experiment, changes in other cell growth properties (survival time, viability, time-lag of growth response and growth rate) are determined by monitoring cells in embryo dishes, exposed to North Atlantic gyre seawater (NAGSW) for varying periods of time before addition of nutrients.

3.3 Methods

3.3.1 Maintenance of *Neoceratium* cultures

Neoceratium strains (*N. hexacanthum*, strain number P10B2; *N. candelabrum*, strain number P37C2) were obtained from the Gulf of Villefranche (Point B, 0-80 m), in The Mediterranean Sea between 2007 and 2008. They were cultured in K/5 medium (Keller et al. 1987), minus silicate, made from NAGSW (Table 3.1) – collected from the surface of the central gyre in October 2009 during Atlantic Meridional Transect (AMT) 19, onboard the Royal Research Ship (R.R.S.) James Cook. All cultures were maintained in 100 ml borosilicate Erlenmeyer flasks and kept at 18°C in a temperature controlled incubator with a 12:12 h light/dark photocycle, with a photon flux density of 60 µmol quanta m^{-2} s^{-1}.

3.3.2 Isolation into experimental flasks

Prior to all experiments, *Neoceratium* were isolated from their culture medium into experimental medium using the following method. The concentration of cells in the stock culture (late exponential/stationary growth phase) was determined in order to calculate the volume required to achieve desired experimental concentrations (~10-30 cells ml^{-1}). Prior to transfer to experimental Erlenmeyer flasks (acid washed with hydrochloric acid and autoclaved), this predetermined volume of stock culture was collected on a 20 µm nylon net filter (NY20; Millipore) and rinsed with filtered NAGSW, using a pipette, in order to remove excess nutrients. Cells were rinsed from the filter into one of the experimental flasks, and then evenly divided (by volume) between all the flasks. All experiments were performed in triplicate.

Experiments were conducted in 100 ml Erlenmeyer flasks, using 50 ml of LNSW or nutrient replete seawater (RSW) (Table 3.1). Experiments were incubated at 18°C on a 12:12 h light/dark cycle at a photon flux density of 60 µmol quanta

m^{-2} s^{-1}. Every four days (starting on day one) sub-samples from each experimental treatment were taken, from which: cell numbers, number of dividing cells, estimated protein per cell, photosynthetic efficiency of photosystem II (PSII; *Fv/Fm*), and dissolved inorganic nutrient concentrations (NO_3^- + NO_2^-, and PO_4^{3-}; only for the *N. candelabrum* experiment) were determined.

Table 3.1. Initial nutrient concentrations for each of the three different experimental nutrient treatments that *Neoceratium* were subjected to (measured from experiments on *N. candelabrum*). All experimental seawater was made from NAGSW; the only amendments made were to concentrations of nitrate and phosphate. *Measurements that were below the detection limit of the nutrient analyser.

Experimental Seawater	Nitrate concentration (µM)	Phosphate concentration (µM)
Low nutrient (LNSW)	0.58	0.04
Nutrient replete (RSW)	185	1.40
Surface North Atlantic gyre (NAGSW)	<0.02*	<0.02*

3.3.3 Cell numbers

Cell numbers were determined by enumeration of 1 ml of experimental medium in a 1 ml plastic Sedgewick-Rafter (S-R) chamber, under an inverted microscope. In addition to cell numbers, observations on motility were made and the number of dividing cells was recorded.

3.3.4 Protein content of cells

In the reaction of the bicinchoninic acid (BCA) reagents with protein, the reduction of Cu^{2+} to Cu^{+}, by protein in an alkaline medium, is followed by the reaction of BCA with Cu^{+} – resulting in an intense purple-coloured reaction product (BCA/Copper complex) that exhibits a strong linear absorbance at 562 nm (Smith et al. 1985). The BCA method is favourable to other protein detection methods (e.g. Lowry assay) as it is a one-step process, is more tolerant of interfering substances, has greater working reagent stability, and increased sensitivity (Smith et al. 1985); additionally there is less variability caused by protein compositional differences – other assays are strongly influenced by four amino acid residues (cysteine, cystine, tyrosine and tryptophan) in the protein, whereas in the BCA assay the universal peptide backbone also contributes to colour formation.

1.5 ml of experimental medium was frozen in 1.5 ml cryoviles (-80°C). The average protein content of *Neoceratium* cells was measured using the BCA method (Smith et al. 1985), using bovine serum albumin (fraction 5) as a standard. Prior to analysis, samples were defrosted at room temperature prior to being centrifuged (10 mins, 4 °C, 12000 rpm). Under the protocol recommended by Smith et al. (1985), BCA reagents would simply be added at this point, and the colour change would be allowed to occur over a 24 hour period before taking measurements with a spectrophotometer. However, due to the relatively low number of cells in the samples, combined with the fact that the cell shape of *Neoceratium* prevented them from forming a pellet when centrifuged, the method had to be optimised in order to make it sensitive enough to measure protein in the experimental samples. 1.3 ml (out of 1.5 ml total volume) was carefully removed from each centrifuged sample. In order to maximise cell numbers and minimise seawater volume (necessary to achieve detectable protein concentrations), the remaining 0.2 ml was transferred to a S-R chamber (rinsed with MilliQ) and individual cells from each sample were picked (using a 10 µL micropipette) into polymerase chain reaction (PCR) tubes – in order to further reduce sample seawater volumes, once cells had settled to the bottom of the tube, some seawater was carefully removed from the PCR

tubes using a 10 µL micropipette. Following this, the exact number of cells, transferred to PCR tubes, was confirmed under a dissecting microscope, and blanks were prepared by pipetting a set volume of cell-free media into PCR tubes (for each sample). BCA reagents were added in an 8:1 ratio (reagents:sample), and samples were left at room temperature for 24 hours, prior to analysis on a Nanodrop 1000 Spectrophotometer, in order to allow colour development to occur. Data values more than two standard deviations (i.e. outside of 95 % confidence limits) from the mean were omitted from the final analysis as recommended by Fowler and Cohen (1991) (*N. hexacanthum*: 1/54 samples; *N. candelabrum*: 2/54 samples). To ensure that the BCA protocol had been sensitive enough, the number of cells from each sample analysed was plotted against protein measured for that sample for both *Neoceratium* species (Fig. 3.1). A positive relationship between cell number and protein measured was found for *N.hexacanthum* (Fig. 3.1A, R^2=0.66, P<0.001) and *N. candelabrum* (Fig. 3.1B, R^2=0.74, P<0.001), providing confidence that the method had been sensitive enough to measure the protein concentrations in the samples.

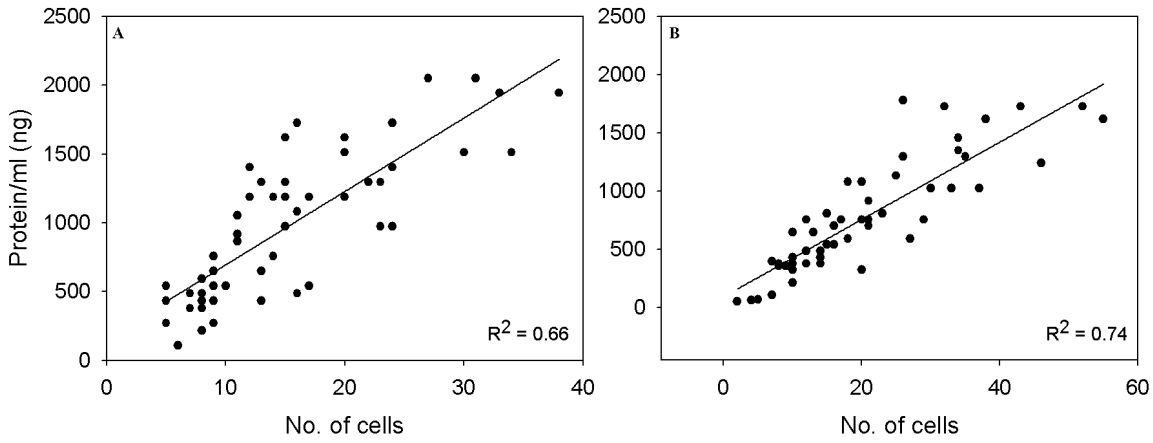

Fig. 3.1. Comparison of protein ml^{-1} (ng) measured from individual samples with the number of *N. hexacanthum* (A) and *N. candelabrum* (B) cells in those same samples.

3.3.5 Fast repetition rate fluorometry (FRRf)

Fast repetition rate fluorometry (FRRf) was used to assess the maximum PSII photochemical efficiency (F_v/F_m), which typically decreases under periods of 'stressful' growth such as nutrient starvation (Kolber et al. 1988; Kolber and Falkowski 1993). 2 ml of each experimental medium was transferred to a 15 ml darkened Falcon tube for at least 1 hour prior to FRRf analysis, allowing the primary receptor molecules of PSII (quinones) to be fully oxidised and ready to receive electrons (Suggett et al. 2009). FRRf measurements were made using the 'standard' protocols described by Suggett et al. (2003) and Moore et al. (2005). A Chelsea Instruments Fasttracka FRR fluorometer was programmed to deliver single photochemical turnover saturation of PSII from 100 flashlets of 1.1 µs at 1 µs intervals. Fluorescence transients generated were then fitted to the Kolber-Prasil-Falkowski (KPF) (Kolber et al. 1998) model to yield values of F_v/F_m (Moore et al. 2006).

3.3.6 Nutrient measurements

Dissolved inorganic nutrients (nitrate + nitrite and phosphate) were analysed from subsamples taken from LNSW experimental flasks (*N. candelabrum* experiments only). 10 ml subsamples were filtered through 0.2 µm Millipore filters into 15 ml Falcon tubes; subsamples were the result of combining 3.5 ml subsamples from triplicate experimental flasks; this was done in order to provide sufficient volume for analysis. Samples were stored at -80°C prior to analysis within 1 month of collection. Nitrate and phosphate measurements were analysed using a Skalar SanPlus Autoanalyser at NOCS according to Sanders and Jickells (2000) by Mark Stinchcombe.

3.3.7 Changes in cell growth properties over 30 days of exposure to NAGSW

N. hexacanthum cells (exponential growth phase) were reverse filtered in order to remove excess nutrients from the culture medium. Following this, approximately 10 cells (average: 9; range: 5-14) were transferred to 30 embryo dishes containing 2.5 ml of NAGSW, and covered with a glass lid to prevent evaporation (the mass of each dish was monitored to ensure no evaporation occurred). Exact cell numbers were confirmed, and every day for 30 days (starting on day 1) nutrients were added (0.5 ml of K-medium) to a single dish. Following nutrient addition cell numbers and dividing cells were monitored every 2 days, allowing for the estimation of the following:

Maximum viability time: The longest period that any single cell survived and went on to divide.

Changes in growth rate: Growth rate was estimated, after initial time-lags in growth response following nutrient addition, by fitting an exponential growth model [Stirling Model; $y=y0+a(exp(b\times x)-1)/b$] to the data using SigmaPlot (**Systat Software Inc.)** software – where "x" refers to x-axis values (experiment day number), "y" refers to y-axis values (cell number), and "a" and "b" are coefficients provided by the software. The slope of the line was then used to estimate growth rate in divisions per day (d^{-1}). Several different exponential models were tested for how well they fitted the data. The Sterling model was used as it had the highest R^2 values of all the exponential models (11 in total) fitted to the data using SigmaPlot.

Change in the percentage of viable cells (cells capable of growth): For each embryo dish, on the day of nutrient addition, attempts were made to calculate the number of viable cells present that contributed to the increase in cell numbers. To do this the first two data points from each of the growth curves

were removed and then the Stirling growth model (discussed above) was fitted to the data in order to estimate how many cells were viable on day 1 (y=0). It was decided to remove the first two data points as this was found to provide the best compromise between removing the influence of early data points and reducing the error of the estimate of y=0. For dishes where no growth was observed, the number of viable cells was taken to be zero. By combining data together into three groups (day 1-10, day 11-20 and day 21-30), and comparing the number of viable cells from each group to the total number of cells upon nutrient addition, it was possible to estimate the percentage of viable cells during each of these three periods.

Changes in time-lag of growth response: The growth time-lag for each dish was estimated from the number of days it took, after nutrient addition, for the first sign of growth to occur: either an increase in cell number, or the presence of dividing cells.

3.4 Results

3.4.1 Growth at nutrient concentrations typical of OSGs – *N. hexacanthum*

In experiments on *N. hexacanthum*, in LNSW, cell numbers showed little variation over 21 days (Fig 3.2A: range, 17.7 to 20 cells ml^{-1}). Cell numbers increased in RSW up until day 13, from 28 to 49 cells ml^{-1}; after this point cell numbers decreased from 49 to 33 cells ml^{-1}. The percentage of dividing cells observed broadly mirrored the above pattern (Fig. 3.2C): no dividing cells were observed in LNSW; in RSW dividing cells increased from 0 to 4.8 % between day 1 and 9, before decreasing to 0.7% by day 17. Motile cells were observed throughout the 21 day experiment in RSW, but no motile cells were observed after day 17 in LNSW.

Average protein content per cell (Fig 3.2E) remained stable in LNSW between day 1 and 13 (8.4 to 9.1 ng $cell^{-1}$), before decreasing to 4.3 ng $cell^{-1}$ by day 21. In RSW average protein per cell fluctuated between 6.9 and 11.3 ng $cell^{-1}$, but was similar on day 1 and day 21 (8.7 and 9.9 ng $cell^{-1}$ respectively).

There was little difference in *Fv/Fm* values between the two nutrient treatments, where a small decrease occurred over the 21 days: from 0.274 to 0.245 in LNSW, and from 0.307 to 0.235 in RSW (Fig. 3.2G).

3.4.2 Growth at nutrient concentrations typical of OSGs – *N. candelabrum*

In experiments on *N. candelabrum*, in LNSW, cell numbers (Fig. 3.2B) showed a small decrease over 21 days, from 21 to 15 cells ml^{-1}, whereas cell numbers increased in RSW over the course of the whole 21 day period, from 16 to 156 cells ml^{-1}. The percentage of dividing cells (Fig. 3.2D) mirrored the above

pattern: the percentage of dividing cells on day 1 was roughly similar across both scenarios (9 and 12 %). Beyond day 5 no dividing cells were observed in LNSW; in RSW there was an increase in dividing cells, between day 1 and 5, from 12-19 %, followed by a decrease to 2 % by day 21. Motile cells were observed throughout the experiment under both nutrient scenarios.

The average protein content per cell (Fig 3.2F) remained relatively stable in both nutrient scenarios between day 1 and 21, with some indication of a downward trend over time: in the LNSW scenario protein concentrations were 5.5 ng $cell^{-1}$ on day 1 and 2.7 ng $cell^{-1}$ on day 21; In the RSW scenario protein concentrations were 6.4 ng $cell^{-1}$ on day 1 and 4.0 ng $cell^{-1}$ on day 21

Fv/Fm values (Fig. 3.2H) closely mirrored changes in cell numbers (Fig. 3.2B). In LNSW values stayed relatively constant up until day 9 (range, 0.089 to 0.116); this was followed by a decrease, to 0.014, by day 21. In RSW there was a rapid increase between day 1 and 9 (from 0.107 to 0.325), followed by a gradual increase until day 17 (to 0.394), before falling to 0.319 by day 21

In LNSW PO_4^{3-} concentrations remained between the detection limit of <0.02 µM and 0.04 µM. NO_3^- concentrations ranged between 0.41 µM and 0.86 µM (Fig. 3.3).

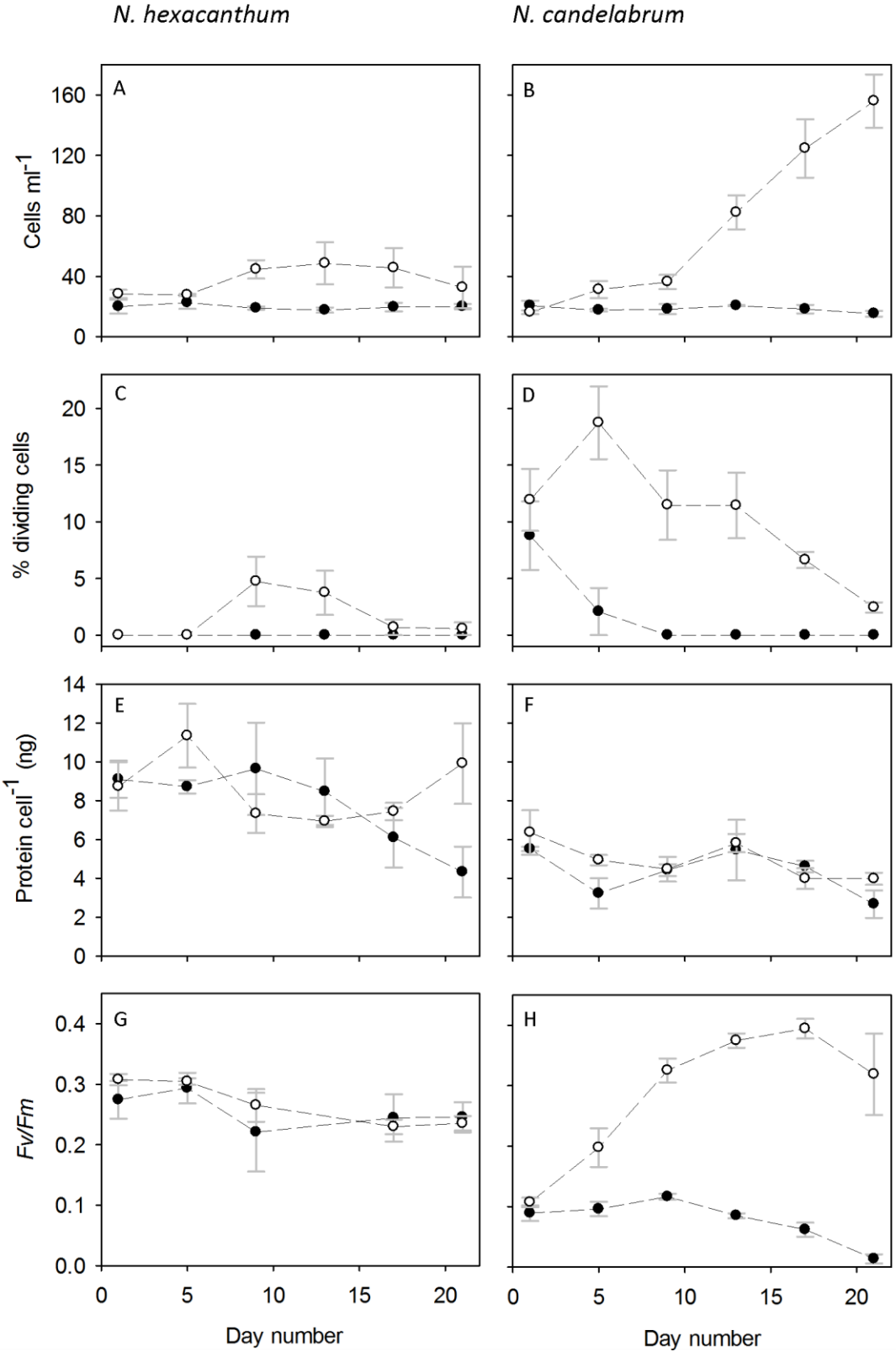

Fig. 3.2. Changes in *N. hexacanthum* and *N. candelabrum* cell numbers (A,B), % of dividing cells (C,D), protein cell^{-1} (E,F) and *Fv/Fm* (G,H) over the course of 21 days, under two different nutrient treatments: LNSW (filled symbols) and RSW (hollow circles). Error bars represent the standard error of triplicate experimental flasks.

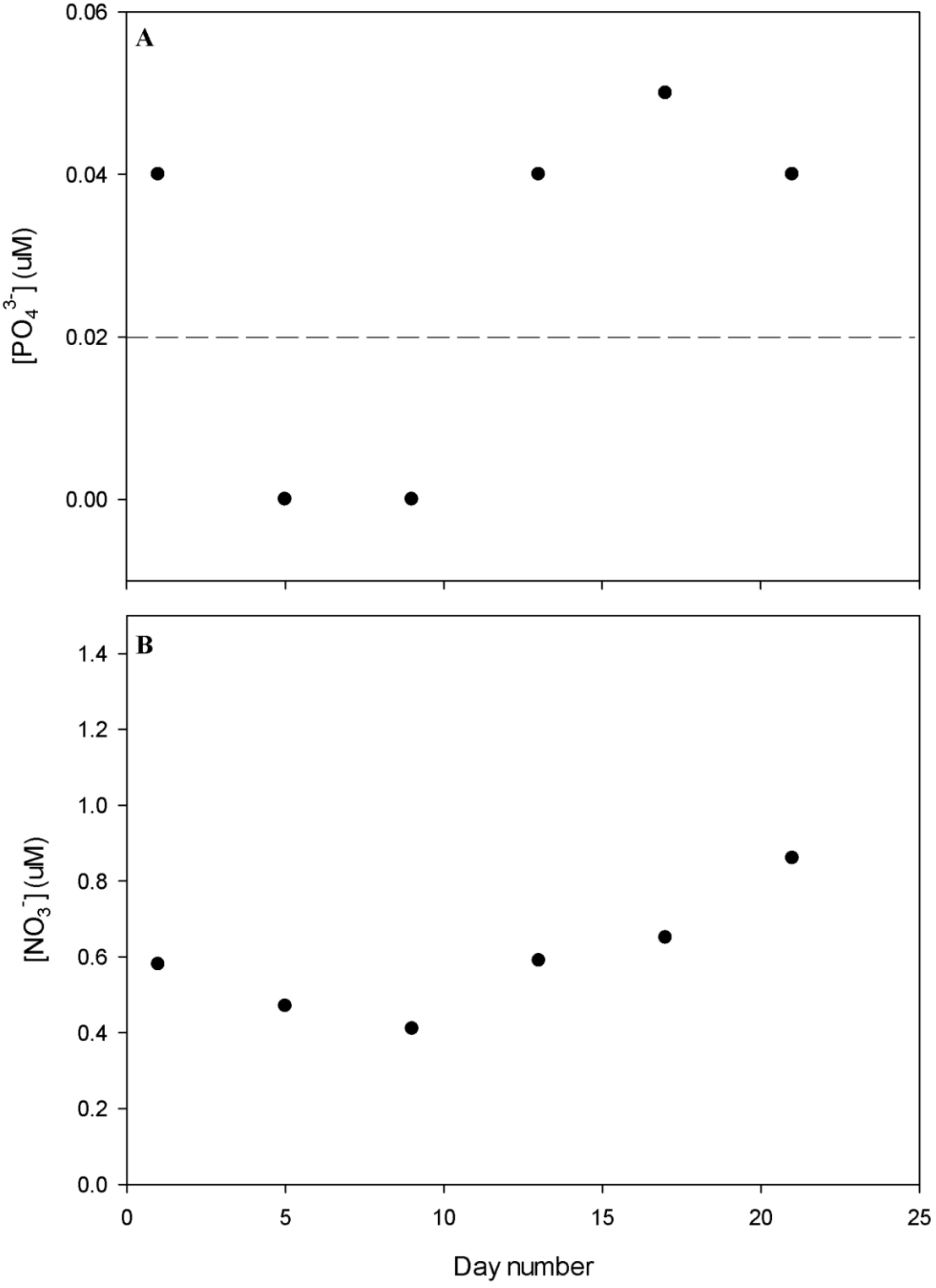

Fig. 3.3. Nutrient concentrations measured over the course of 21 days for experiments performed on *N. candelabrum* (Fig. 3.2). PO_4^{3-} and NO_3^- concentrations are shown for the LNSW treatment. Dashed line represents limit of detection.

3.4.3 Changes in cell growth properties over 30 days of exposure to NAGSW

In almost all embryo dishes cell numbers either remained the same or decreased before nutrients were added (Fig. 3.4). The longest time any single cell survived in NAGSW, and then went on to re-grow after addition of nutrients, was 26 days (Fig. 3.4). Motile cells were observed after 28 days, but none of these cells were able to re-establish growth when nutrients were added.

The percentage of viable cells decreased over the course of the experiment (Fig. 3.5A): between 1-10 days, the percentage of viable cells was 68 % (71/105 cells); this dropped to 40 % between day 11-20 (44/110 cells), and 3 % (2/64 cells) between day 21-30.

The time-lag between nutrient addition and the first sign of growth appearing generally increased over the course of the experiment (Fig. 3.5B): the time-lag was 2 days up until day 10; with the exception of day 13. From day 11 onwards the time-lag was always greater than 2 days (between 4-8 days).

Once growth did commence, the growth rate of cells appeared to be unaffected by the length of exposure to NAGSW (Fig. 3.5C). The mean growth rate (once time-lag had been accounted for) observed was 0.16 d^{-1} (range: 0.07-0.31 d^{-1}), and for most embryo dishes observed (12 out of 17) the growth rate was within a fairly narrow range of 0.11-0.19 d^{-1}. Although the lowest growth rate (0.07 d^{-1}) was observed on day 26, the growth rate just one day before (day 25) was close to the mean growth rate observed (0.15 d^{-1}).

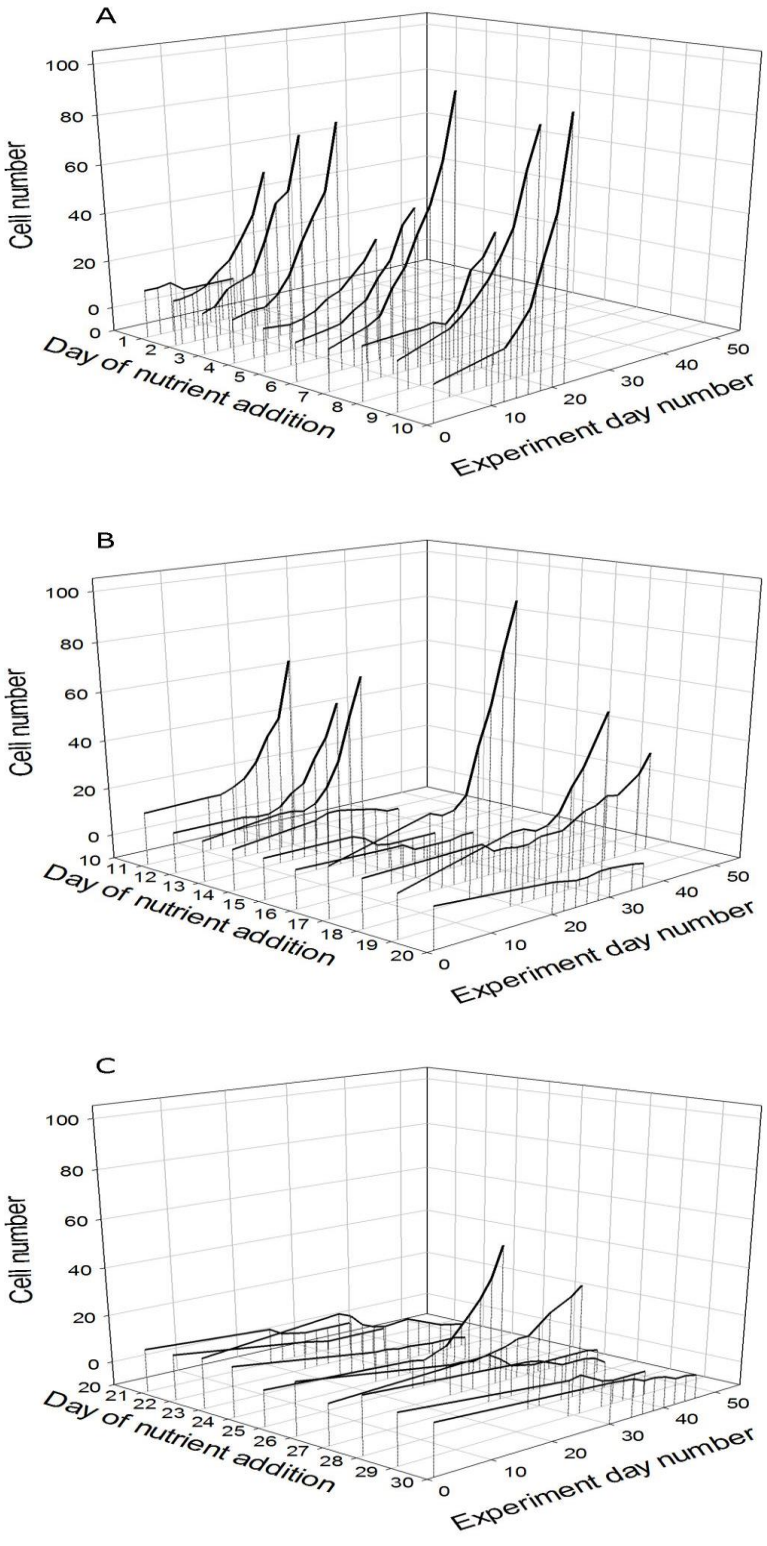

Fig. 3.4. Growth curves of *N. hexacanthum* demonstrating the effect of exposure to NAGSW for between 1 and 10 days (A), 11 and 20 days (B), and 21 and 30 days (C). Changes in cell number (y-axis) for each day of nutrient addition (z-axis, day 1-30) over the course of 50 days (x-axis) is shown. The second drop-line for each growth curve represents the point at which nutrients were added.

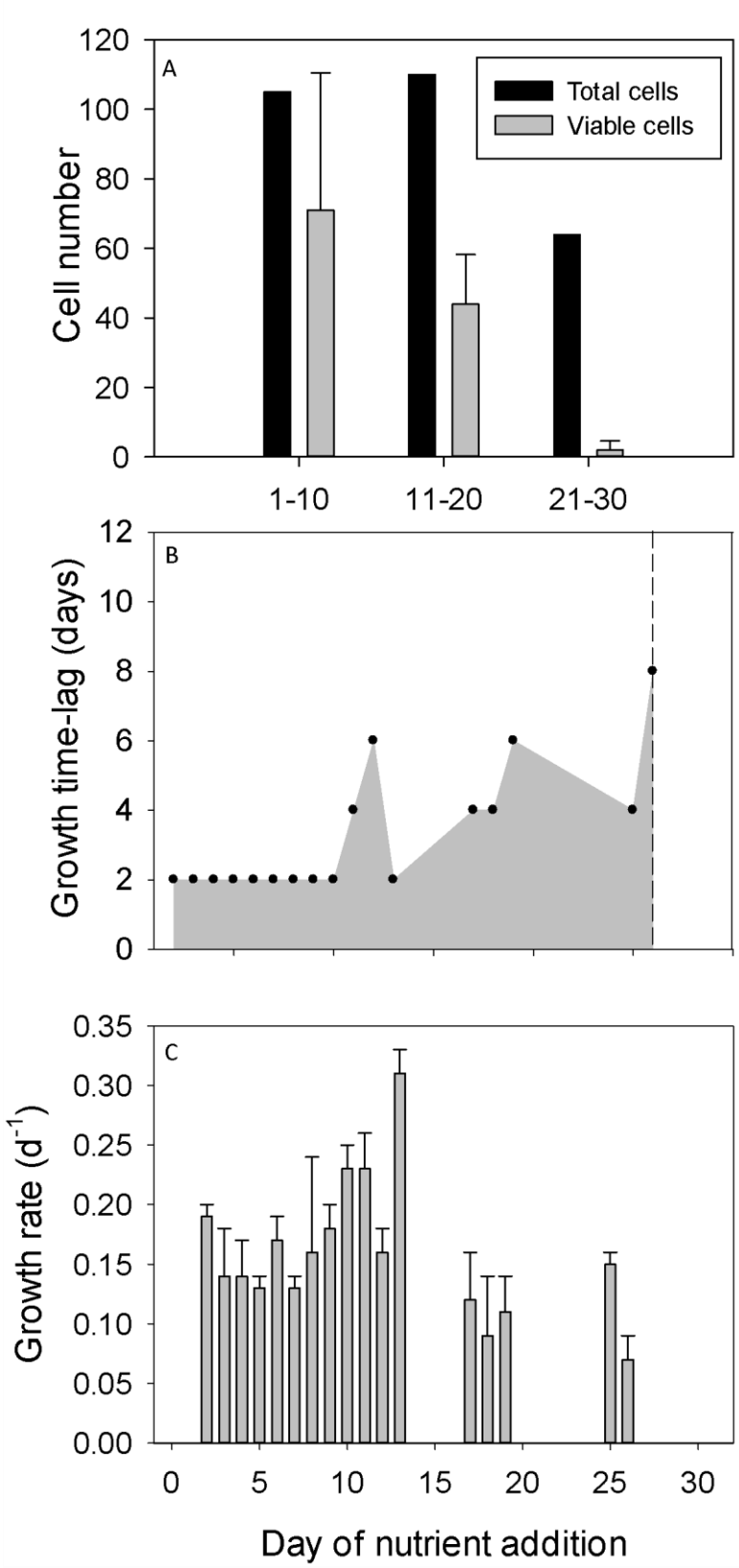

Fig. 3.5. Changes in the number of viable cells (A), time-lag in growth (B; dashed line represents maximum survival time), and growth rate (C) of *N. hexacanthum* cells exposed to NAGSW for 1-30 days. Error bars (A and C) represent the standard errors of estimates made.

3.5 Discussion

3.5.1 *Neoceratium* cell growth at low nutrient concentrations

Observations, on *N. hexacanthum* and *N. candelabrum*, revealed that ontogenetic growth (cell division) did not occur at the low nutrient concentrations used here (starting concentrations: NO_3^-, 0.58 µM; PO_4^{3-}, 0.04 µM), and cells became more nutrient stressed with time, as shownby decreasing *Fv/Fm* values. *Fv/Fm* worked differently as an indicator of "nutrient stress" in both species; the reduction in *Fv/Fm* was far more pronounced in *N. candelabrum*. An obvious explanation for why this occurred is not available, but considering all the parameters that were measured it appears that the "health" of both species did suffer under low nutrient concentrations. In addition to the absence of ontogenetic growth, the possibility that cells were slowly increasing in size (somatic growth), and therefore potentially dividing on timescales longer than the experimental period (21 days), is eliminated as average protein content per cell roughly halved over the course of the experiment in both species. This suggests that *Neoceratium* could not survive in OSGs if they were entirely dependent on the nutrient concentrations found in surface waters (above the nutricline), much less achieve the high growth rates (0.09-0.13 d^{-1}) that have been previously observed in the North Pacific subtropical gyre (Weiler, 1980).

N:P ratios were higher in the RSW than in LNSW (132:1 compared to 15:1), which may have enhanced the growth rate in the RSW treatment – *Neoceratium* has previously been shown to grow faster at higher N:P ratios (Baek et al., 2008). However, these differences in ratios would not account for why there was no growth at all in the LNSW, as there is no evidence that low N:P ratios prevent *Neoceratium* from growing (Baek et al. 2008a). Increases in swimming speed, sinking rate and turbulent shear can all reduce nutrient diffusion limitation in larger cells to some extent (Chisholm 1992). In this experimental set-up, which uses culture flasks, sinking rate and turbulent shear would have been negligible compared to the natural environment. However, it has been pointed out that these two factors could, at most, scarcely double nutrient uptake rates in a cell with a diameter of 200 µm (Chisholm, 1992). Therefore,

it seems unlikely that this factor would account for growth of *Neoceratium* in OSG surface waters. The possibility that, in the natural environment, *Neoceratium* exploit nutrient micropatches in OSG surface waters (Lehman and Scavia 1982) cannot be ruled out; here, *Neoceratium* cells may be able to take up nutrients at the same rate as smaller algal cells based on a recent suggestion that phytoplankton uptake rates are not dependent on cell size (Marañón et al. 2013). The uptake of dissolved organic nutrients may also provide an additional source of phosphorus and nitrogen to *Neoceratium* in OSGs. As these fractions are thought to turn over on time periods of minutes to days (Bronk et al. 2007) it is unlikely that the concentrations of these nutrients, in the experimental media used, were representative of concentrations found in the natural environment. It is known that *Neoceratium* produce the enzyme alkaline phosphatase, which may allow for the exploitation of dissolved organic phosphorus pools (Girault et al., 2013; Mackey et al., 2012). Until recently it was believed that the dissolved organic nitrogen pool was largely refractory and, therefore, unavailable to phytoplankton. However, a review by Bronk (2007) presents evidence that phytoplankton, and particularly some dinoflagellate species, may be able to access this pool – especially some of the more labile fractions such as urea, dissolved free amino acids and nucleic acids. In fact, data presented by Baek et al. (2008a) suggests that *Neoceratium* are able to use urea as a nitrogen source. It is clearly important to identify which dissolved organic nitrogen sources *Neoceratium*, and other phytoplankton, are able to utilise in order to determine what role they may play in controlling autotrophic production within OSGs.

3.5.2 *Neoceratium* survival time in oligotrophic seawater

Results from experiments on *N. hexacanthum* in embryo dishes containing NAGSW, where growth did not occur until the addition of nutrients, support the conclusion that cell growth is not possible at nutrient concentrations common in OSG surface waters. These experiments, however, did demonstrate that cells can potentially survive in OSG surface waters, and remain viable, for a long period of time (>3 weeks; Fig. 3.4). This survival time is consistent with the

measurements of *Fv/Fm* on *N. candelabrum*, which showed that after 21 days in LNSW the value for this parameter had fallen to almost zero, indicating severe nutrient stress. Few other studies have focussed on the long term survival of phytoplankton under oligotrophic conditions. However, one study on the dinoflagellate *Gymnodinium splendens* demonstrated that this species could survive for 65 days under oligotrophic conditions (Dodson and Thomas 1977) – nearly three times longer than *N. hexacanthum* in the present study. In addition to inter-specific nutrient tolerances between *Gymnodinium* and *Neoceratium*, this significantly longer survival time is probably the result of the higher nutrient concentrations that were used in that study (NO_3^-, 0.08 µM; PO_4^{3-}, 0.46 µM) compared to this one (NO_3^-, <0.02 µM; PO_4^{3-}, <0.02 µM). It is likely that this ability to survive long periods of time in the absence of sufficient nutrients may partly explain the success of *Neoceratium* in oligotrophic regions, and also, their success in stratified coastal regions during summer.

Due to the sampling resolution (2 days), time-lags in growth response, upon nutrient addition, could only be resolved within 2 day intervals. Even so, a clear pattern emerged. The time-lag in growth response increased beyond 10 days of exposure to NAGSW. This increase in time-lag is consistent with studies that have found the delay in growth response to be positively related to duration of nutrient "starvation", especially in species that are capable of storing nutrients internally. This is a strategy that is proposed to be ecologically advantageous in environments where nutrients are only encountered periodically (Collos 1986). Once cells began to grow, however, there did not appear to be a detrimental impact on growth rates. This suggests that the adverse effects of prolonged exposure to surface oligotrophic conditions, of greater than 10 days, do not persist once cells overcome the initial delay in growth.

There are several important implications of these findings. *Neoceratium* cells must periodically access an external source of nutrients in order to survive and grow in surface waters of OSGs. To maintain a healthy population in a steady state of growth this nutrient source would ideally need to be accessed, at most, every 10 days, but could be accessed over a longer timescale (10-20 days) whilst still allowing for a relatively high chance (~40%) of survival. Under extreme circumstances, a small number of cells (~3%) could survive nutrient

starvation for longer than 20 days, enabling a "seed population" to survive. In the long-term, however, this strategy would not be ecologically successful as cell losses would be too high to maintain a population.

3.5.3 Possible sources of nutrients for *Neoceratium*

In the final part of this chapter, possible mechanisms by which *Neoceratium* may encounter nutrients periodically in OSGs are discussed. Karl (1999) identified at least four physical mechanisms that can increase phytoplankton productivity by introducing nutrients into surface waters of subtropical gyres: internal waves and tides, cyclonic mesoscale eddies, wind-driven Ekman pumping, and atmospheric storms. Of these four physical mechanisms, mesoscale eddies occur in the most predictable manner, and the increase in nutrient concentrations associated with these events would appear to be great enough to support the growth of *Neoceratium* (McGillicuddy and Robinson 1997; Baek et al. 2007, 2008a). These events alone, occurring approximately once per month in the Sargasso Sea (Siegel et al. 1999) and in the North Pacific subtropical gyre (Johnson et al. 2010), would be almost sufficient to enable *Neoceratium* to survive via periodic nutrient exposure. It is worth considering, however, that the nutrient concentrations used (nitrate: 185 µM) to "recover" nutrient deprived cells had much higher concentrations of nitrate and phosphate than would be found at the nutricline in OSGs (nitrate: no more than 5-10 µM) (Moore et al., 2013), and therefore may not provide a completely accurate proxy for how *Neoceratium* react when exposed to these waters. For example, a study by Baek et al. (2008a) on *N. fusus* and *N.furca* showed that although growth rates peak at 5 µM of nitrate, with additional increases making no difference to how fast cells divide, nutrient uptake rates continue to increase even when growth rates have plateaued; a finding that was interpreted by these authors as *Neoceratium* storing excess nutrients in vacuoles.

Another strategy may be to obtain nutrients via phagotrophy: a tactic that is thought to be widespread amongst small eukaryotic algae (<5µm) in the OSGs of the Atlantic Ocean (Zubkov and Tarran 2008; Hartmann et al. 2011, 2012), and one thought to be used by a number of *Neoceratium* species, which commonly feed on ciliate prey (Bockstahler and Coats 1993b; Li et al. 1996;

Smalley et al. 1999, 2003, 2012; Smalley and Coats 2002). Some important questions here would be: how much prey would *Neoceratium* need to ingest in order to obtain sufficient nutrients for survival and growth, and whether encounter rates with prey species are high enough to support this method of nutrient acquisition (these questions are discussed in chapter 4).

Finally, vertical advection and vertical migration are likely to play a role in obtaining nutrients. Vertical advection, aided by turbulent mesoscale eddies, internal waves and Langmuir cells, is capable of transporting cells tens of metres over a period of a few hours (Denman and Gargett 1983), and may transport *Neoceratium* cells to the nutricline – or at least close to the nutricline, where vertical migration may become important. Villareal and Lipschultz (1995) have previously suggested that all large phytoplankton (>100 µm) in the Sargasso Sea are capable of vertical migration, and that they use this mechanism to acquire nutrients from the nutricline. A number of studies indicate that *Neoceratium* undergo cell division at depth around dawn (Weiler and Chisholm 1976; Weiler and Eppley 1979; Baek et al. 2009), followed by upward migration before the transition from dark to light, with downward migration occurring before dusk.

3.6 Conclusion

This study demonstrates that *Neoeceratium* cells are unable to grow phototrophically at low nutrient concentrations representative of surface waters in OSGs. Nevertheless, cells can survive and remain viable for over 3 weeks, suggesting that the presence of *Neoceratium* in OSGs may be explained by them enduring long periods in surface waters above the nutricline, with periodic exploitation of alternative nutrient sources. Ephemeral upwelling of nutrients, mixotrophy, vertical migration and /or passive advection to the nutricline appear to be the most feasible mechanisms by which nutrients may be obtained. In the next two chapters of this thesis the potential roles of mixotrophy and vertical migration are considered.

4. Mixotrophy and its potential role in nutrient acquisition for *Neoceratium* in oligotrophic subtropical gyres

4.1 Abstract

Some species of *Neoceratium* are capable of mixotrophy when intracellular nutrient concentrations are altered by nutrient limitation (N or P). This behaviour would confer an advantage to *Neoceratium* in oligotrophic subtropical gyres (OSGs) as it would provide a major source of nutrients. Here, attempts to observe feeding in *N. hexacanthum, N. candelabrum, N. horridum* and *N. tripos* were unsuccessful, although possible food vacuoles were observed in cells collected from the North and South OSGs onboard AMT 20. Using previously published data, combined with some data discussed previously in the thesis, it is demonstrated that nutrient ratios in large areas of Atlantic OSGs surface waters are favourable to mixotrophy (86 % of sites in the North and South Atlantic OSGs). Based on changes in cellular protein concentrations (from Chapter 2), it is estimated that 0.01 to 0.44 ciliates day^{-1} would need to be ingested for *Neoceratium* to survive in OSGs. Ingestion rates from a previous study on *N. furca*, under a range of prey concentrations, are used to estimate that, at typical prey concentration ranges found in the OSGs, 0.002 to 0.053 ciliates d^{-1} would typically be consumed, which is at the lower range required for survival and growth. Therefore, mixotrophy is likely to be an important source of nutrients for *Neoceratium* in OSGs but probably does not account, on its own, for their widespread presence in these environments.

4.2 Introduction

It has been suggested that *Neoceratium* supplement their nutrient requirements via phagotrophy (Weiler 1980): a strategy that is thought to be widespread amongst small eukaryotic algae (<5µm) in the oligotrophic subtropical gyres (OSGs) of the Atlantic Ocean (Zubkov and Tarran 2008; Hartmann et al. 2011, 2012). The predominantly coastal species *Neoceratium furca* (Matrai 1986) has been shown to primarily ingest ciliates (Bockstahler and Coats 1993b; Li et al. 1996; Smalley et al. 1999, 2003, 2012; Smalley and Coats 2002), via direct engulfment of prey when nutrients (N or P) are limited – more specifically, when intracellular ratios of C:N:P are altered by nutrient limitation (Smalley et al. 2003, 2012). There is also non-conclusive evidence (observations of inclusion bodies that are speculated to be food vacuoles or prey) for mixotrophy in *N. declineatum*, *N. fusus*, *N. longipes*, *N. lunula*, *N. teres*, *N. balechii* and the freshwater species *C. hirundinella*, (Norris 1969; Chang and Carpenter 1994; Jacobson and Anderson 1996; Callieri et al. 2006; Mackey et al. 2012). Additionally, it has been suggested that mechanical stimulation of the flagella, causing the contraction-relaxation cycle of the various structures, may trap food particles between the folds of the flagellar membrane, which would be subsequently carried into the flagellar pocket (diameter of ~6 µm) and then towards the mouthpart, or cytostome (Cachon et al. 1991). This may allow *Neoceratium* cells to feed on cyanobacteria such as *Synechococcus*. In freshwater ecosystems *Synechococcus* has been shown to be strongly associated with *Ceratium hirundinella*, suggesting a predator-prey relationship (Callieri et al. 2006). In the same study *Synechococcus* was found in the vacuole of *C. hirundinella* in a sample from late summer, when nutrient concentrations are typically depleted.

Here the ability of two *Neoceratium* species (*N. hexacanthum, N. candelabrum*) to feed via direct engulfment is investigated, on laboratory grown cultures of *Rhodomonas marina*; the ability of *N. tripos* to feed on *Mesodinium rubrum* is also tested. In both of these experiments, this is achieved by observing whether cells can grow following the addition of the prey under nutrient-depleted conditions, and by trying to observe ingested prey using

epifluorescence microscopy. Also investigated is the potential of three *Neoceratium* species (*N. hexacanthum*, *N. candelabrum* and *N. horridum*) to feed via contraction of the flagellar into the flagellar pocket by using epifluorescence microscopy to look for ingested fluorescent microbeads and *Synechococcus* cells (see appendix 2 for a summary of the different experimental designs: *Neoceratium*/prey species, nutrient conditions etc.). Samples collected from the North and South Atlantic subtropical gyres during Atlantic Meridional Transect (AMT) 20 (October to November 2010) are also visually analysed for signs of mixotrophy. This chapter concludes with a review of what is known regarding *Neoceratium* mixotrophy. Previously published data is used in conjunction with data from chapters 2 and 3 in order to examine the likely contribution of mixotrophy to *Neoceratium* nutrition in OSGs.

4.3 Method

4.3.1 Isolation and culture of *N. tripos*

N. tripos cells were collected from Station L4, off the coast of Plymouth UK (50˚ 15.00' N, 4˚ 13.02' W) during August 2012, using a plankton net (mesh size 120 µm). All other *Neoceratium* species (*N. hexacanthum*, *N. candelabrum*, *N. horridum*) were obtained from culture collections (Appendix 3). The reason *N. tripos* was "newly isolated" was due to concerns that species cultured for long periods may have lost their ability to feed, having spent many generations growing autotrophically (P.J. Hansen, University of Copenhagen, Personal Communication). Individual cells were initially isolated into Embryo dishes containing K/5 medium and incubated at 60 µmol quanta m^{-2} s^{-1} on a 12:12 light/dark cycle, replicating conditions cells would have been exposed to *in situ*. Once over one hundred cells were present in the embryo dish they were transferred to 20 ml Erlenmeyer flasks, and then to 50 ml Erlenmeyer flasks.

4.3.2 Isolation and culture of potential prey organisms

All cultures (see Appendix 3 for further details) were incubated on a 12:12 light/dark cycle at 18ºC with a photon flux of 60 µmol quanta m^{-2} s^{-1}. *Synechococcus* was cultured in 50 ml Nunc plastic culture flasks containing K/5 media. *R. marina* and *Isochrysis galbana* were cultured in 25 ml Erlenmeyer flasks containing F/20 media. *M. rubrum* was cultured in 50 ml Nunc plastic culture flasks in K/5 media; once a week 1 ml of *Teleaulax spp.* (cultured under the same conditions as *M. rubrum* but in 25 ml Erlenmeyer flasks) was added to *M. rubrum* which rely on the chloroplasts from this prey organism for photosynthesis and survival (Hansen and Fenchel 2006). Tintinnids, *Strobilidium* spp. and *M. rubrum* were also isolated from Southampton Water using a plankton net (20 µm-mesh size), and used for qualitative attempts to observe feeding (Section 4.3.2).

4.3.3 Initial qualitative attempts to observe feeding

N. hexacanthum, *N. horridum,* and *N. candelabrum* were transferred to oligotrophic seawater for 11 days in order to deplete cells of nutrients, as in previous observations with *N. furca*, ingestion rates have been demonstrated to be increased by nutrient limitation (Smalley et al. 2003). 5 to 10 cells of each *Neoceratium* spp. were then transferred, using a 10 µl micropipette, to a drop of NAG seawater on a Sedgewick-Rafter chamber containing a variety different potential prey organisms (tintinnids, *Strobilidium* spp., *Mesodinium rubrum*, and *Isochrysis galbana*). Observations were made over approximately a two hour time period.

4.3.4 Feeding on *Rhodomonas marina*

Experiments were conducted in 50 ml conical flasks, using 20 ml of Nutricline seawater (NUSW; Table 3.1). *N. hexacanthum* and *N. candelabrum* were added to flasks to provide final concentrations of ~10 to 30 cells ml^{-1}. 5ml of *R. marina* (grown in F/20 medium) was added to half of the flasks, providing a final concentration of ~15 to 20,000 cells ml^{-1}. To the other flasks, used as controls, 5 ml of *R. marina* medium (filtered through a 0.2 µm Millipore filter) was added. Each experiment was performed in duplicate. Experiments were incubated at 18°C on a 12:12 light/dark cycle. Cell numbers (*Neoceratium spp.* and *R.marina)* were determined every four days (for 28 days) via enumeration of 1 ml of culture in a 1 ml plastic Sedgewick-Rafter chamber, under an inverted microscope.

On day 28 the remaining culture media (~10 ml) was collected on a 20 µm filter and rinsed with 10 ml of filtered seawater to remove *R. marina*. *Neoceratium* cells were then washed onto, and filtered through, a 0.2 µm black PC filter. The filter was mounted on a slide and immersion oil was added so that both sides were covered. The slide was examined using epifluoresence

microscopy, under ultraviolet and blue/green excitation, in order to identify any ingested *R. marina* cells, which emit orange fluorescence when exposed to blue/green light.

4.3.5 Feeding on *Mesodinium rubrum*

N. tripos cells were reverse filtered through a 20 µM nylon filter with filtered North Atlantic gyre seawater (NAGSW; Table 3.1) in order to remove excess nutrients. Cells suspended in NAGSW were then split equally between 6 flasks and topped up with 40 ml of K/75 medium. After nutrients had become depleted – determined from the point when cell division ceased – cultures were further diluted by removing 20 ml of culture and adding 40 ml of NAGSW. Cells were then monitored for a number of days to make sure no growth was occurring. *M. rubrum* from cultures (reverse filtered through a 10 µM nylon filter) were added to half the flasks to provide final concentrations of ~50 to 200 cells per ml. To the other half of flasks (used as controls), the same volume of *M. rubrum* was filtered through a 0.2 µM milipore filter to remove prey before addition to flasks. Changes in the numbers of *N. tripos* and *M. rubrum* were then monitored for 11 days (1 ml counts using a plastic Sedgewick-Rafter chamber). 24 hours after prey addition, cells were washed onto, and filtered through, a 0.2 µm black polycarbonate (PC) filter. The filter was mounted on a slide and immersion oil was added so that both sides were covered. The slide was examined using epifluoresence microscopy, using ultraviolet and blue/green excitation, in order to identify any ingested *M. rubrum*, which emits orange fluorescence when exposed to green light.

4.3.6 Feeding on fluorescent microbeads

N. horridum, *N. hexacanthum*, and *N. candelabrum* containing culture media were collected on a 20 µm filter and rinsed with 6 ml of filtered North Atlantic gyre seawater (NAGSW; Table 3.1), using a pipette, in order to remove excess nutrients. Cells collected on the filter were then rinsed into a 50 ml conical

flask (acid washed and autoclaved) with 6 ml of nutricline seawater (NUSW; Table 3.1). After gentle agitation, to evenly distribute the cells, 3 ml was transferred to another 50 ml conical flask: to one flask, 1 ml of 0.5 µm fluorescent microbeads (~1,000,000 beads per ml) was added; to the other, 1 ml of 3 µm beads was added (~1,000,000 beads per ml). Each flask was then topped up to 47 ml with NUSW media to give final bead concentrations of approximately 20,000 beads ml^{-1} and final *Neoceratium* concentrations of 30 to 50 cells ml^{-1}. Experiments were incubated at 18°C on a 12:12 light/dark cycle.

Every five days [starting on day 0, where a subsample of cells were fixed with paraformaldehyde (PFA) prior to bead addition], 5 ml of medium was collected on a 20 µm filter and rinsed with 10 ml of filtered seawater to remove beads. *Neoceratium* cells were then washed onto a 0.2 µm black PC filter. The filter was mounted on a slide and immersion oil was added. The slide was examined using epifluoresence microscopy, using ultraviolet and blue excitation, in order to identify any ingested beads. For the first 50 cells encountered, the number of cells appearing to contain beads (and the number of beads present) was recorded.

4.3.7 Feeding on *Synecococcus*

In order to maximise the visibility of any *Synechococcus* cells ingested by *Neoceratium*, experiments were carried out to find the optimum concentration of ethanol for reducing chlorophyll fluorescence (red), while leaving phycoerythrin (orange) in *Synechococcus* unaffected. Cells were filtered onto a 0.2 µm black polycarbonate filter and, before being mounted on slides in preparation for epifluorescence microscopy using UV and blue excitation, were either left untreated (Fig. 4.1A), rinsed for 30 seconds with 10 % (Fig. 4.1B), 20 % (Fig. 4.1C), 30 % (Fig. 4.1D), or 40 % ethanol (Fig. 4.1E). After rinsing with ethanol, cells were rinsed again with filtered seawater to remove any traces of ethanol. The optimum concentration for reducing chlorophyll fluorescence while maintaining the resolution of the cell was 30 % (Fig. 4.1D). Phycoerythrin

fluorescence was largely unaffected by the ethanol treatment at concentrations of up to 40 % (Fig. 4.1F-G).

N. hexacanthum were transferred to a petri-dish containing K/5 medium (minus phosphate) and incubated at 18°C on a 12:12 light/dark cycle. After 15 days 1 ml of this medium was transferred into a well plate (12 mm) containing 2.5 ml of *Synechococcus* (transferred from culture medium into filtered oligotrophic seawater); a second well plate containing *N. hexacanthum* only (no *Synechococcus*) was set up as a control. Cells were incubated for 24 hrs on a 12:12 light/dark cycle and then fixed with paraformaldehyde (PFA) (final concentration 1 %). Cells were filtered onto a 20 µm filter, rinsed with 5 ml of filtered (0.2 µm Milipore filter) oligotrophic seawater in order to remove free *Synechococcus*, and then rinsed into a Petri dish. Following this cells were collected on a 0.2 µm black polycarbonate filter. The filter was mounted on a glass slide and immersion oil was added so that both sides were covered. The slide was examined using epifluoresence microscopy, with ultraviolet and blue/green excitation in order to identify any *Synechococcus* cells that had been ingested by *Neoceratium* (50 cells examined). *Synechococcus*, if ingested, would be visible as orange fluorescent spheres within the protoplasm of *Neoceratium* cells (Jeong et al. 2005, Apple et al. 2011).

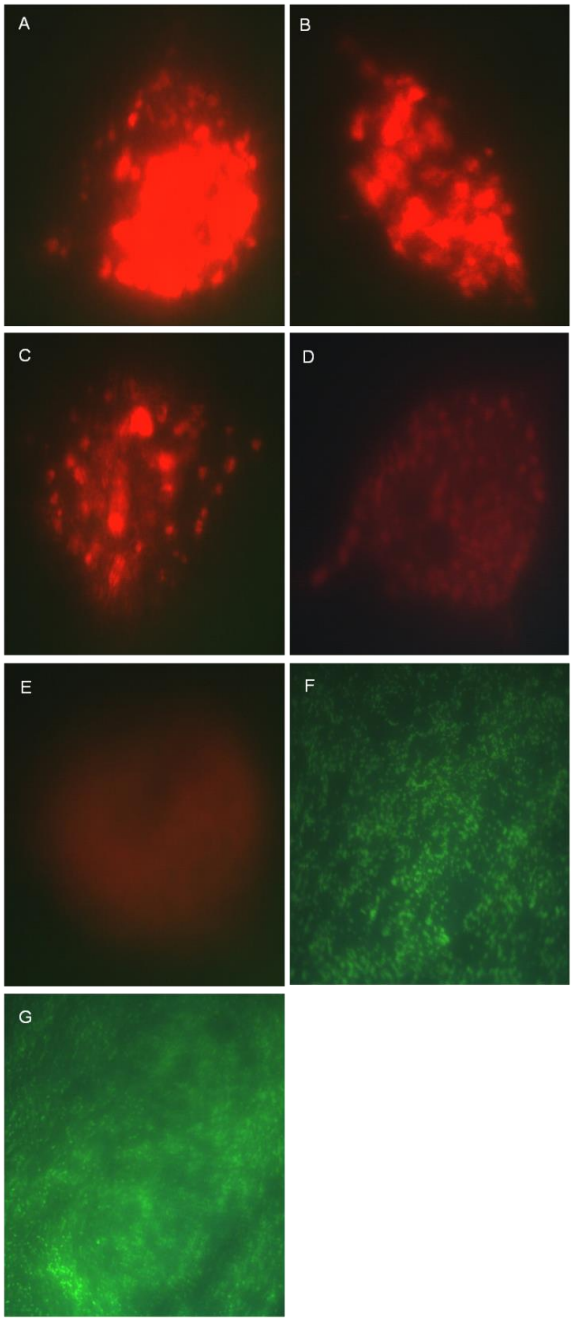

Fig. 4.1. Effect of ethanol on the fluorescence of *N. hexacanthum* and *Synechococcus*. A-E, Single cells of *N. hexacanthum* exposed to a number of different concentrations of ethanol for 30 seconds: (A) untreated, (B) 10 %, (C) 20 %, (D) 30 %, and (E) 40 %. *Synechococcus* (which appeared orange through the microscope eyepiece, but green when photographed) is shown untreated (F) and exposed to 40% ethanol (G). All images are at x670 magnification.

4.3.8 AMT samples

During AMT 20, between October 18th and November 15th 2010, samples were collected, at various locations in the Atlantic Ocean (Chapter 2), using an 11m long size-fractionating microzooplankton net, with an opening of 18 cm (diameter). The net was deployed vertically to 100 metres in the water column and then slowly raised to the surface at approximately 10 m $minute^{-1}$, filtering approximately 2835 L of seawater. Size fractions collected were 20 µm, 40 µm, and 100 µm. Live samples were analysed under a dissecting microscope within 4 hours of collection and *Neoceratium* cells were photographed using a hand-held camera (Fujifilm XP).

4.4 Results

4.4.1 Initial qualitative attempts to observe feeding

N. hexacanthum, *N. horridum,* and *N. candelabrum* showed no ability to catch or capture larger prey items (tintinnids, *Strobilidium* spp., or *Mesodinium rubrum*), nor did the ingestion of the smaller algae species, *Isochrysis galbana*, occur. However, two potential feeding strategies that may be used for smaller prey items were observed: beating of the longitudinal flagella generated what could potentially be a feeding current from the apical to antapical end of the cell, and the longitudinal flagella was occasionally extended and then rapidly withdrawn into the flagellar pocket.

4.4.2 Attempts to observe ingestion of *R. marina*

In all three species examined there was no positive growth of *Neoceratium* when cultured with *R. marina* (Fig. 4.2A-C), which itself displayed positive growth rates before declining in abundance beyond day 9 of the experiment. This contrasts with positive growth in the controls for *N. hexacanthum* and *N. candelabrum*.

On day 28, the remaining culture media (~10 ml) was examined using epifluoresence microscopy, under ultraviolet and blue/green excitation, in order to identify any ingested prey (orange fluorescence; Fig. 4.2E), within *Neoceratium* cells (red fluorescence; Fig. 4.2C-D). Between 20 and 72 cells were examined and, although a number of *R. marina* cells were observed on the slide, none were observed inside cells of *Neoceratium* (Table 4.1).

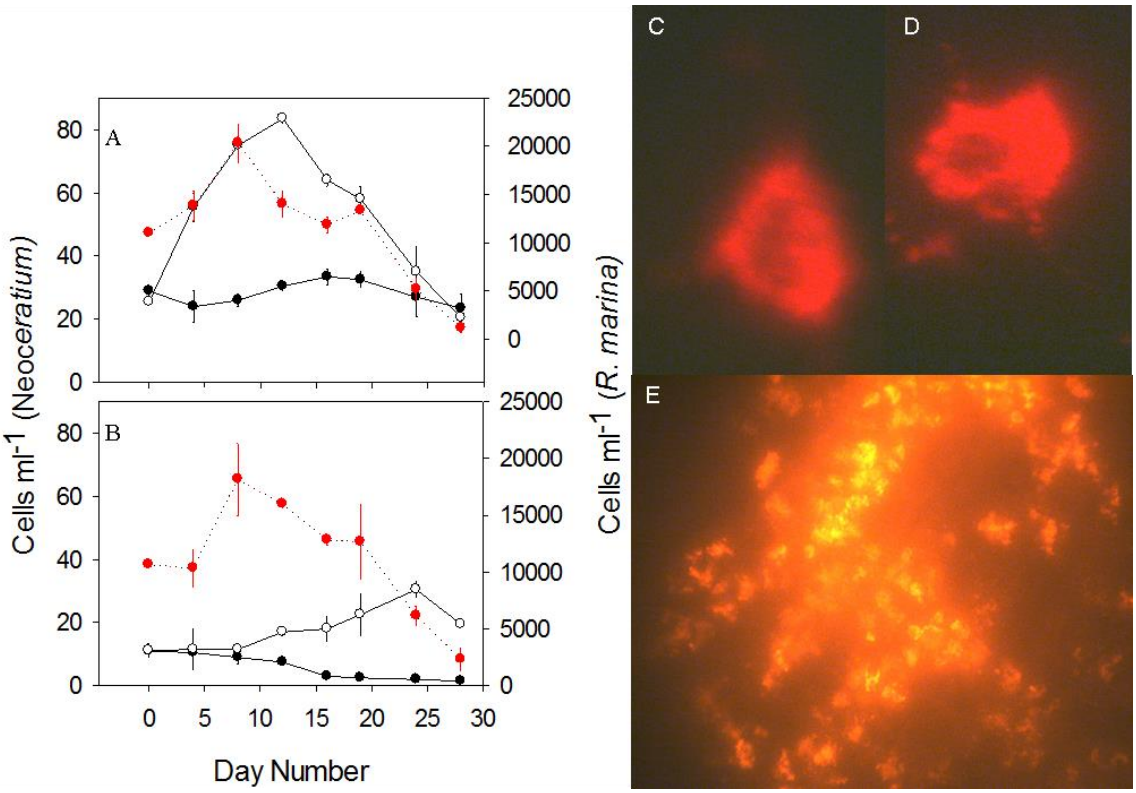

Fig. 4. 2 . Feeding experiments where *N. hexacanthum* (A) *and N. candelabrum* (B) were grown in the presence (filled black circles) and absence (hollow black circles) of *R. marina* prey (red filled circles) in F/20 culture medium. Error bars represent the standard error of duplicate experimental flasks. On day 28, epifluoresence microscopy was used to determine if *N. hexacanthum* (C) or *N. candelabrum* (D) ingested *R. marina*, which fluoresces orange under green excitation (E). No ingested prey were observed (between 20 and 72 cells of each species were counted). Image magnification = x400.

Table 4.1. The number of *Neoceratium* cells observed for each species using epifluorescence microscopy and the number of ingested *R. marina* prey.

	Number of cells observed	Number of cells containing *R. marina*
N. hexacanthum	72	0
N. horridum	28	0
N. candelabrum	20	0

4.4.3 Feeding on *Mesodinium rubrum*

N. tripos cells initially increased under both experimental and control conditions (Fig. 4.3): from ~50 to 150 cells per ml between day 1 and 6. From day 6 to 9 cell numbers remained constant under both conditions. After further dilution with NAGSW on day 9, cells numbers remained below 50 cells per ml until day 26. In the experimental treatment, this pattern was observed even after the addition of *M. rubrum* (on day 13 and 20). However, *M. rubrum* numbers did decrease rapidly once added to the experimental flasks (Fig. 3B). Examination of *N.tripos* cells under an epifluorescence microscope, following *M.rubrum* addition (24 hours), revealed that, although present and visible on the slide (Fig. 4.4), no *M. rubrum* had been ingested by *N. tripos* (> 50 cells examined).

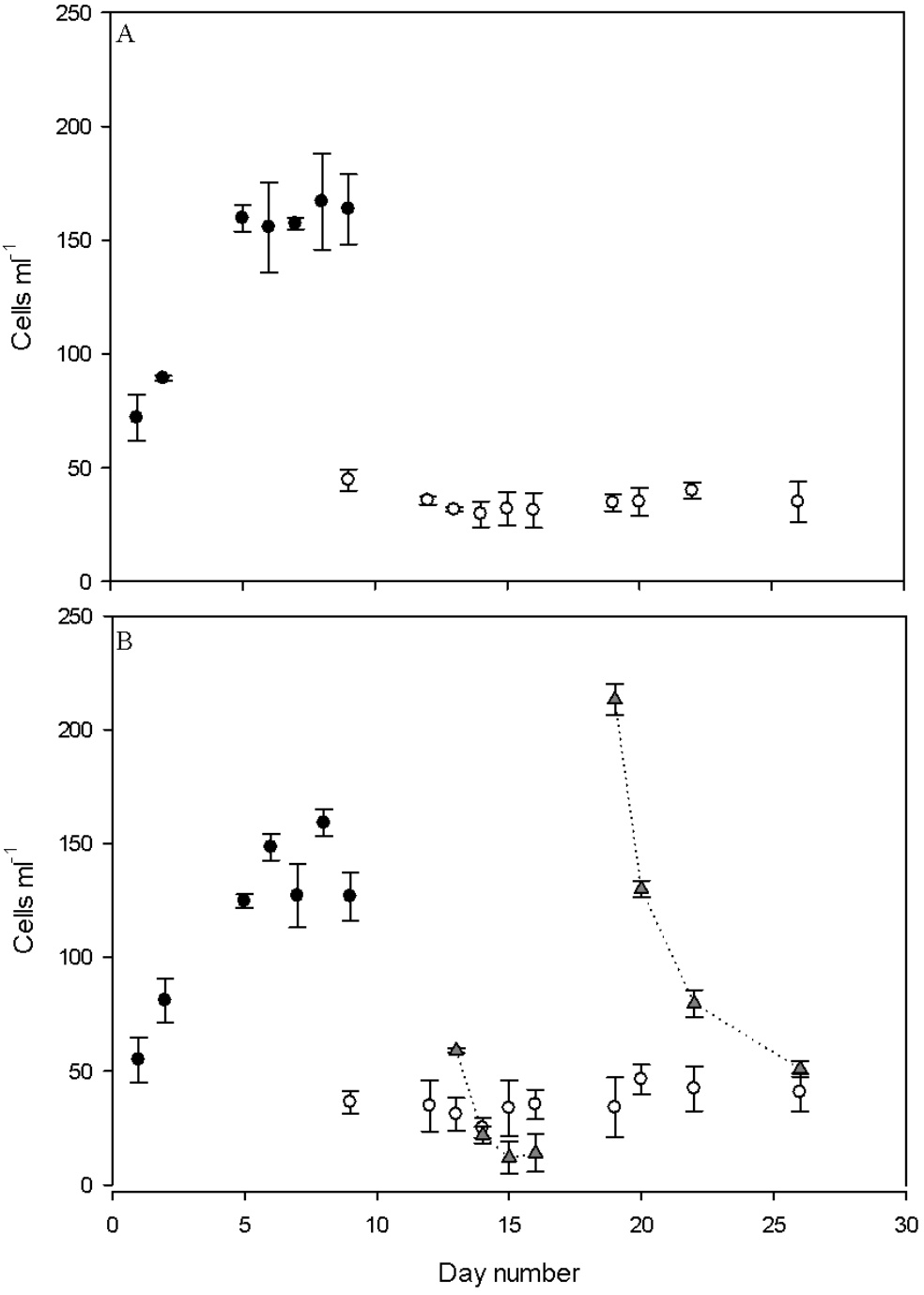

Fig. 4. 3. Changes in *N. tripos* cell numbers cultured under low nutrient concentrations for 26 days in the absence (A) and presence (B) of *M. rubrum*. Cells were initially cultured with K/75 medium (filled circles), which was then diluted with NAGSW (clear circles) once growth had stopped. *M. rubrum* were added to the experimental treatment (B) on day 13 and 20 (filled triangles).

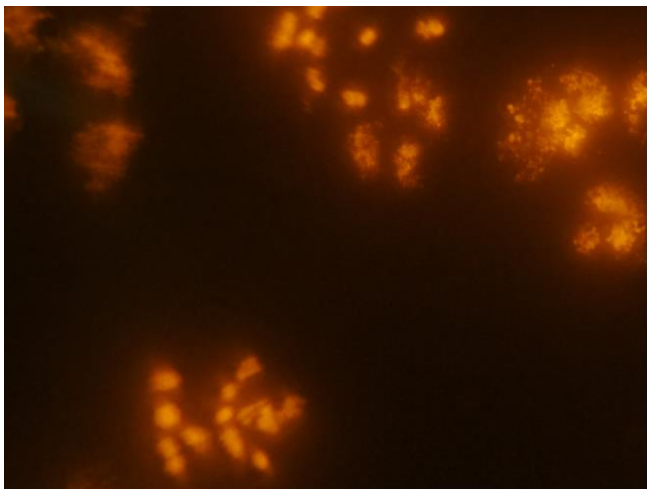

Fig. 4.4. Orange auto-fluorescence of *M.rubrum* when excited with green light using epifluorescence microscopy. Image magnification = x400.

4.4.4 Attempts to observe ingestion of fluorescent microbeads

A small number of beads were observed under the epifluoresence microscope associated with *N. hexacanthum, N. horridum* and *N. candelabrum* (Fig. 4.5). However, as beads were also observed associated with cells fixed with PFA (Fig. 4.6), prior to addition of the beads (day 0), it is clear that the rinsing of beads from the cells was not 100 % effective (a fact re-enforced by higher abundances of the smaller, more adhesive 0.5 µm beads associated with the cells). By comparing the number of beads appearing to be 'ingested' on day 0 with the number that occurred on days 5, 10, 15, and 20 it is possible to infer whether microbeads were ingested during the experiment (Fig 4.6). As the number of 'ingested' beads does not appear to increase throughout the experiment, it seems unlikely that ingestion of beads (0.5 µm or 3 µm) occurred.

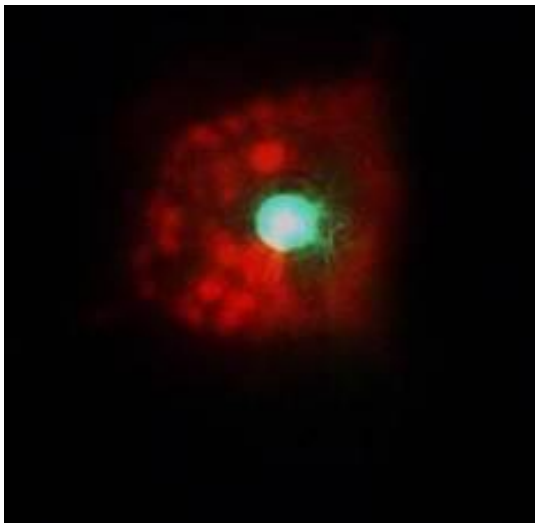

Fig. 4.5. *N. hexacanthum* associated with a fluorescent microbead. Image magnification = x670.

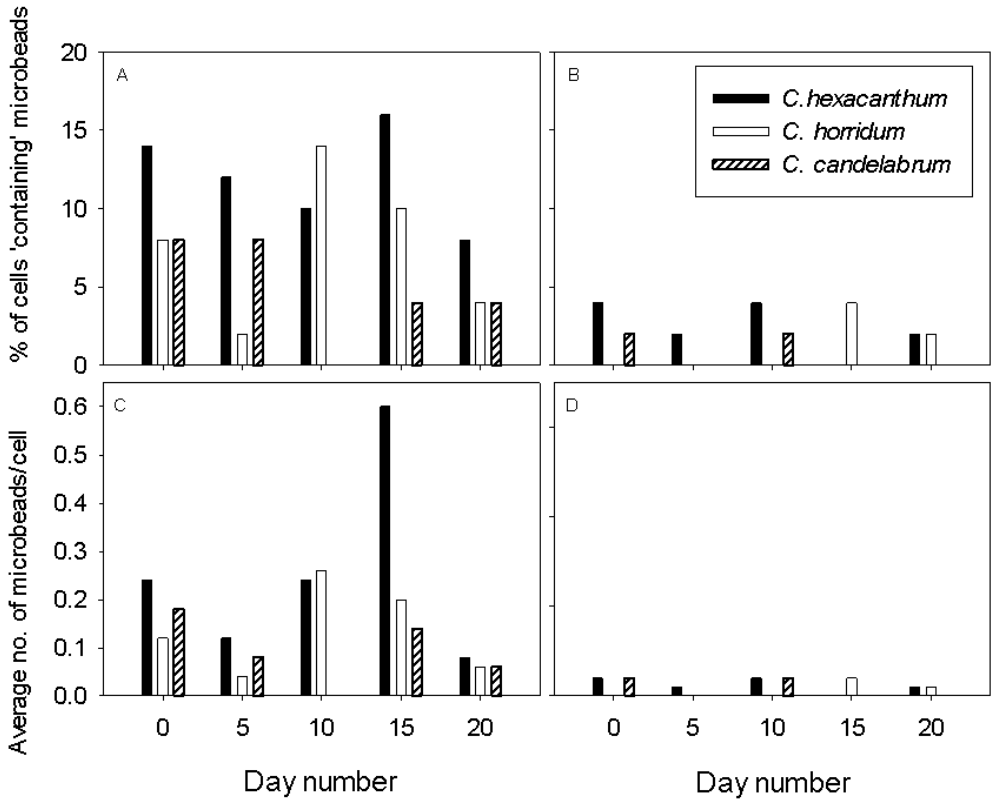

Fig. 4. 6 . The percentage of *N. hexacanthum*, *N. horridum*, and *N. candelabrum* cells appearing to contain fluorescent microbeads of 0.5 µm (a) and 3 µm (b) size, and the average number of microbeads observed per cell that were 0.5 µm (c) and 3 µm (d). All numbers are based on epifluoresent microscopy counts of 50 cells for each species. Day 0 numbers were obtained following addition of microbeads added to cells fixed with PFA.

4.4.5 Feeding on *Synechococcus*

Synechococcus cells were observed associated with *N. hexacanthum* (10 out of 50 cells, 3-6 *Synechococcus* cells per *N. hexacanthum* cell), but appeared "stuck" to the outside of *Neoceratium* cells, rather than ingested. It was not possible to obtain pictures of this using the integrated (or hand-held) camera as the camera was not sensitive enough to pick up the orange fluorescence emitted from *Synechococcus*.

4.4.6 AMT samples

A number of photographs of *Neoceratium* cells obtained during AMT 20 in 2010, from the North and South Atlantic subtropical gyres, appeared to show cells with inclusions that could be interpreted as being food vacuoles (Fig. 4.7A-F), and a few cells that appeared to be in the process of ingesting prey (Fig. 4.7E,G).

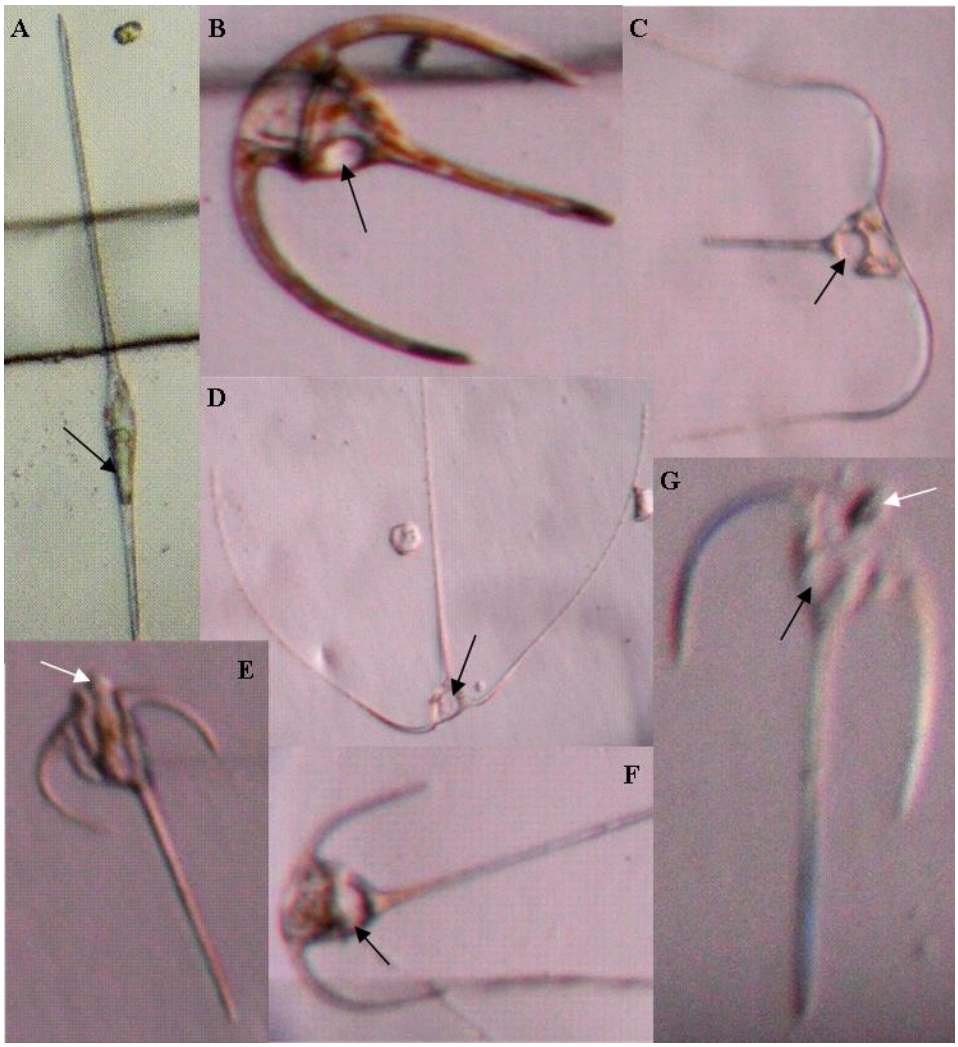

Fig. 4.7. *Neoceratium* cells, collected during AMT 20 in the North and South Atlantic subtropical gyres, showing cells that appear to contain food vacuoles (black arrows), and/or appear to be ingesting prey (white arrows).

4.5 Discussion

4.5.1 Experiments to observe mixotrophy

Neoceratium are likely to feed on prey either by inadvertently trapping small organisms (<6 µm) in their flagella pocket, following mechanical stimulation and subsequent retraction of their longitudinal flagellum, as suggested by Cachon et al. (1991, 1992); and/or by direct engulfment of larger prey organisms (between 10 and 40 µm) through the sulcus, as is suggested for *N. furca* (Smalley et al., 1999, 2003; Smalley and Coats, 2002).

The experimental design used here attempted to investigate whether these potential methods of feeding were utilised. No convincing evidence was found to suggest that these four *Neoceratium* species were ingesting any of the potential prey items: no feeding was seen when *Neoceratium* were observed in the presence of a variety of potential prey species (including *Strobilidium* spp., *R. marina, Mesodinium rubrum*, *Isochrysis galbana* and tintinnids). Following exposure to fluorescent microbeads (3 and 0.5 µm) and *Synecochoccus*, no ingested particles were seen under epifluorecent microscopic observation; and all three species, grown in the presence of *R. marina*, exhibited little growth when compared to prey-free controls, suggesting that *Neoceratium* growth in experimental flasks was inhibited, likely due to *R. marina* outcompeting them for inorganic nutrients – an observation that was reinforced by the fact that *R. marina* concentrations approximately doubled in all experiments up until about day 7, prior to declining, suggesting that a rapid uptake (and assimilation) of nutrients was followed by nutrient limitation.

Possible reasons for why mixotrophy was not observed include: 1) the wrong sort of prey was being provided, 2) that the *Neoceratium* cultured cells had spent too long maintained under autotrophic conditions and had therefore lost their ability to feed, or 3) cells were being exposed too rapidly to limiting nutrient conditions, causing excess stress that may have been preventing them

from performing phagotrophy. In a final attempt to observe mixotrophy *N.tripos* cells were isolated in September 2012, from off the coast of Plymouth, and feeding experiments were performed less than 6 months after this date with *M. rubrum*, which *N. furca* has previously been shown to feed on (See Table 4.2). In these experiments *N.tripos* were left to use up a small quantity of excess nutrients before *M. rubrum* were introduced. It was considered that evidence of mixotrophy would constitute positive growth upon *M. rubrum* addition when compared to prey-free controls and/or the presence of *M.rubrum* within *N. tripos* cells when observed under a fluorescent microscope. Neither of these events was observed, strongly suggesting that *N. tripos* did not ingest *M. rubrum* in these experiments.

Live *Neoceratium* cells collected during AMT 20 showed a number of inclusion bodies similar to those previously seen in *in situ* samples from Chesapeake Bay (Bockstahler and Coats 1993b; Chang and Carpenter 1994); some cells even appeared to be in the process of ingesting prey. Although the position of these inclusion bodies within the cells was consistent with those observed by others (Bockstahler and Coats 1993b), it was not possible to definitely prove whether these were food vacuoles. They could, as has previously been pointed out (Bockstahler and Coats 1993b; Chang and Carpenter 1994), be inclusions such as accumulation bodies, autophagic vacuoles, parasites or symbionts. The development of general fluorescence in-situ hybridisation (FISH) probes for ciliates, or ones specific for common prey such as *Strobilidium* spp., would greatly assist in estimating the prevalence of mixotrophy in OSGs as it would allow for the conclusive identification of food vacuoles containing ciliate prey.

4.5.2 Evidence of mixotrophy from the literature

Although mixotrophy was not observed in these four species of *Neoceratium,* there is little doubt that some species of this genus are capable of mixotrophy (See Table 4.2 for summary). Mixotrophy is difficult to observe experimentally: some species only feed under certain conditions, have low feeding rates, or are

specialised predators on particular types of prey (Li et al. 1996; Stoecker et al. 1997); dinoflagellates kept in culture for long periods of time may also lose their ability to feed (P.J. Hansen, University of Copenhagen, Personal Communication).

In the event that mixotrophy had been successfully observed under laboratory conditions, subsequent work would have involved estimating growth rates of *Neoceratium* at prey concentrations typical of OSGs in order to determine if mixotrophy alone could account for survival and growth in this environment. As this was not possible, it was instead decided to collate data from previous studies in order to try and answer this question (Table 4.2).

Table. 4.2. Details on studies that have provided strong (direct) evidence for mixotropy in *Neoceratium*. *Abbreviations: Location – CB = Chesapeake Bay, CS = Caribbean Sea, C = culture study; Evidence – PFV = prey in food vacuoles, IB = inclusion bodies, DAPI = DAPI staining of inclusion bodies, CMFDA = CMFDA pre-staining of prey, PCC = prey that have ingested cryptophyte prey, CFM = ciliates that pre-ingested fluorescent microbeads.*

Study	Species	Location	Evidence	Prey ingested	Main findings
Bockstahler & Coats (1993b)	*N. furca*	CB	PFV	Ciliates (*Strobilidium* spp., *Mesodinium* spp., *Balanion* spp.)	-Average food vacuole size of 7.51 µm -Usually only one prey item per vacuole -3 % of cells on average possessed inclusion bodies; most frequent in August
Chang & Carpenter (1994)	*N. teres* *N. declinatum* *N. furca* *N.fusus*	CS	IB DAPI	NA	-8-30% of cells had inclusion bodies; 7% of these inclusion bodies contained DNA
Li *et al*. 1996	*N. furca*	CB	CMFDA PCC	Ciliates (esp. *Strobilidium*	-Yellow-orange inclusions seen in cells from un-amended water samples; possibly due to *M. rubrum* ingestion

				sp.)	
Smalley *et al.* 1999	*N. furca*	CB	CFM	Choreotrich ciliates (particularly *Strobilidium sp.*)	-Ingestion rate 0-0.11 prey h^{-1} (mean, 0.010 prey h^{-1}) -Mean food vacuole diameter 12.1 µm (range, 6-32 µm) -Feeding rate correlated with prey abundance -Authors mention that feeding on *M. rubrum* previously observed
Smalley & Coats 2002	*N. furca*	CB	CFM	Choreotrich ciliates (particularly *Strobilidium sp.*)	-N-content of *Strobilidium* ~7% of *N. furca* N-content -P-content of *Strobilidium* ~4% of *N. furca* P-content -Feeding stimulated by low nutrient concentrations (N or P) and ceased when nutrients added to field populations -Daily consumption of prey biomass averaged 6.5% (51% max.) body N and 4.0% (32% max.) body P -Strong positive correlation between ingestion rate and prey density -Assuming gross growth efficiency of 40%, *N. furca* could meet 12% (92% max.) of N and 7% (57% max.) of P requirements for reproduction (division) through phagotrophy

Smalley *et al.* 2003	*N. furca*	C	CFM	*Strobilidium sp.*	-Feeding only after 11 days of nutrient limitation; ingestion rates continued to increase until day 36 -Food vacuoles only seen in cells >60µm in length -Feeding only in nutrient-limited cells, triggered by changes in intracellular nutrient ratios -P-depleted cells only fed when intracellular ratios of C:P >130:1 and N:P >19:1 -N-depleted cells only fed when intracellular ratios of C:N >10:1 and N:P <7:1 -Feeding ceased hours after nutrients added to cultures -High irradiance increases C:P/N and therefore increases demand for N and P to utilise additional C. *N. furca* responds by increasing feeding
Smalley et al. 2012	*N. furca*	CB	CFM	Choreotrich ciliates	-No clear relationship between absolute nutrient concentrations and feeding response -Feeding controlled by nutrient ratios (measured from seawater), and ceased once nutrients were added to experiments: .P-depleted cells only fed when ratios of N:P >17-22:1 .N-depleted cells only fed when ratios of N:P <7:1

					.Suggests that nutrient concentrations may be an adequate substitute for intracellular nutrient values when the nutrient environment is relatively stable -Ingestion rate increased in the dark under some treatments, but dependent on relative not absolute irradiance levels -No experiments showed increased feeding in complete darkness (therefore mixotrophy is to obtain inorganic nutrients not carbon) -Ingestion rates increased in morning and remain high throughout the day -Author's devised conceptual model: anything changing intracellular nutrient ratios can affect feeding: .Nutrient limitation increases feeding by increasing C:N/P .Limiting and photo-inhibitory irradiance reduces C-fixation and therefore nutrient demand via reductions in C:N/P .Implies that feeding should remain high under light-limiting conditions if nutrient demand in cell not met during daylight hours

4.5.3 Would mixotrophy be feasible in OSGs

Intracellular nutrient ratios have been shown to be the best way in which to predict mixotrophy in *Neoceratium* (Smalley et al. 2003, 2012), but inorganic nutrient ratios in seawater have been shown to be an adequate substitute in relatively stable environments (Smalley et al. 2012), such as those found in OSGs. Under N-limitation, N:P ratios of <7:1 have been linked with mixotrophy in *Neoceratium* (Smalley et al. 2003, 2012). By reanalysing the nutrient data (converting to N:P ratios) from chapter 2 (Fig. 2.12 and 2.14) it is shown that in surface waters of the NAG (Fig. 4.8) and SAG (Fig. 4.9), 86 % of sites (NAG, 90/105; SAG, 207/240) have N:P ratios that would favour mixotrophy. In the nutricline the percentage was much lower: 16 % (8/49) of sites in the NAG and 39 % of sites (37/94) in the SAG. This would suggest that *Neoceratium* cells in the NAG and SAG at least have the capability to ingest prey in these regions, and that this behaviour is more prevalent in surface waters where nutrient concentrations are known to be limiting.

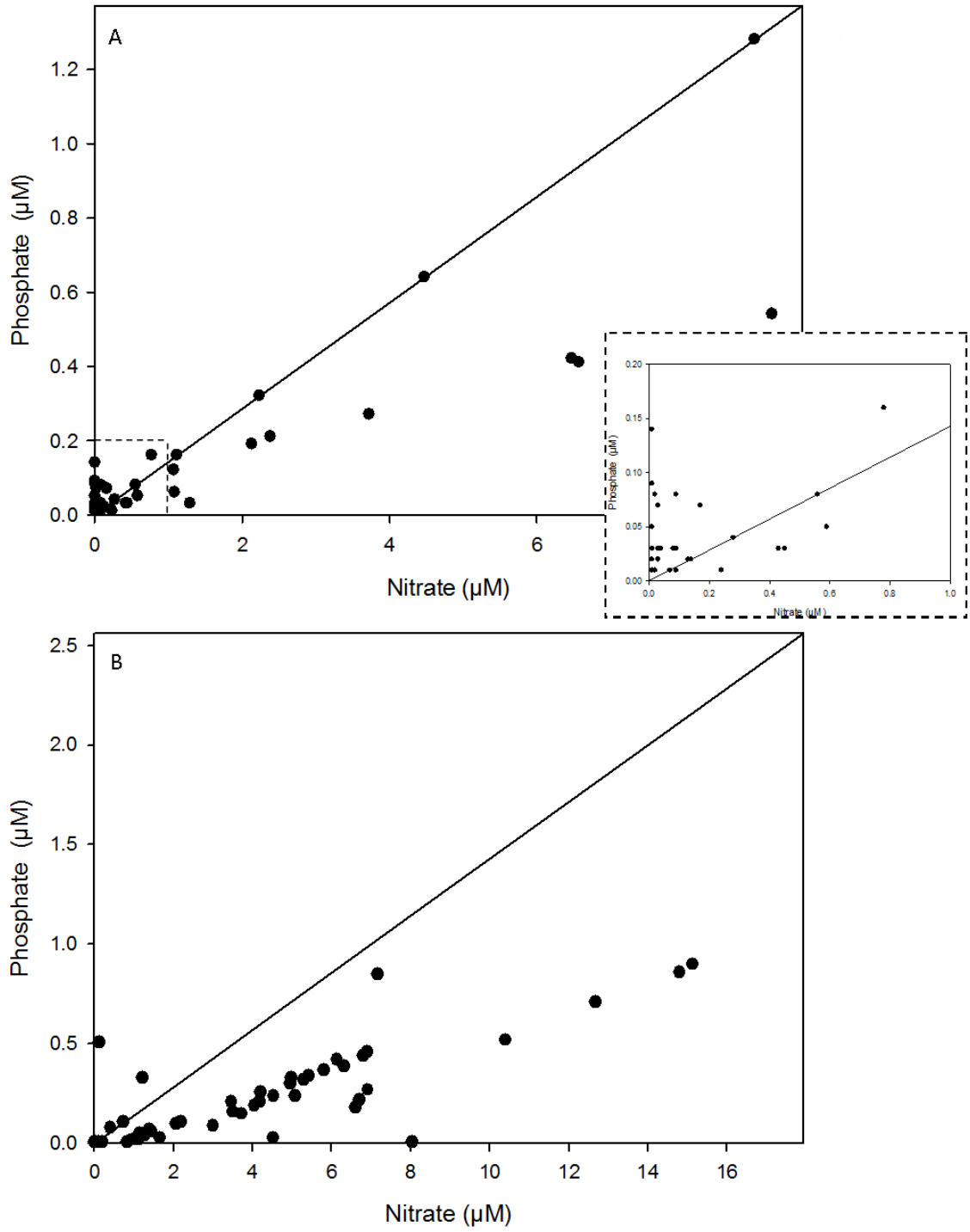

Fig. 4.8. Nutrient ratios (N:P) above (A, 0 to 100 m) and below (B, 101 to 200m) the nutricline in the North Atlantic subtropical gyre. A solid line, representing N:P ratios of 7:1, is shown for reference. Data points above this line (surface, 90/105 sites; nutricline, 8/49 sites) represent nutrient ratios that favour mixotrophy according to Smalley et al. (2003, 2012).

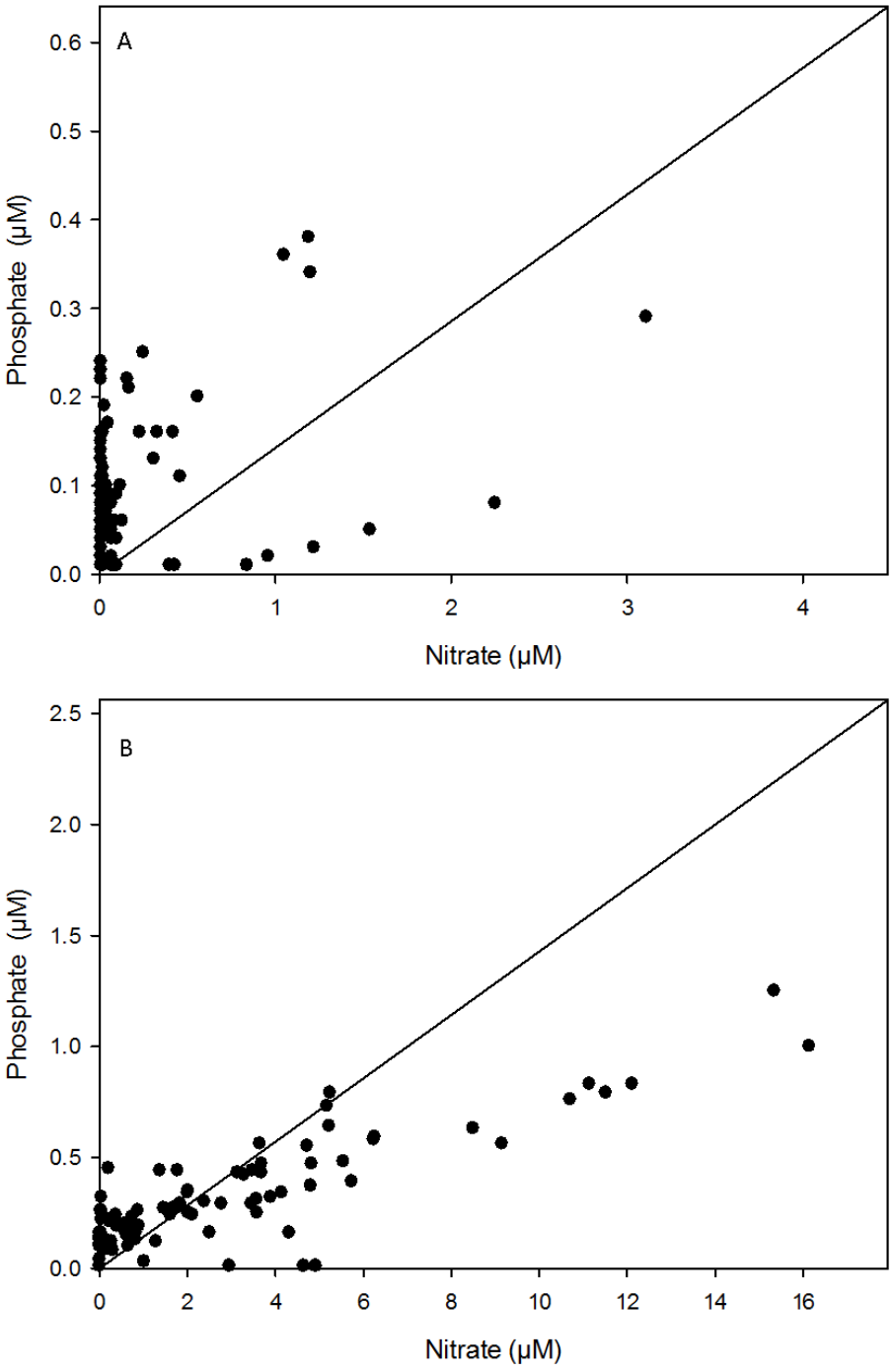

Fig. 4.9. Nutrient ratios (N:P) above (A, 0 to 130 m) and below (B, 131 to 200m) the nutricline in the South Atlantic subtropical gyre. A solid line, representing N:P ratios of 7:1, is shown for reference. Data points above this line (surface, 207/240 sites; nutricline, 37/94 sites) represent nutrient ratios that favour mixotrophy according to Smalley et al. (2003, 2012).

4.5.4 How much prey would be required for *Neoceratium* survival and growth in OSGs?

It is possible, by making a few assumptions to calculate approximately how much prey (in the form of ciliates) would be required for survival and growth of *Neoceratium*. Measurements of intracellular protein (Chapter 3) showed that, in *N. hexacanthum* exposed to low nutrient seawater (LNSW), protein concentrations decrease by 5 ng (±2 ng) over 21 days. Therefore, to maintain their cells, *Neoceratium* need approximately 0.14-0.33 ng day^{-1} of protein to supplement their nitrogen demands. Estimates for nitrogen assimilation efficiencies in the literature vary from 0.4 to 1 (Anderson and Hessen 1995; Stickney et al. 2000; Flynn and Mitra 2009). Here, an intermediate nitrogen assimilation efficiency of 0.75 for type II mixotrophs feeding on microzooplankton (Stickney et al. 2000) is assumed. Under these circumstances, *Neoceratium* would need to ingest 0.19-0.44 ng of protein per day. Using previously published protein contents of a number of ciliate species (1-15 ng) (Zubkov and Sleigh 1996, 2000), it would appear that an ingestion rate of 0.01-0.44 ciliates day^{-1} would be required for *Neoceratium* to survive in OSGs. For *Neoceratium* to divide at the rate observed by Weiler (1980) (0.09-0.16 d^{-1}), adding the further assumption that the complete asexual division process requires the ultimate doubling of cellular protein concentrations, it is calculated that *Neoceratium* would need to consume 0.9-1.8 ng protein d^{-1}, or 0.06-1.8 ciliates d^{-1}. This rate of feeding would appear to be feasible given that the maximum feeding rate observed for *N. furca* in coastal waters is 2.6 ciliates d^{-1} (Smalley and Coats 2002). However, whether ingestion rates at OSG prey concentrations are high enough is unknown, but can be estimated.

4.5.5 Would ingestion rates be high enough in OSGs to support survival and growth?

By using ingestion rate estimates, under different prey concentrations from Smalley *et al.* (1999) it is possible to estimate ingestion rates of *Neoceratium*

in OSGs. In chapter 2 (Fig. 2.15), ciliate concentrations in the upper 160 m were shown to range from ~500 to 3000 cells L^{-1}. However, Smalley *et al.* (1999) showed that ingestion rates were most strongly associated with the ciliate genus *Strobilidium* ($n = 30$, $r = 0.84$, $P = <0.0001$) compared to total ciliates ($n = 30$, $r = 0.53$, $p=0.002$). This would seem logical as *Strobilidium* is suggested as the favoured prey of *Neoceratium* (Table 4.2). For this reason *in situ Strobilidium* plus *Strombilidium* abundances (mean, 200 L^{-1}), previously reported in the NE subtropical Atlantic (Quevedo 2003), are used to estimate *Neoceratium* ingestion rates in OSGs – this study demonstrated that these two genera dominate the ciliate population here, but unfortunately grouped them together in their microzooplankton counts. Using the linear relationship between *Strobilidium* abundance and prey ingested per hour discussed above (Fig. 4.10) it is estimated that at mean *Strobilidium (+Strombilidium)* abundances of 200 L^{-1} (0.2 ml^{-1}) *Neoceratium* ingestion rates would be approximately 0.018 prey cells day^{-1}. This is just above the lower range of prey *Neoceratium* would need to ingest to survive in OSGs (0.01-0.44 ciliates day^{-1}), but significantly lower than the 0.06-1.8 ciliates d^{-1} that would be required to grow at the rate observed by Weiler (1980).

The above scenarion, however, would be the situation under average conditions. The range of prey concentrations in OSGs is useful for determining the importance of mixotrophy as homogenous distributions of protistan biomass are not the norm in these environments (Quevedo 2003). By using this author's data on the range of abundance of total ciliates (100 to 1160 cells L^{-1}, which is comparable to the abundance range shown in chapter 2 of ~500 to 3000 cells L^{-1}) in combination with their finding that *Strobilidium* and *Strombilidium* contribute on average 27% (by abundance) of ciliate abundance, the concentration range of ciliates within OSGs is estimated to be 27 to 594 cells L^{-1} (the upper value observed was attributed largely to mesoscale eddy activity, raising the possibility that mesoscale eddy activity benefits *Neoceratium* not just through increased supply of inorganic nutrients, but also by concomitant increases in prey availability). By once again applying the feeding rate considerations of Smalley et al. (1999) the feeding rate range of *Neoceratium* in OSGs on *Strobilidium/Strombilidium* is estimated to be 0.002 to 0.053 ciliates d^{-1} (compare this to the previously calculated range required

for survival of 0.01-0.44 ciliates day^{-1}). This implies that in some areas of OSGs prey concentrations are not high enough to support the survival of *Neoceratium*, but, in others, prey concentrations are sufficient for survival and could also probably sustain growth close to those observed by Weiler (1980) (requiring 0.06-1.8 ciliates d^{-1}). Where prey concentrations are not high enough to support survival, the ability to survive long periods of time (>3 weeks) without nutrients is no doubt important (Aldridge et al. 2014) until such a time where higher prey abundances are encountered

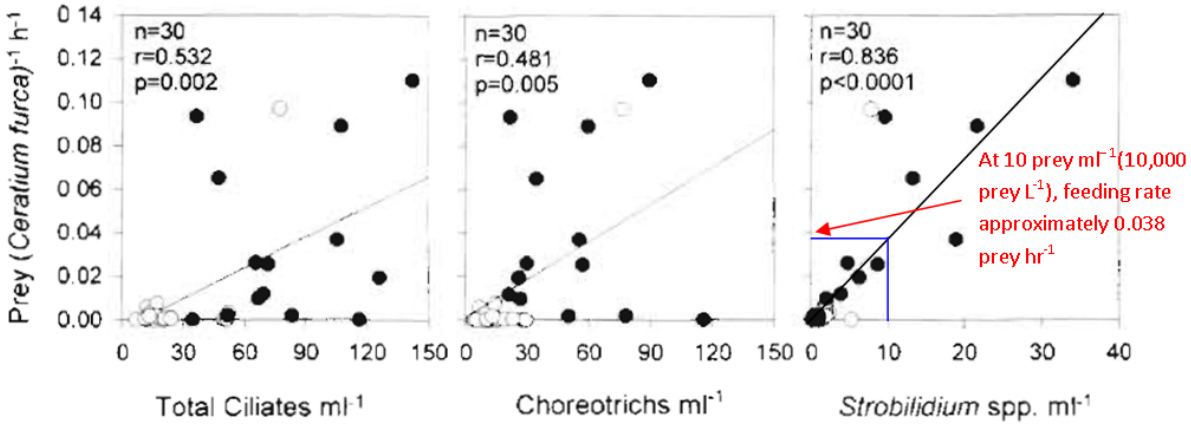

Fig. 4.10. The relationship between ciliate prey concentration and *N. furca* ingestion rates. The relationship between *Strobilidium* spp. concentration and *N. furca* ingestion rates (right panel) is used here to estimate ingestion rates of *Neoceratium* in OSGs. Modified from Smalley et al. (1999).

4.6 Conclusion

No direct evidence of phagotrophy was observed in multiple experiments on *Neoceratium* in culture, using a variety of potential prey items. However, using observations from the literature, combined with some data discussed in previous chapters, it is revealed that nutrient ratios (N:P) in OSG surface waters would be favourable to mixotrophy, especially in surface waters. Furthermore, based on the number of ciliate prey that *Neoceratium* would have to ingest to survive and grow in OSG, in addition to previously published ingestion rates at ciliate abundances typical of OSGs, it appears that mixotrophy may allow cells to survive in OSGs under normal prey abundances, and perhaps even grow under peak prey abundances. However, due to the temporal and spatial "patchiness" of ciliate distributions, there are also likely to be periods where prey abundances are too low to support survival. Therefore, whilst mixotrophy is likely to be a useful source of nutrients, it probably does not solely explain the reason why *Neoceratium* are prevalent in OSGs. In the next chapter, the potential role of vertical migration, to and from the nutricline, is considered.

5. Assessing the viability of vertical migration as a means by which *Neoceratium* may access the nutricline in oligotrophic subtropical gyres.

5.1 Abstract

In oligotrophic subtropical gyres (OSGs) the nutricline offers a source of nutrients to *Neoceratium*. By performing laboratory experiments on *Neoceratium hexacanthum* it was confirmed that cell growth is possible (at a mean rate of 0.14 day^{-1}) at nutrient concentrations representative of the nutricline (NO_3^-, 2.1 µM; PO_4^{3-}, 0.05 µM). However, when cells were exposed to a range of irradiances (6 to 60 µmol quanta m^{-2} s^{-1}), growth was only observed above 22 µmol quanta m^{-2} s^{-1}; an irradiance that is typically only found 15 to 22 metres above the nutricline. The implication is that movement between the euphotic zone and the nutricline would be required for growth to occur. It is demonstrated that cells could survive for more than 2 weeks at reduced irradiances associated with migration to the nutricline and suggested that this movement may ultimately be triggered by phosphate-limitation. This is based on the increased sinking rates (mean increase 1.4 m day^{-1}) and reduced numbers (>20 %) of buoyant *N. tripos* cells following phosphate-limitation of cultures. The increased sinking rates observed are shown to provide ample time for cells to access the nutricline from the euphotic zone, and a mechanism for how this migration is likely to occur is discussed.

5.2 Introduction

Neoceratium are frequently found in oligotrophic subtropical gyres (OSGs), where nutrient concentrations are severely depleted in surface waters (Moore et al. 2013). Although *Neoceratium* can survive for prolonged periods of nutrient starvation – up to 3.5 weeks – they cannot grow in these environments and require an external source of nutrients (Aldridge et al. 2014). One potential source of nutrients is the nutricline, which often lies over 100 metres below the sea surface (see chapter 2). The nutrient concentrations present in the nutricline would appear to be great enough to sustain growth of *Neoceratium* based on studies where *Neoceratium* have grown at nutrient concentrations slightly lower than those found at the nutricline in OSGs (Baek et al. 2008a).

At the nutricline in OSGs, irradiance values are on average <10 µmol quanta m^{-2} s^{-1} during the middle of the day (range <2 to 21 µmol quanta m^{-2} s^{-1}; see Chapter 2). Whether *Neoceratium* cells are able to survive and grow at these irradiances is unknown, but seems unlikely based on previous studies. Falkowski et al. (1985) studied three species of phytoplankton (*Thalassiosira weisflogii, Isochrysis galbana* and *Prorocentrum micans*), and predicted, based on positive measured growth rates between 30 and 600 µmol quanta m^{-2} s^{-1}, that below 20 µmol quanta m^{-2} s^{-1} growth rates would be zero. Although Chang and McClean (1997) showed that, at 25 µmol quanta m^{-2} s^{-1}, the dinoflagellate *Alexandrium minutum* is able to grow slowly (0.15 d^{-1}), this would be at the very highest range of light intensities found at the nutricline in OSGs.

Other studies have considered the compensation irradiance – the irradiance where photosynthesis is equal to respiration. *In situ* population measurements for the compensation irradiance range from 0.1 to 1.7 mol photons m^{-2} d^{-1} (Siegel et al. 2002; Marra 2004). Estimates from laboratory cultures suggest a range of 0.06 to 1.8 mol photons m^{-2} d^{-1} (Falkowski and Owens 1978; Langdon 1987), with the highest value being for the large dinoflagellate, *Gonyaulax tamerensis*. If this daily irradiance value (1.8 mol photons m^{-2} d^{-1}) is considered to be a likely value for *Neoceratium*, and is converted into an instantaneous

irradiance requirement, assuming 12 hours of daylight, then an instantaneous irradiance value in the region of 40 µmol quanta m^{-2} s^{-1} would be required during daylight hours to balance photosynthesis with respiration in *Neoceratium*.

As the instantaneous light values discussed above are significantly higher than typical values that would be encountered in the nutricline in OSGs, vertical migration (VM) may be a useful strategy for *Neoceratium* in these environments, as has previously been observed for *Neoceratium* in coastal environments (Blasco 1978; Baek et al. 2009), freshwater environments (Heaney and Furnass 1980; Taylor et al. 1988; James et al. 1992; Whittington et al. 2000), and under laboratory conditions (Weiler and Karl 1979; Baek et al. 2009).

If VM is used as a strategy to cope with the vertical separation of nutrients and light, it is important to know survival time of *Neoceratium* at low irradiances, as this will contribute towards setting the maximum vertical distance under which vertical migration can occur. Baek et al. (2008) showed that *N. furca* and *N. fusus* can survive in complete darkness (re-establishing growth once transferred to higher irradiances) for up to 10 days. Presumably, *Neoceratium* could survive for longer at low irradiances found close to the nutricline; but, for how long, is unknown.

From previous studies of vertical migration in *Neoceratium* and *Ceratium hirundinella* (a freshwater species), light seems to be the primary controlling factor influencing this behaviour: cells migrate upwards early in the morning and downwards before dark (Blasco 1978; Weiler and Karl 1979; Heaney and Eppley 1981; Baek et al. 2009). Very high irradiances (>1300 µmol quanta m^{-2} s^{-1}), however – occurring at noon for example – can lead to *Neoceratium* migrating downwards out of surface waters (Blasco 1978; Heaney and Furnass 1980; Whittington et al. 2000), presumably to avoid cell damage. Evidence that this behaviour may follow an endogenous rhythm comes from work by Weiler and Karl (1979), who found that the above migration pattern continued to occur under 6 days of constant darkness.

It would also appear that migration can occur against physical water movements (Blasco 1978), provided the mixing intensity is not too high

(Whittington et al. 2000). However, downward migration does appear to be prevented by even a weak gradient in seawater density (Blasco 1978; Heaney and Furnass 1980).

In terms of factors that secondarily control VM, the role of internal cellular stimuli, such as nutrient concentrations within the cell, appear to be important. Heaney and Eppley (1981) demonstrated that, when nitrate is depleted, *Neoceratium* descend earlier in the day, thus allowing more time at the nutricline. Additionally, there is a suggestion that cells exhausted in phosphate cease to migrate (Heaney and Eppley 1981; Taylor et al. 1988); the reason proposed for this is that phosphate limitation leads to reduced motility due to a shortage of ATP. The importance of VM for obtaining phosphate has been demonstrated by James et al. (1992): when VM of *C. hirundinella* was restricted by anoxia in the water column of a freshwater reservoir, cellular phosphate concentrations fell and alkaline phosphatase activity (a proxy for phosphate limitation) increased. This mechanism of controlling VM in *Neoceratium* would logically be important in OSGs considering the low standing stocks of phosphate in these environments (Zubkov et al. 2007; Mather et al. 2008; Van Mooy et al. 2009).

Here, the ability of *N. hexacanthum* and *N. candelabrum* to grow at nutricline nutrient concentrations, as has been reported previously, is verified. Additionally, the ability of *N. hexacanthum* to grow and survive at the low irradiances that are encountered at the nutricline in OSGs is tested. Then, using a recently isolated strain of *N. tripos*, we examine whether cells show a diurnal migration response, and if this changes as cells become increasingly phosphate-limited. Finally, it is determined whether phosphate depletion leads to motility-related buoyancy changes, and the effects this would have on the sinking rates of these cells is quantified.

5.3 Methods

5.3.1 Isolation of *N. hexacanthum* and *N. tripos* cells

N. hexacanthum cells were isolated and cultured as described in Chapter 3 (3.3.1), and *N. tripos* cells were isolated and cultured as described in Chapter 4 (4.3.1).

5.3.2 Investigating growth at nutricline nutrient concentrations

Measurements of cell numbers, percentage of dividing cells, protein per cell and *Fv/Fm* were performed on *N. hexacanthum* and *N. candelabrum* cells cultured in nutricline seawater (NUSW) and low nutrient seawater (LNSW). This was part of an experiment already discussed in Chapter 3 (section 3.3.2 – 3.3.5). Nutrients were monitored simultaneously and analysed as described previously in Section 3.3.6 of this thesis. Growth rates (d^{-1}) were estimated from initial increases in cell numbers between day 1 and 5 using the following equations recommended by Anderson (2005), where N1 and N2 represent the number of cells present at time points one (T1) and two (T2):

$$Growth\ rate\ (K) = Ln\ (N2 / N1) / (t2 - t1) \qquad (Eq.\ 1)$$

$$Divisions\ per\ day^{-1} = K / Ln2 \qquad (Eq.\ 2)$$

This method of estimating growth rates was chosen, in preference to the method used in Chapter 3 (described in Section 3.3.7), as growth curves did not appear exponential – a fact that indicates that growth rates quickly became

nutrient limited, and were probably only exponential for a short time. For this reason, growth rates were calculated using the first two data points only. The same method was used for estimating growth rates from cultures based on cell counts performed every 10 to 15 days over the course of 2.5 years.

5.3.3 Growth responses of *N. hexacanthum* under a range of different irradiances

Approximately 20 *N. hexacanthum* cells (average: 22; range: 13-28) were transferred to 15 embryo dishes containing 2.5 ml of K/5 medium, and covered with a glass lid to prevent evaporation (the mass of each dish was monitored to ensure no evaporation occurred). Exact cell numbers were confirmed, and 3 replicate dishes were transferred to 5 different light intensities (6, 13, 22, 38 and 60 µmol quanta m^{-2} s^{-1}; achieved with black plastic sheeting material and monitored using a Licor LI-1000 light meter throughout the experiment), maintained on a 12:12 light/dark cycle. Following this, cell numbers were monitored every 2 days, and patterns of growth were compared.

5.3.4 Survival time under reduced irradiance

Approximately 30 *N. hexacanthum* cells (average: 29; range: 19-44) were transferred to 14 embryo dishes containing 2.5 ml of K/5 medium, and covered with a glass lid to prevent evaporation (the mass of each dish was monitored to ensure no evaporation occurred). Exact cell numbers were confirmed, and dishes were transferred to low light conditions (2 µmol quanta m^{-2} s^{-1}), and maintained on a 12:12 light/dark cycle. Low light conditions were achieved with multiple sheets of black plastic screening material and monitored using a Licor LI-1000 light meter throughout the experiment (irradiances ranged from 1.5 to 2.5 µmol quanta m^{-2} s^{-1}). Every day for 22 days (starting on day 1) a single dish was transferred to higher light conditions (60

μmol quanta m^{-2} s^{-1}). Following this, cell numbers and dividing cells were monitored every 2 days, allowing for the estimation of the following:

Maximum viability time: The longest period that any single cell survived and went on to divide.

Percentage of cells remaining: This was calculated for each dish by comparing the number of cells present on day 1 to the number of cells present upon transfer to higher light conditions.

Changes in growth rate: Growth rate was estimated, after initial time-lags in growth response following transfer to higher light conditions, by fitting an exponential growth model [Stirling Model; $y=y0+a(exp(b\times x)-1)/b$] to the data using SigmaPlot (**Systat Software Inc.)** software – where "x" refers to x-axis values (experiment day number), "y" refers to y-axis values (cell number), and "a" and "b" are coefficients provided by the software. The slope of the line was then used to estimate growth rate in divisions per day (d^{-1}). Several different exponential models were tested for how well they fitted the data. The Sterling model was used as it had the highest R^2 values.

Changes in time-lag of growth response: The growth time-lag for each dish was estimated from the number of days it took, after transfer to higher light conditions, for the first sign of growth to occur: either an increase in cell number, or the presence of dividing cells.

5.3.5 Effect of phosphate limitation on vertical migration and sinking rates

N. tripos cells were gently reverse-filtered a number of times to remove excess nutrients present in the K/5 medium. Cells were then transferred to a 1 Litre Ehlenmeyer flask and topped up to 800ml with K/75 medium with no phosphate added. Every day, cell counts were performed using a 1 ml plastic Sedgewick-Rafter chamber (3 X 0.33ml replicates), following gentle agitation to evenly distribute cells.

For nutrient analysis, 10 ml subsamples were filtered through 0.2 µm Millipore filters into 15 ml Falcon tubes. Samples were stored at -80°C prior to analysis within 1 month of collection. Nitrate (total oxidised nitrogen;TON) and phosphate measurements were analysed according to Sanders and Jickells (2000).

Every 3-4 days, at 12:00, 25ml of stock culture was added to a 25ml measuring cylinder and incubated on a 12:12 L:D cycle (60 µmol quanta m^{-2} s^{-1}), with only the top 10 ml of the cylinder exposed to light (sideways illuminated). Cells were left for 8 hours to acclimate before the first sampling point (20:00). 0.3 ml of culture was sampled from various points in the measuring cylinder using a Pasteur pipette (taking care not to agitate the water column), and cell counts were performed using a 1 ml Sedgewick Rafter chamber under an inverted microscope. Samples were taken at 5 time-points (20:00, 22:00, 08:00, 10:00 and 14:00) over an 18 hour time period. After the required sample was removed it was replaced by an equivalent volume of culture from the stock culture, and introduced very gently into the top of the cylinder. Additional information on the percentage of buoyant cells over the course of this experiment was inferred by comparing the average number of buoyant cells throughout the water column (cells ml^{-1}) to the total number of cells estimated from the stock culture (cells ml^{-1}).

Every day 4-5 ml of cell-containing culture media was added to 18 ml of oligotrophic seawater, gently mixed to evenly distribute cells, and then added to a settling chamber (50 mm height, 23mm diameter). The settling chamber

had a square (9 x 9 mm) drawn onto the base. A dissecting microscope, fitted with a camera (Canon IXUS 125), was used to determine the number of cells that settled in this box at various times over a 1 hour time period, from which cell sinking speeds were calculated. As cells were evenly mixed at the beginning of the experiment, sinking speeds were calculated assuming that all cells reached the base from halfway up the settling chamber (25 mm); in reality, some cells would have started from closer to the base of the chamber and others from further away. The number of buoyant cells was determined by counting the number of cells 'swimming' above this defined area after 1 hr. This experiment was performed on both motile and immotile (paraformaldehyde fixed) cells. Mean sinking rate changes of immotile and motile cells (day 1-7 compared to day 15-21) were statistically analysed using a t-test.

5.4 Results

5.4.1 Growth at nutrient concentrations typical of the nutricline in OSGs

In Figure 5.1 trends in cell numbers, dividing cells, protein per cell and *Fv/Fm* for *N. hexacanthum* and *N. candelabrum* grown in NUSW and LNSW are shown. Here, only the trends for experiments using NUSW are used, as the trends for LNSW were previously described in Chapter 3 (Section 3.4.1 and 3.4.2). The reason for showing data for NAGSW experiments here is merely to compare NUSW experiments to a control scenario where growth did not occur. These experiments were carried out simultaneously and, therefore, provide useful comparisons.

N. hexacanthum cell numbers increased up until day 13, from 16 to 23 cells ml^{-1}; after this point cell numbers decreased until day 21 from 23 to 16 cells ml^{-1} (Fig. 5.1A). The percentage of dividing cells broadly mirrored the above pattern (Fig. 5.1C), increasing from 0 to 2.1 % between day 1 and 5, remaining at approximately 2 % until day 12, before falling to 0 % on day 16. Motile cells were observed throughout the experiment. Average protein content per cell (Fig 5.1E) showed an initial increase between day 1 and day 9 (8.9 to 10.9 ng $cell^{-1}$), followed by a decrease down to 5.6 ng $cell^{-1}$ by day 21. There was little difference in *Fv/Fm* values over the course of the experiment, where a small decrease occurred over the 21 days, from 0.29 to 0.26. (Fig. 5.1G).

In *N. candelabrum*, cell numbers increased from 20 to 34 cells ml^{-1}, between day 1 and 13, before levelling off (Fig. 5.1B). The percentage of dividing cells (Fig. 5.1D) broadly mirrored the above pattern, slowly decreasing from 9 % on day 0, to 1 % on day 21. Motile cells were observed throughout the experiment. The average protein content per cell (Fig 5.1F) remained relatively stable between day 1 to 13 (4.6 to 6.2 ng $cell^{-1}$). This was followed by a decrease down to 3.2 ng $cell^{-1}$ by day 21. *Fv/Fm* values (Fig. 5.1H) closely reflected

changes in cell numbers (Fig. 5.1B). Values increased from day 1 to 9 (from 0.130 to 0.224), followed by a steady decline to 0.105 by day 21.

5.4.2 Nutrient concentrations

In NUSW PO_4^{3-} concentrations (Fig. 5.2A) were depleted from 0.05 µM, on day 1, to near the detection limit of the instrument on day 5 (~0.02 µM); between day 5 and day 21, concentrations remained within this range (undetectable to 0.02 µM). NO_3^- concentrations (Fig. 5.2B) followed an almost identical pattern to PO_4^{3-} : they fell from 2.1 µM, on day 1, to 1.65 µM, on day 5; concentrations remained at this level (between 1.57 and 1.68 µM) until day 17, after which there was a rise to 1.88 µM by day 21.

5.4.3 Growth rates

Mean growth rates for *N. hexacanthum* in NUSW (Fig. 5.3) were 0.14 d^{-1} (range: 0.08-0.24 d^{-1}) – just under half the mean growth rate observed in cells cultured in K/5 medium (mean, 0.31 d^{-1}; range, 0.18-0.65 d^{-1}), and within the range of *in situ* growth rates (for this genus) observed in the North Pacific gyre (0.09-0.16 d^{-1}; Weiler 1980).

Mean growth rates for *N. candelabrum* in NUSW (Fig. 5.3) were 0.28 d^{-1} (range: 0.16-0.43 d^{-1}); this is close to the growth rates observed in K/5 medium (0.36 d^{-1}; range, 0.18-0.58 d^{-1}), and higher than average *in situ* growth rates (for this genus) observed in the North Pacific gyre (0.09-0.16 d^{-1}; Weiler 1980).

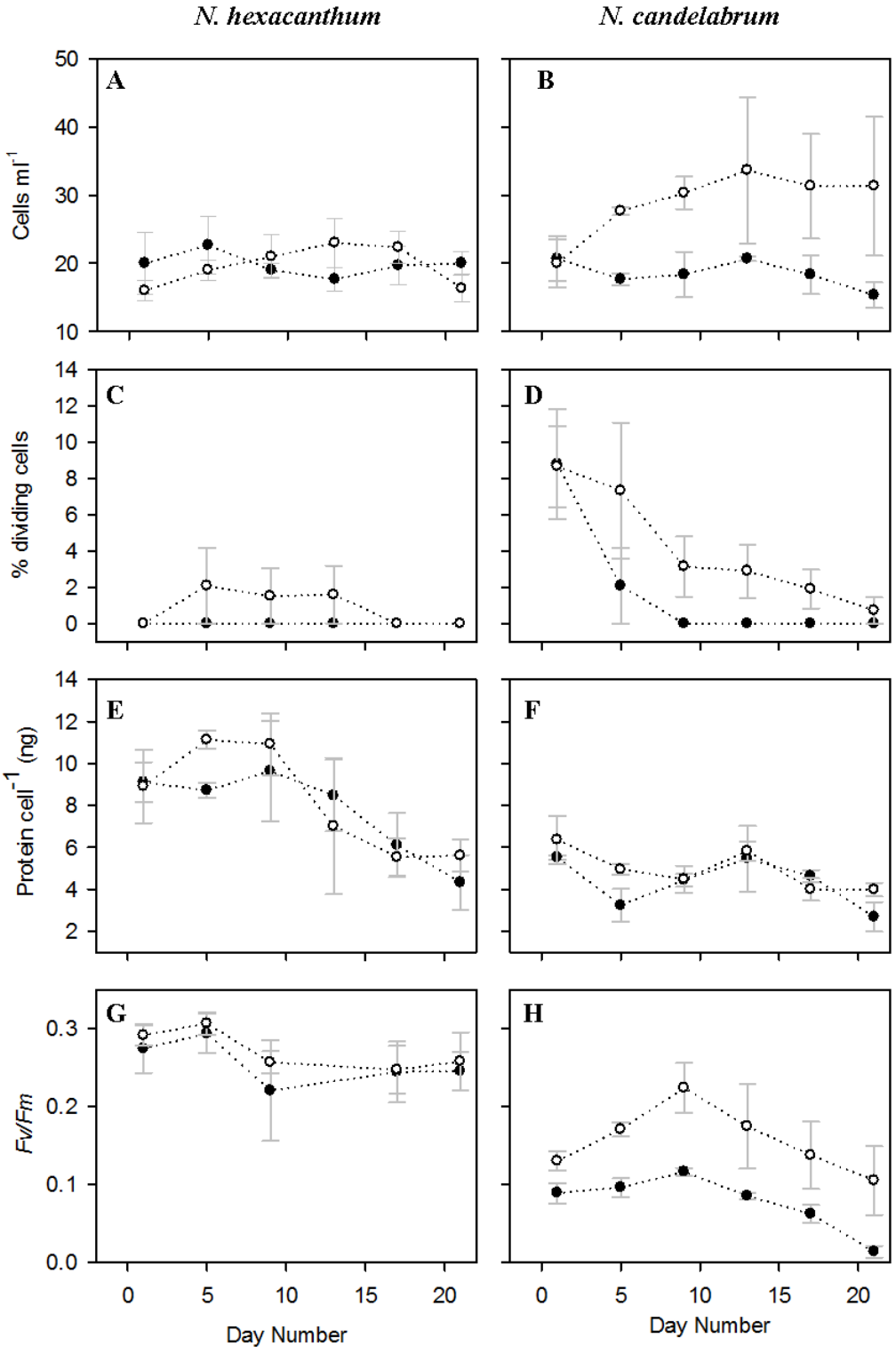

Fig. 5.1. Changes in *N. hexacanthum* and *N. candelabrum* cell numbers (A,B), % of dividing cells (C,D), protein cell^{-1} (E,F) and *Fv/Fm* (G,H) over the course of 21 days, under two different nutrient treatments: LNSW (filled symbols) and NUSW (hollow circles). Error bars represent the standard error of triplicate experimental flask.

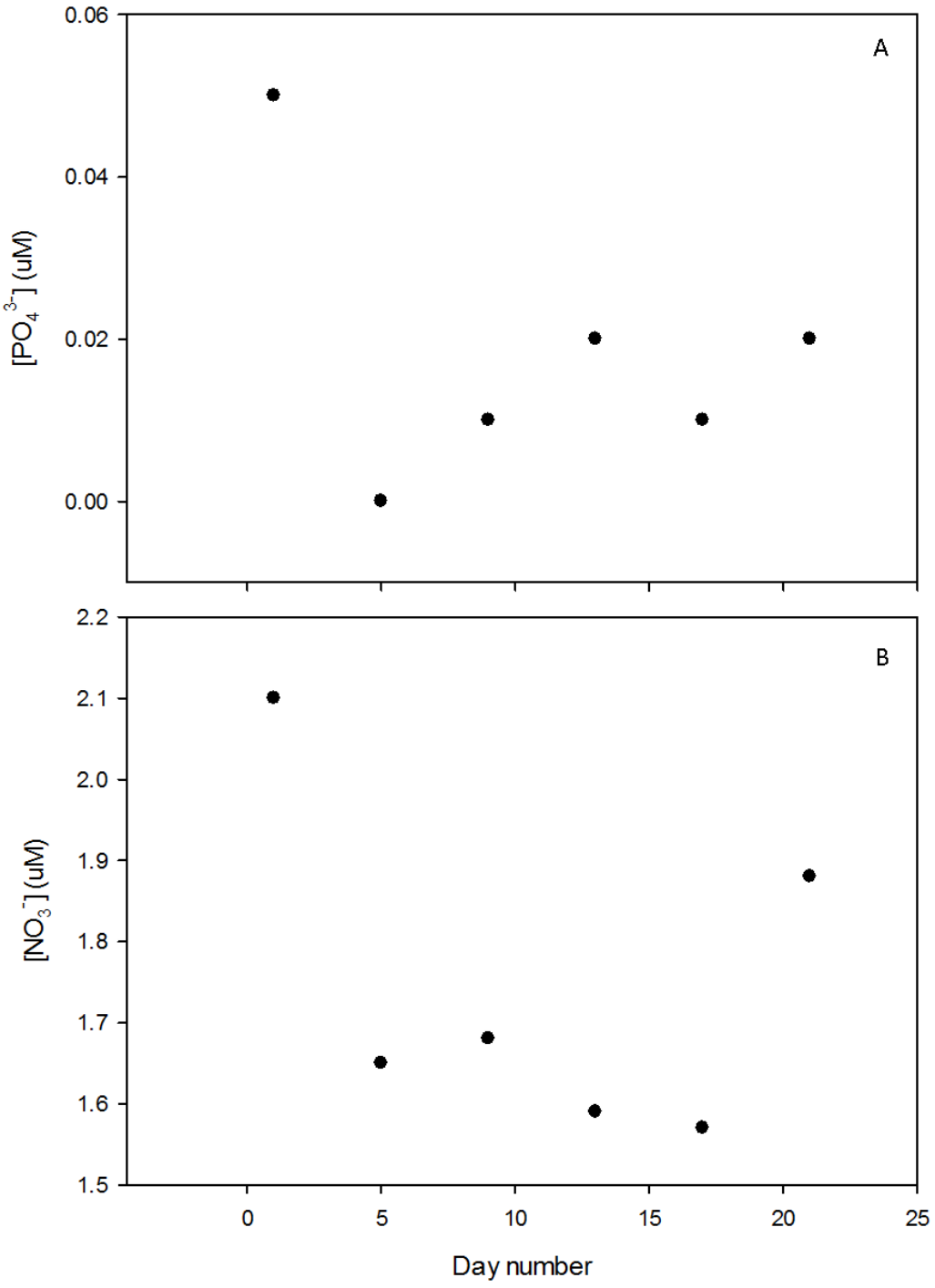

Fig. 5.2. Nutrient concentrations measured over the course of 21 days for experiments performed on *N. candelabrum* (Fig. 5.1). PO_4^{3-} and NO_3^- concentrations are shown for the NUSW treatment.

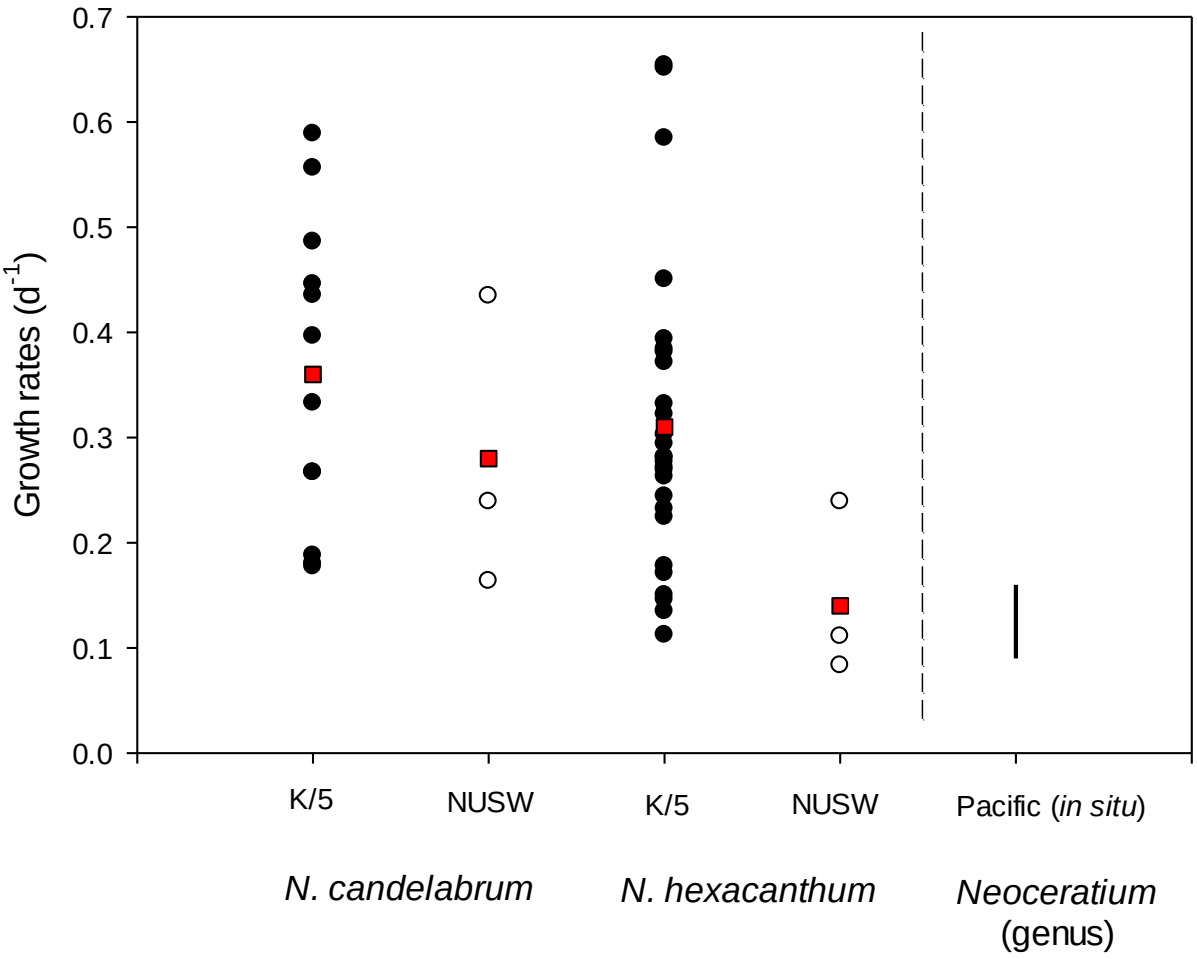

Fig. 5.3. A comparison of growth rates (μ, d^{-1}) of *N. hexacanthum* and *N. candelabrum* in K/5 and NUSW growth mediums. Discrete measurements of growth rates are denoted by black circles for different nutrient scenarios (filled = K/5 medium; hollow = NUSW). Red squares show the average growth rate under each scenario. The range of published growth rates for *Neoceratium* (genus), in the central subtropical North Pacific gyre (Weiler, 1980), is shown by a continuous black line.

5.4.4 Growth and survival at irradiances typically found at or near the nutricline in OSGs

Irradiance had a clear effect on the growth of *N. hexacanthum* (Fig. 5.4), with higher light intensities leading to increased cell numbers. At 60 µmol quanta m^{-2} s^{-1} growth was rapid over the first 6 days with average cell numbers increasing from 24 to 63. Between day 6 and 11 a smaller increase occurred, from 63 to 78 cells. At 38 µmol quanta m^{-2} s^{-1} a similar pattern was evident, although growth occurred more slowly: from 19 to 39 cells between day 1 and 11. There was a very small increase in cell numbers at 22 µmol quanta m^{-2} s^{-1}: from 22 to 25 cells. At 13 and 6 µmol quanta m^{-2} s^{-1} cell numbers decreased: from 22 to 17 in the former, and from 20 to 9 in the latter.

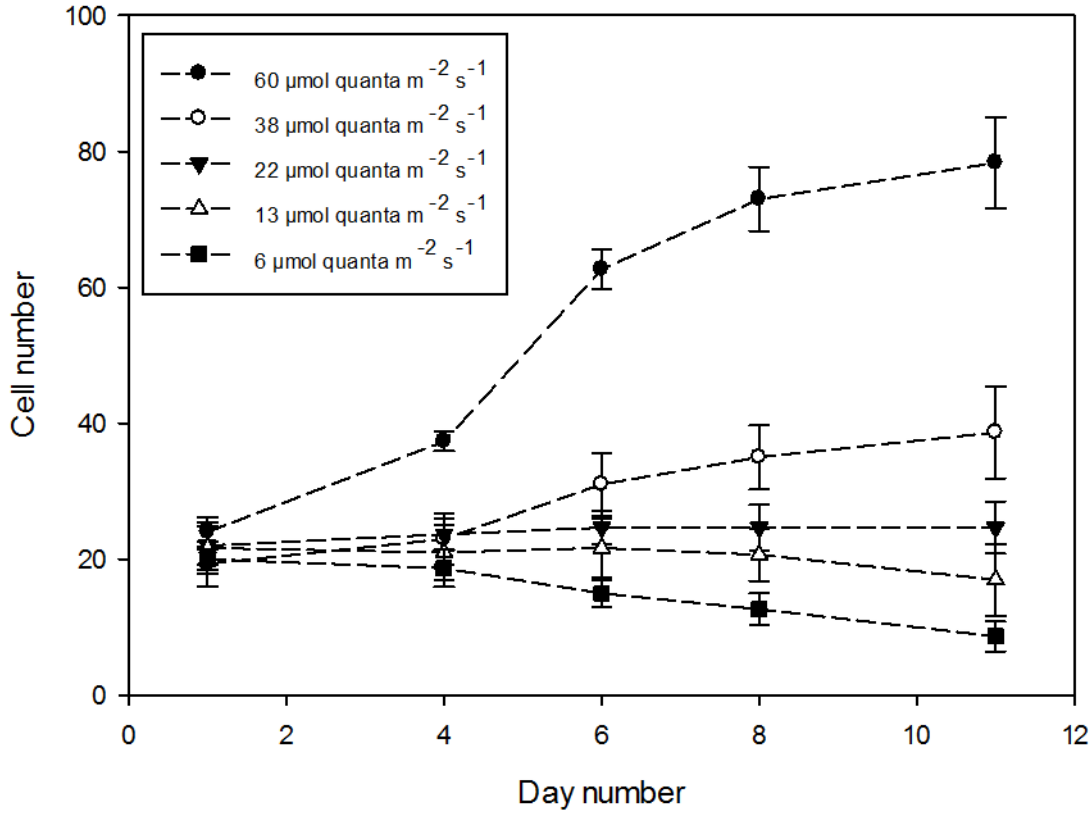

Fig. 5.4. Growth responses of *N. hexacanthum* under a range of different light intensities over 11 days. Error bars represent the standard error of triplicate experiments.

The survival time of *N. hexacanthum* exposed to very low light intensities associated with the nutricline (2 µmol quanta m^{-2} s^{-1}) was also examined. Cell numbers only began to increase once transferred, from this very low irradiance, to a higher irradiance (60 µmol quanta m^{-2} s^{-1}) that was able to support cell growth (Fig. 5.5). The longest time any single cell survived at 2 µmol quanta m^{-2} s^{-1}, and then went on to re-grow upon transfer to higher irradiance, was 16 days.

The percentage of cells remaining (as a percentage of cells present on day 1) decreased over the course of the experiment, from 100 % on day 1 to 0 % on day 22 (Fig. 5.6A). On day 16 – the last day where cells were able to regrow – there were approximately 60 % of cells still remaining. The time-lag between movement to higher irradiance and the first sign of growth remained at 2 days between day 1 and 9 (Fig. 5.6B). Beyond this, on days 14 and 16, the time-lag had increased to four days. However, once growth did commence, the growth rate of cells appeared unaffected by the length of exposure to low irradiance. The mean growth rate observed (after accounting for the time-lag) was 0.25 d^{-1} (range, 0.08 – 0.32 d^{-1}). For most embryo dishes (7/9) the growth rate was within a narrow range (0.22 – 0.32 d^{-1}), and on the last day that growth was observed (day 16) the growth rate was still relatively high (0.29 d^{-1})

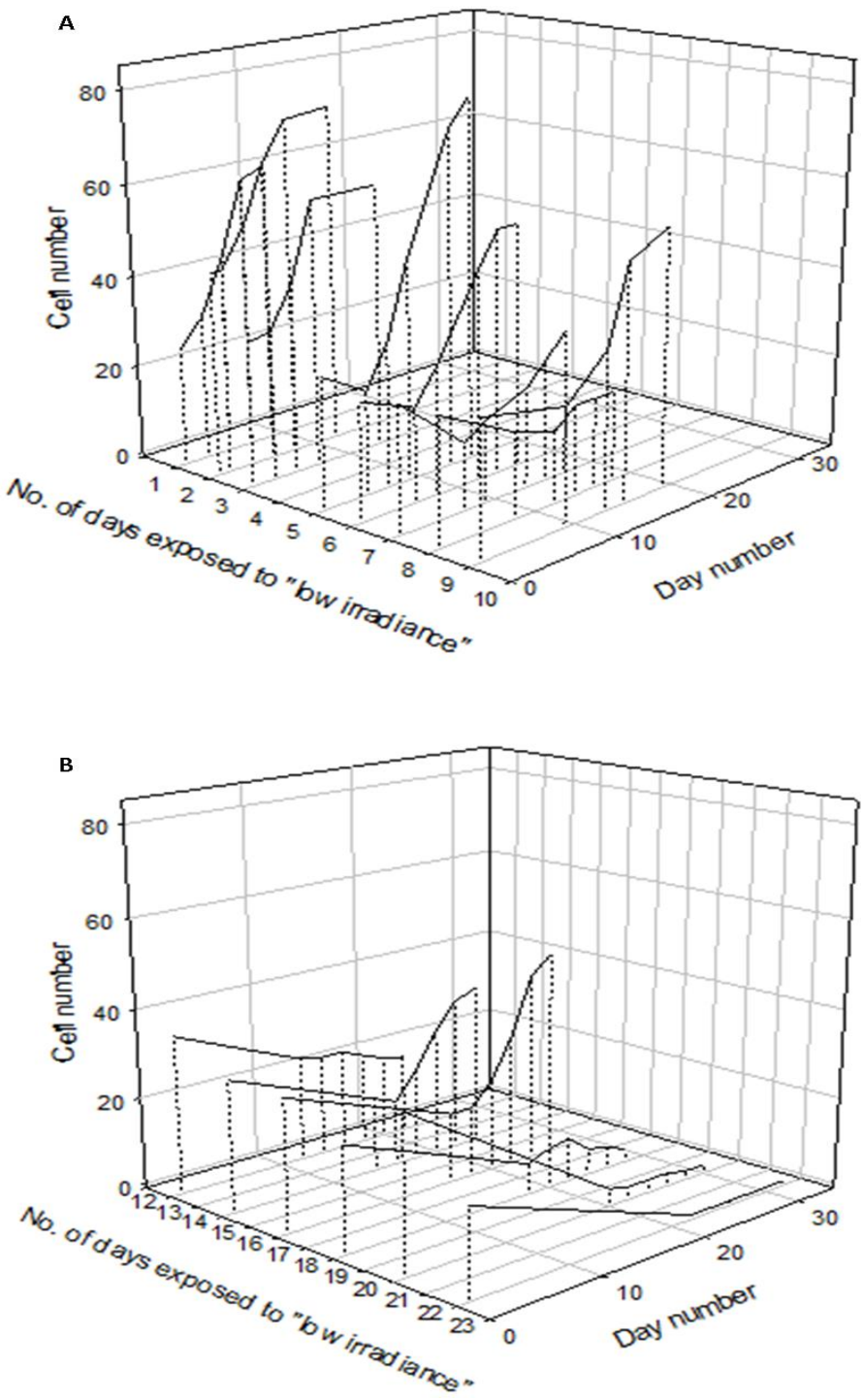

Fig.5.5. Growth curves of *N. hexacanthum* demonstrating the effect of exposure to "low irradiance" (2 µmol quanta m^{-2} s^{-1}) for between 1 and 9 days (A), and 12 and 22 days (B). Changes in cell numbers (y-axis) for each day that cells were moved to higher irradiance (z-axis, day 1-22) over the course of 32 days (x-axis) are shown. The second drop-line for each growth curve represents the point at which cells were moved from low irradiance (2 µmol quanta m^{-2} s^{-1}) to higher irradiance (60 µmol quanta m^{-2} s^{-1}).

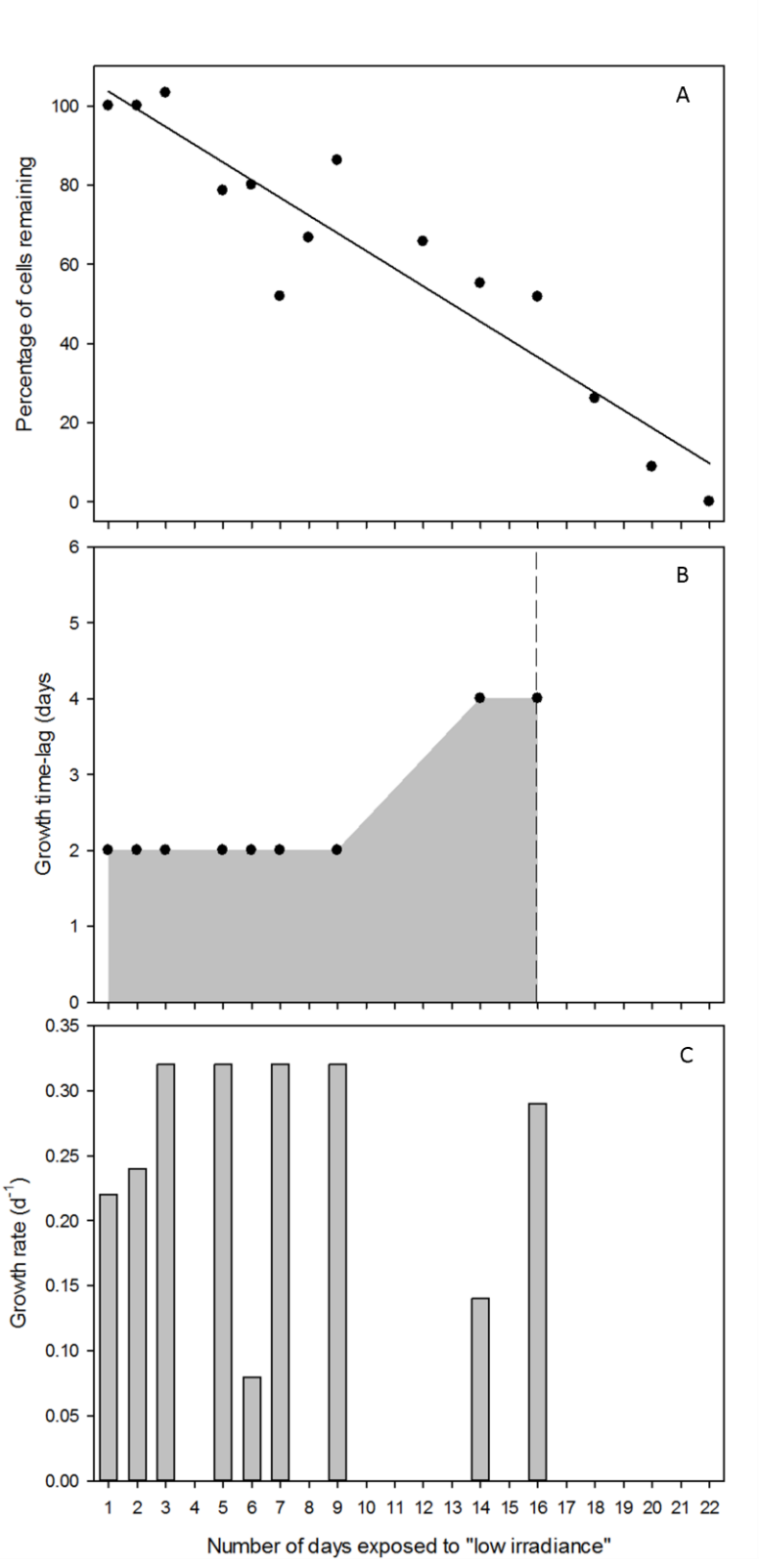

Fig. 5.6. Changes in the number of cells present (percentage remaining compared to day 1, A), time-lag in growth (B; dashed line represents maximum survival time), and growth rate (C) of *N. hexacanthum* cells exposed to low irradiance (2 µmol quanta m^{-2} s^{-1}) for 1-22 days.

5.4.5 Effects of phosphate limitation on the vertical migration patterns of *N. tripos*

N.tripos abundances increased from 80 to 148 cells over 21 days (Fig. 5.7A) when grown under replete nitrate concentrations (Fig. 5.7B), but limiting phosphate concentrations (undetectable, < 0.02 µM). This increase in abundance slowly decreased over the 21 day period. Nitrate (TON) concentrations mirrored this trend, decreasing from 23 to 15 µM between day 1 and 13, at which point they remained stable until day 21.

The decision was taken to split this 21 day experimental period into 3 equal time-periods to aid analysis of the data. This was predominantly based on nitrate removal rates from the culture (Fig. 5.7B): day 1 – 7 (relatively high removal), day 8 – 14 (reduced removal) and 15 – 21 (zero removal).

No clear patterns of *N. tripos* vertical distribution emerged when the vertical distribution of buoyant cells was compared, either, at different times of day (Fig. 5.8), or as phosphate became increasingly limiting (Fig. 5.9). Under both circumstances cells appeared to be evenly distributed throughout the measuring cylinder: 10 depths were monitored and the percentage of cells present was typically about 10 % at each depth. However, if the percentage of buoyant cells over the course of the experiment is looked at, a clear pattern emerges (Fig. 5.10). The percentage of buoyant cells remained stable (50-56 %) until day 13. After this there was a decrease to 32 % by day 17, and to 24 % by day 21. This change in buoyancy corresponds to the point at which cells are no longer growing (Fig. 5.7A) and where nitrate uptake appears to have stopped (Fig. 5.7B).

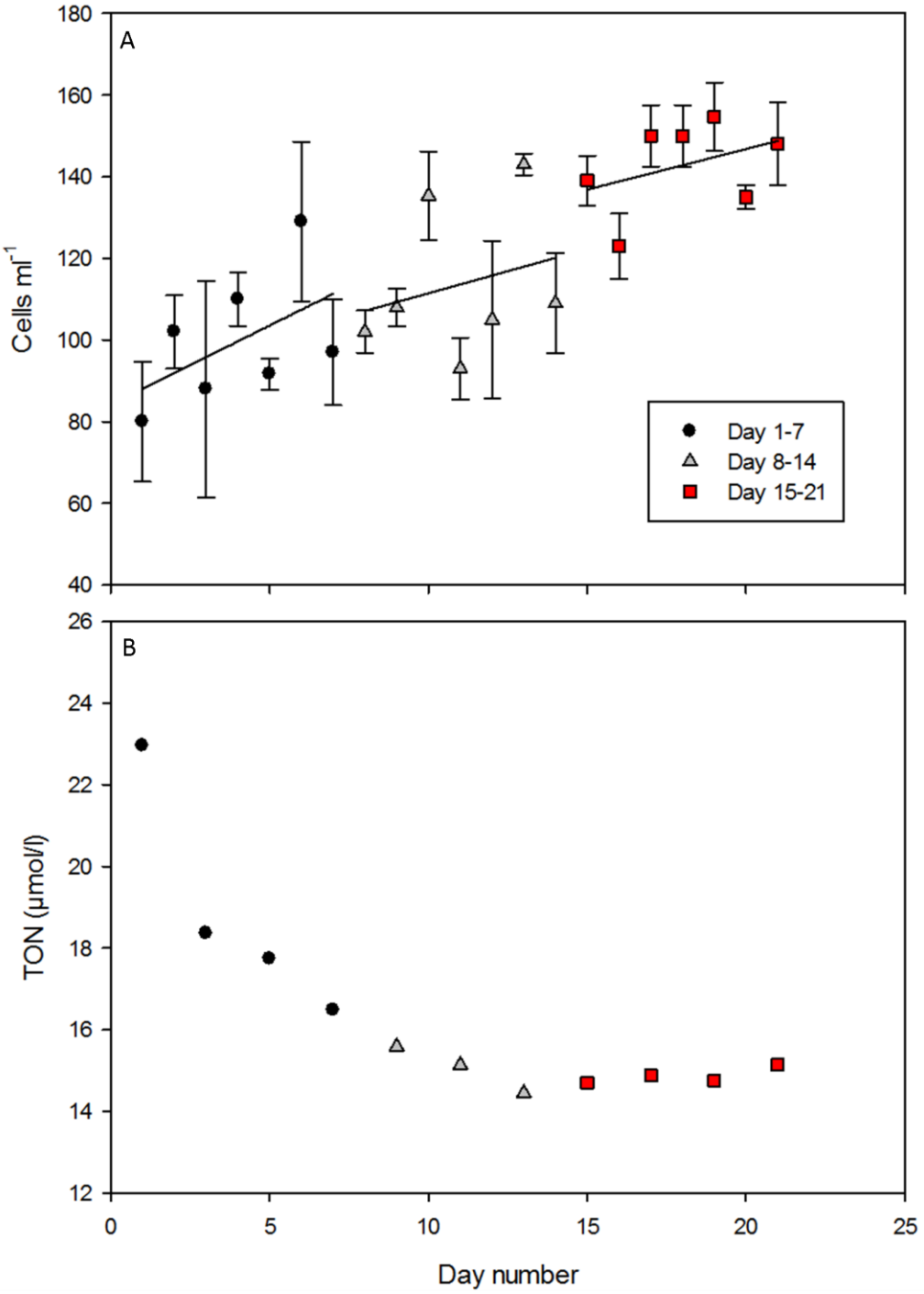

Fig. 5.7. Changes in cell numbers of *N. tripos* grown in phosphate depleted seawater over 21 days (A) and changes to nitrate (total oxidised nitrogen) over the same period of time (B). Phosphate concentrations remained at or below the detection limit (0.02 µM) throughout the experiment. Error bars for A represent the standard error of triplicate measurements.

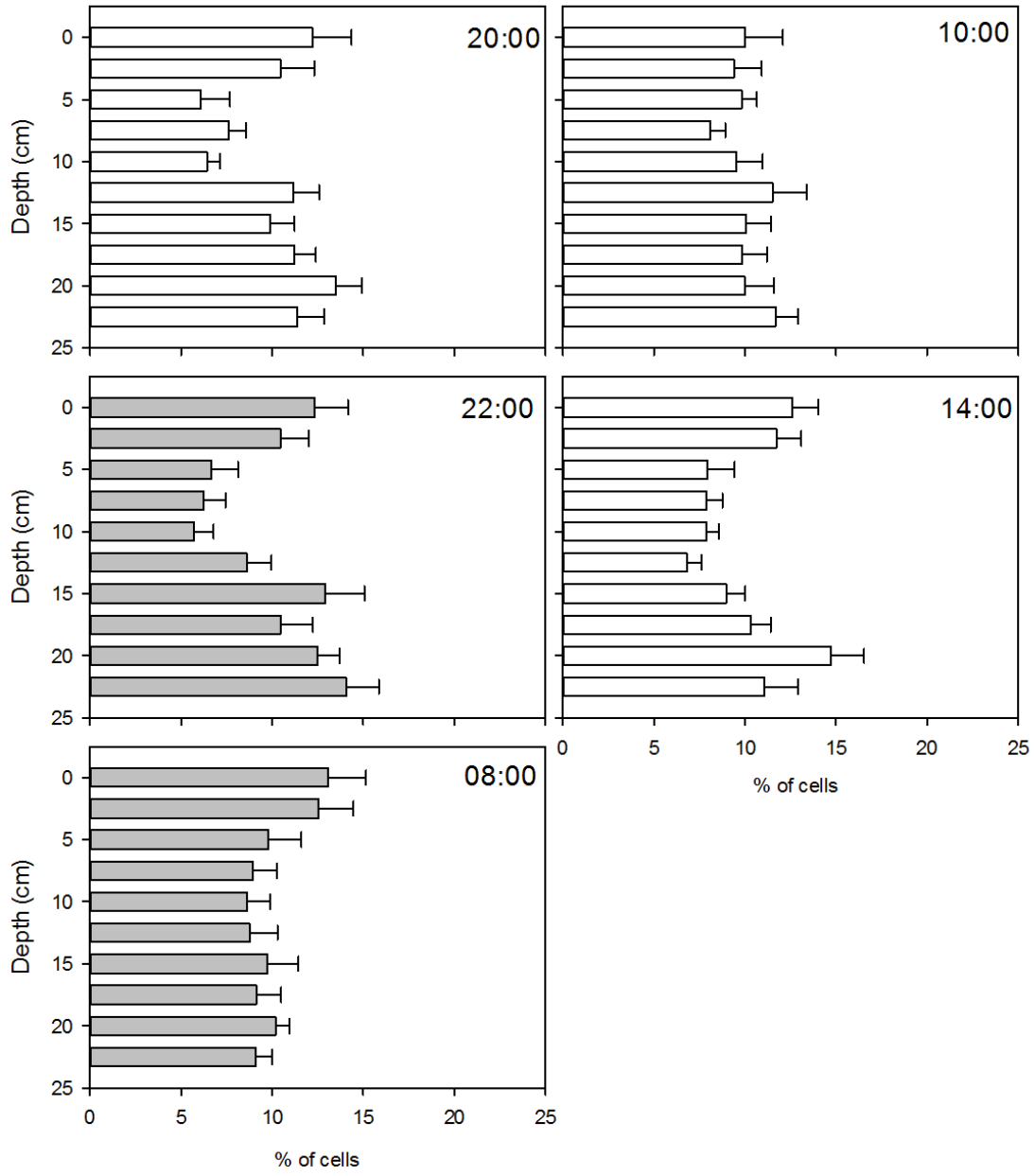

Fig. 5.8. Vertical distributions of *N. tripos* cells at different times of the day, averaged over the 21 day period of the experiment (day 4, 7, 10, 13, 17 and 21; see Appendix 4 for results from individual experiments). Grey columns represent periods in the dark; white columns represent periods in the light. Error bars represent the standard error of these averages.

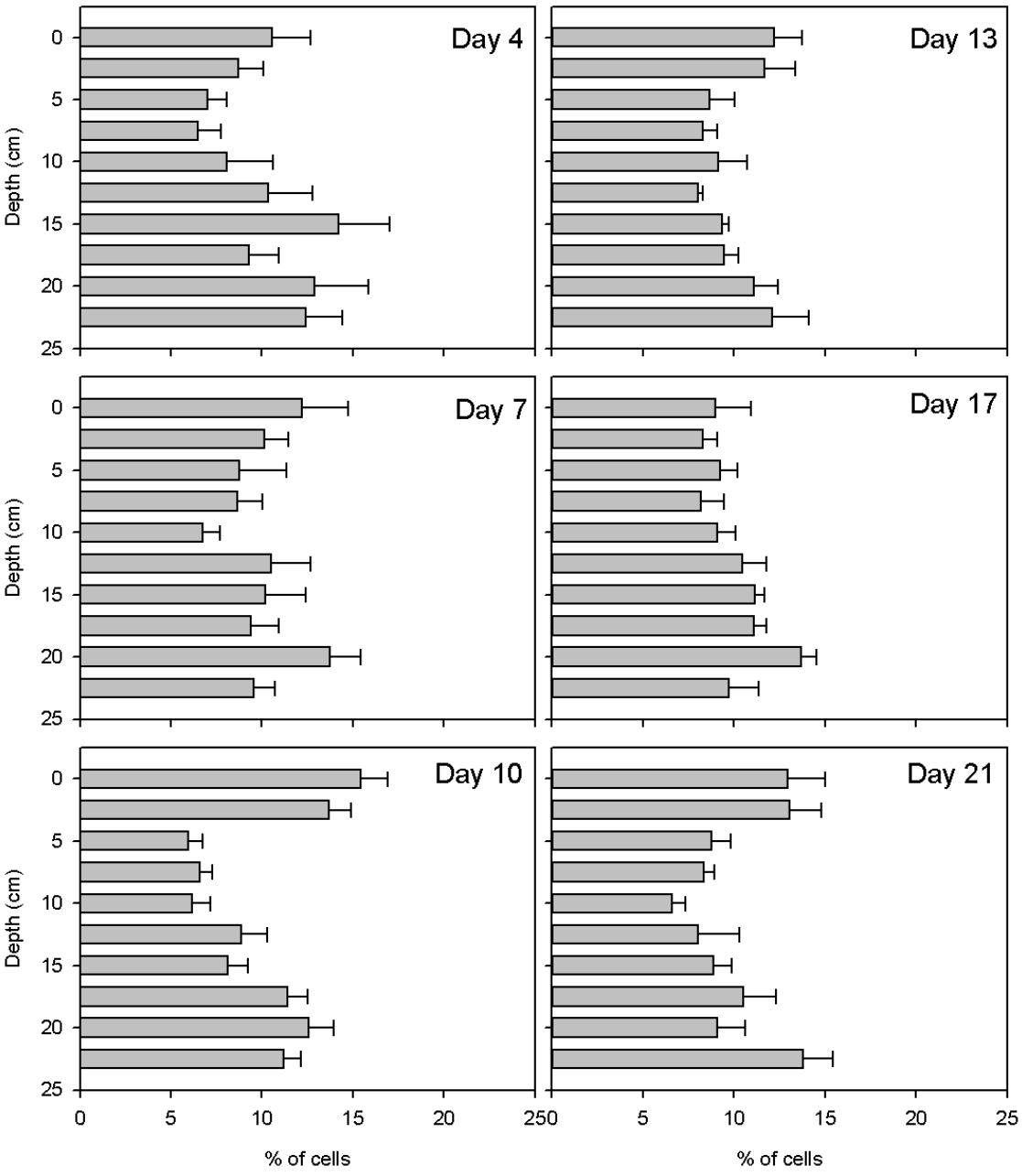

Fig. 5.9. Vertical distributions of *N. tripos* cells at various different time points in the experiment, averaged across all times of day (2000, 2200, 0800, 1000 and 1400). Error bars represent the standard error of these averages.

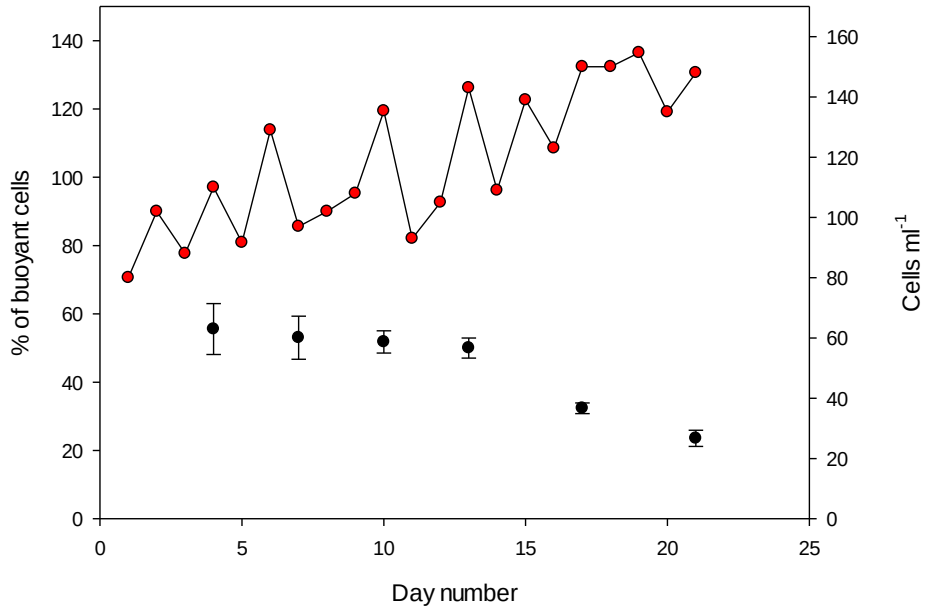

Fig. 5.10. Changes in the percentage of buoyant *N. tripos* cells (filled black circles) with increasing PO_4^{3-} limitation, inferred by comparing the average number of buoyant cells (Figs. 5.8 and 5.9) to total cell numbers (Fig. 5.7A). Error bars represent the standard error of triplicate cell counts. Shown for comparison is the total cell number (from Fig. 5.7A).

Amongst immotile cells, 97-98 % were non-buoyant (Fig. 5. 11) and had sinking speeds that ranged from 0.026 – 1 m hr^{-1}. However, there was little change in the sinking speed distributions with increasing phosphate limitation. There was, however, a significant increase in mean sinking speed between days 1-7 and 15-21, from 0.29 to 0.34 m hr^{-1} (t-test, D.F. = 1195, $P < 0.05$).

Amongst the motile cells, sinking speeds were lower (mean of 0.15 compared to 0.32 m hr^{-1}), and the majority of cells were buoyant (up to 42 %) (Fig. 5. 11). As phosphate became increasingly limiting there was a notable decrease in the number of the buoyant cells (0 – 0.025 m hr^{-1}). Beyond day 14 the percentage of cells in this category fell from over 40 % to less than 20 %, leading to a significant increase (t-test, D.F. = 655, $P < 0.05$) in the mean sinking speed, from 0.12 to 0.19 m hr^{-1} . Accounting for the error, this would result into an increase in mean sinking speed of 0.04–0.10 m hr^{-1}, or approximately 1 to 2.4 metres per day.

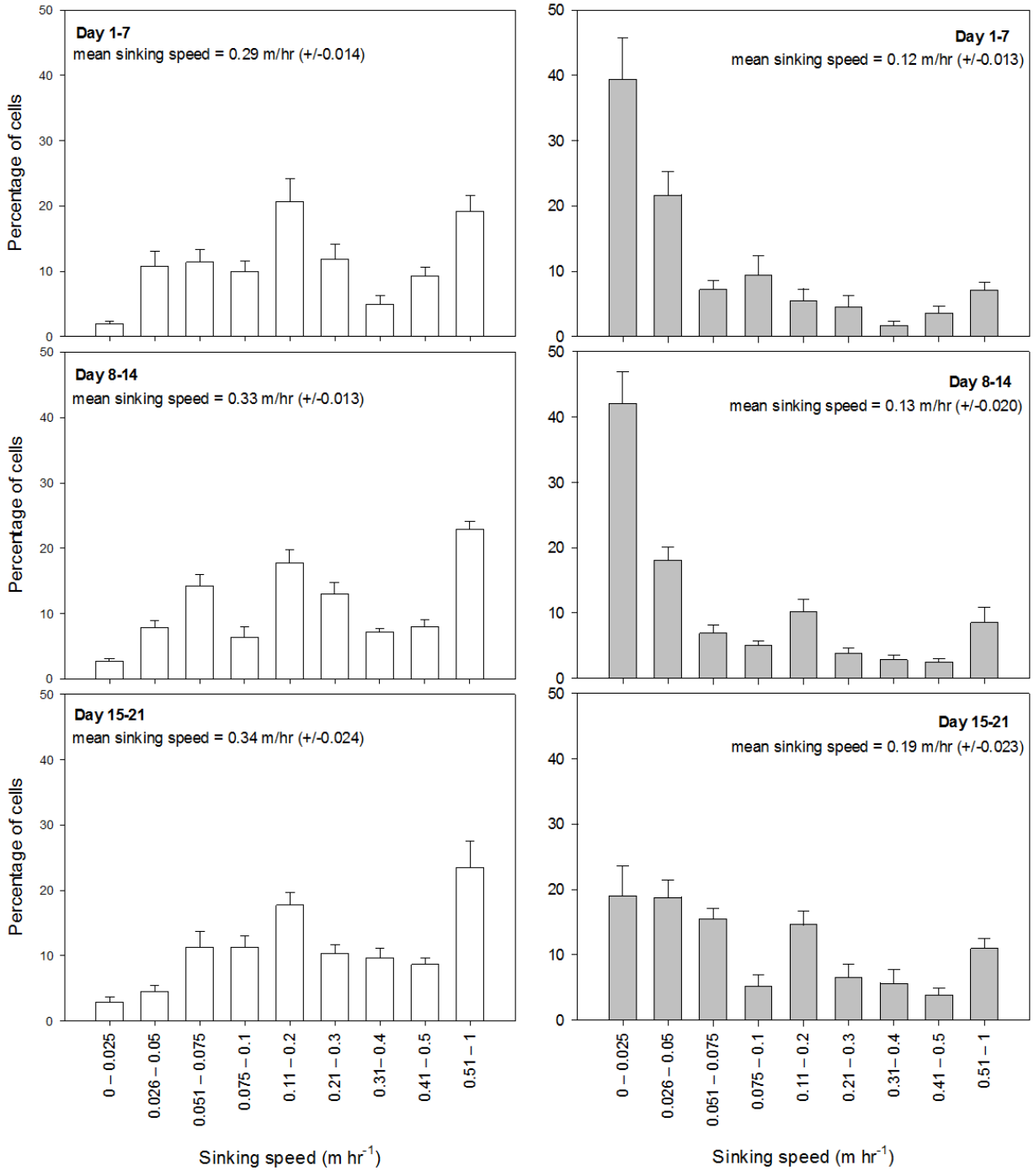

Fig. 5.11. Changes in the sinking rate distributions of immotile (white columns) and motile (grey columns) *N. tripos* cells with increasing PO_4^{3-} limitation (see Appendix 5 and 6) for results from individual experiments. Sinking rate distributions are grouped into three periods: day 1-7 (upper panels), day 8-14 (middle panels) and day 15-21 (lower panels). Error bars represent the standard errors of the seven days making up each group.

5.5 Discussion

These observations demonstrate that autotrophic growth of *Neoceratium* is possible when cells are exposed to nutrient concentrations representative of the nutricline in OSGs (starting concentrations: N, 2.1 µM; P, 0.05 µM). This finding agrees with previous work by Baek et al. (2008a) who showed that *N. furca* and *N. fusus* were able to grow in culture medium containing ≤1.0 µM NO_3^- and ≤0.1 µM PO_4^{3-}. Although the nutrient concentrations used were only confirmed in the experiment on *N. candelabrum*, the fact that the same experimental medium was used, and the same protocols for transferring cells from cultures to experimental flasks, for experiments on *N. hexacanthum*, suggests that starting nutrient concentrations in this experiment would also have been representative of the nutricline. Confidence can be placed in the fact that the increase in cell numbers observed was real, as the number of dividing cells, and *Fv/Fm* mirrored the pattern of growth observed for changes in cell numbers. The protein content of *N. hexacanthum* and *N. candelabrum* cells also remained constant whilst cell numbers were increasing, suggesting that the increase in cell numbers represented an overall increase in biomass. The mean growth rates observed in our experiments (*N. hexacanthum*, 0.14 d^{-1}; *N. candelabrum*, 0.28 d^{-1}) are similar to the *in situ* growth rates observed by Weiler (1980) for *Neoceratium* (genus) in the North Pacific subtropical gyre (0.09-0.16 d^{-1}) during summer/early autumn – a study that collected samples, from between 100 m and the surface, and estimated growth rates from the number of dividing cells. The growth rates seen in the current study are close to these values, suggesting that the relatively high growth rates observed by Weiler (1980) could be explained if cells were able to access the nutricline. However, as growth rates were calculated with only two data points, albeit from triplicate experimental flasks, there are large potential errors in the calculation of these values. This is a drawback of the "batch-culture" approach adopted here: using more data points was not possible due to the fact that growth slowed down quickly because of the low starting nutrient concentrations that were used,

To assess whether *Neoceratium* can grow at the irradiances associated with the nutricline, cells were cultured under a range of different irradiances (from 6 to 60 µmol quanta m^{-2} s^{-1}) on a 12:12 light/dark cycle. 22 µmol quanta m^{-2} s^{-1} appeared to be the compensation irradiance: below this value the growth of *Neoceratium* deteriorated (cell numbers decreased), with positive growth only occurring above this value. An alternative way to view this value would be in terms of the irradiance required over the course of a 24 hour period in order to balance photosynthesis with respiration (i.e. by converting 22 µmol quanta m^{-2} s^{-1}, delivered on a 12:12 L/D cycle, into a daily value). This gives a figure of 0.95 moles photons m^{-2} d^{-1}, which is approximately half the value determined for the dinoflagellate *G. tamerensis* by Langdon *et al.* (1987).

In the North Atlantic subtropical gyre (NAG), the mean depth at which this compensation irradiance of 22 µmol quanta m^{-2} s^{-1} occurs at midday is 85 m (see chapter 2); in the South Atlantic subtropical gyre (SAG) this depth is 108 m. However, the depth at which there are sufficient nutrients for growth occurs beyond 100 m in the NAG and 130 m in the SAG. The implications of this are that *Neoceratium* cannot grow at the irradiances present at the nutricline. Cells would need to change their position in the water column by at least 15 to 20 meters in order to take up nutrients at the nutricline (in reality, it would likely be greater than this due to the fact that these calculations are based on peak midday irradiances). This would require nutrient uptake to occur in the dark, which seems to be common among dinoflagellates (Paasche et al. 1984), especially when nutrient-limited. Not taken into account here, however, are shade species, also called “shade flora” or “knephoplankton” (poetically meaning “the wanderers of twilight”). Seven shade species of *Neoceratium* have been observed to inhabit deeper waters (reviewed by Sournia 1982), and it is proposed that they are adapted to low irradiances via a specific combination of shape, size and number of chloroplasts, varying depending on the species in question. Although these species may be able to avoid migration, not all *Neoceratium* species found within OSGs are “shade species”, so this adaptation can only partly explain how this genus is able to cope with the vertical separation of light and nutrients in OSGs.

Neoceratium cells are unlikely to migrate more than 15 to 20 m in a single diurnal cycle as maximum reported swimming speeds for *Neoceratium* are just

under 1 m h^{-1} (Whittington et al. 2000; Baek et al. 2009). Therefore, VM only seems likely if triggers other than light are involved. Before considering the trigger(s) that may be involved the survival time of cells at reduced irradiances were determined in order to estimate the maximum time and distance over which migrations could take place. At the nutricline most cells receive <9 µmol quanta m^{-2} s^{-1} at midday (see chapter 2). As this is the time when irradiances are at their peak, the average value received during daylight hours will actually be significantly lower than this. Here, survival time of *N. hexacanthum* at 2 µmol quanta m^{-2} s^{-1} (on a 12:12 light/dark cycle) was tested in order to determine likely survival times of *Neoceratium* at nutricline light intensities. The longest survival time recorded was 16 days, at which point >50 % of the original cells remained. There was no survival beyond 16 days, and by 22 days all cells had disappeared – leading up to this point, cells noticeably began to deteriorate: horns disappeared and cells reduced in size and lost definition. Although the time-lag in growth increased beyond 9 days, there were no lasting impacts on growth rates. In a different study Baek et al. (2008c) found that *N. furca* and *N. fusus* could survive in total darkness for up to 15 days. However, this was based on observations of movement – they only observed regrowth of cells after up to 10 days of dark exposure. Our results show that under very low irradiances the viability time of *Neoceratium* is markedly increased from 10 to 16 days, which would give *Neoceratium* a total time of over 2 weeks to complete a migration from the euphotic zone to the nutricline and back.

There is evidence from this present study to suggest that the trigger for such migrations may be related to phosphate, supporting similar suggestions made by Heaney and Eppley (1981) and Taylor et al. (1988). In experiments on *N. tripos*, where the upper section of a cylinder was horizontally illuminated, there was no evidence of VM occurring, but a decrease in the number of buoyant cells (by 25 – 30 %) was observed once phosphate became limiting. Perhaps VM was not observed because horizontal illumination does not provide a sufficient "light gradient" for *Neoceratium* to follow, although other authors (e.g. Weiler and Karl 1979) have successfully observed DVM using this method in the past. Another explanation may be that the light intensity used was not high enough. Others, who have successfully observed VM, have studied illuminated conditions where high irradiances of 232 to >1000 µmol quanta m^{-2} s^{-1} have

been used (Heaney and Eppley 1981; Baek et al. 2009), whereas a maximum irradiance of 60 µmol quanta m^{-2} s^{-1} was used here. It is difficult to see, however, why *Neoceratium* would not respond to these irradiances, especially as these irradiances are more relevant to the light values that would be found at the base of the euphotic zone in OSGs. One final explanation may be related to inter-specific differences in migratory behaviour. Baek et al. (2009) demonstrated that VM coincides with the light regime for *N. furca* but not *N. fusus*, and found the difference to be related to swimming behaviour: *N. furca* swam faster during the light period, but the swimming speed of *N. fusus* was constant irrespective of the light environment. The implication of this is that downward migration may result from a reduction in swimming activity. Results presented are consistent with this: when comparing the mean sinking rates of motile and non-motile cells, sinking rates of the non-motile cells were consistently twice as fast as the motile cells.

Initially, there was an increase in the mean sinking speed of immotile cells, suggesting some aspect of *Neoceratium* cell physiology, unrelated to motility, was causing the cells to sink faster. One possible explanation is that cell size increased due to phosphate-limitation as has previously been observed in *N. furca* (Smalley et al. 2003). However, this increase in sinking speed was not observed in the motile cells during the same time-period (up to day 14), suggesting that this increased tendency to sink was overcome by cell motility. Beyond day 14, however, a difference in the sinking speeds of motile cells was observed: the number of "buoyant" cells decreased by more than 20%, and the mean sinking speed increased by 54 %. Changes in the distribution of sinking speeds, during this period, were not observed in immotile cells, implying that these changes were related to changes in swimming behaviour. The changes observed in mean sinking speed would cause cells to increase their sinking speed by 0.24 to 2.4 m d^{-1}, but if cells became totally immotile, and yet still viable (able to regrow when nutrients were encountered), sinking rates could potentially be >20 meters per day.

If all these findings are combined with what is already known about *Neoceratium* VM, speculations can be made about how VM within OSGs may function:

1) Under non nutrient limited conditions, cells show positive photo-taxis during the day (whilst avoiding strong surface irradiances), maintaining cells in surface waters – the rate of upward migration (0.58 to 0.97 m hr^{-1}; Whittington et al. 2000) is easily high enough to overcome the mean rate of sinking in nutrient-replete cells (mean, 0.11 to 0.13 m hr^{-1}; present study).

2) When nitrate becomes limiting, cells descend earlier in the day (Heaney and Eppley 1981). However, this is still probably not sufficient for cells to reach the nutricline, given its depth below the euphotic zone (>15 metres) and the mean sinking rate of cells (mean, 0.11 to 0.13 m hr^{-1}).

3) When phosphate becomes limiting, positive photo-taxis ceases (Heaney and Eppley 1981; Taylor et al. 1988) and cells become less motile due to a lack of ATP (this occurs after approximately 14 days; present study), causing them to sink towards the nutricline. This could potentially occur at a maximum rate of 24 m d^{-1} in some cells, but initially proceeds at a much lower rate (0.24 to 2.4 m d^{-1}). Density differences associated with the pycnocline prevent cells from sinking below this point in stratified waters of OSGs (Blasco 1978; Whittington et al. 2000).

4) Beyond 14 days, provided the nutricline is reached in a time frame that allows cells to remain viable – up to 12 additional days without nutrients (Aldridge et al. 2014) – cells take up nutrients until a point where ATP concentrations restore motility and positive photo-taxis resumes.

5) Photo-taxis returns cells back to irradiances where growth is possible. Based on an upward migration rate of 0.58 to 0.97 m hr^{-1} (Whittington et al. 2000), for 12 hours of daylight, this would allow cells to move upwards by approximately 7 to 12 meters per day. Taking into account that cells would sink during the dark, at a rate of 0.11 to 0.13 m hr^{-1}, it is calculated that cells would be able to return to a euphotic zone, 30 m above the nutricline, in 3 to 5 days. In the above scenario, cells only

remain viable if total migration times to and from the nutricline do not exceed 2 weeks.

6) Normal DVM patterns in surface waters would resume, in response to the light regime, until a point where cells became phosphate-limited again.

5.6 Conclusion

Here it is demonstrated that *Neoceratium* are able to grow at nutrient concentrations that are typical of the nutricline in OSGs. However, at light intensities found here growth is not possible. In order to access sufficient light and nutrient concentrations *Neoceratium* would need to vertically migrate between the euphotic zone and the nutricline. These migrations could take place over a maximum time-period of two weeks, as this is the amount of time cells are able to survive at the low irradiances associated with the nutricline. A VM mechanism where phosphate limitation is the primary controlling factor is proposed based on observations that phosphate limitation causes cells to sink at a faster rate.

6. Summary and Conclusions

In this thesis attempts have been made to answer the question: how do *Neoceratium* grow and survive in oligotrophic subtropical gyres.

In Chapter 2 it was demonstrated that *Neoceratium* are present all year round in surface waters of oligotrophic subtropical gyres (OSGs), with peak abundances occurring in June. In surface waters, where irradiances are high enough to support growth, average nitrate and phosphate concentrations were shown to be low (nitrate, <0.5 µM; phosphate, <0.08 µM).

In Chapter 3 the ability of *Neoceratium* to survive and grow at nutrient concentrations found in OSG surface waters was tested. No growth was observed at these low nutrient levels; however, some cells were able to survive up to 26 days of "nutrient starvation", with cells beginning to show signs of stress after 10 days without nutrients.

In Chapter 4 unsuccessful attempts to observe *Neoceratium* feeding on a variety of prey organisms were documented. Some of the theoretical aspects of how mixotrophy may function in OSGs were considered: it was demonstrated that large areas of OSG surface waters have N:P ratios that would trigger mixotrophy in *Neoceratium*. An estimate was made of the number of ciliates that *Neoceratium* cells would need to be ingested for survival, and it was shown that this could be achieved in some, but not all, areas of the NAG and SAG.

In Chapter 5 the feasibility of *Neoceratium* using vertical migration (VM) to access nutrients was examined. The ability of cells to survive at nutrient concentrations typical of the nutricline was confirmed, and the need to migrate was established by showing that growth is not possible at irradiances found at the nutricline; the nutricline lies at least 15 metres below irradiances at which *Neoceratium* are able to grow. Evidence was presented that suggests phosphate limitation would, via reduced motility, provide a cue for vertical migration in OSGs.

The challenge remaining is to establish how all of these findings combine to further our understanding of *Neoceratium* nutrient acquisition in OSGs. Below, a conceptual model demonstrates the various mechanisms by which a single *Neoceratium* cell in OSGs may obtain sufficient inorganic nutrients required for survival and growth (Fig. 6.1).

According to the conceptual model, a single non nutrient-limited cell inhabits the euphotic zone. It is maintained there by positive phototaxis during the day, but sinks towards the nutricline at night (Heaney and Furnass 1980; Taylor et al. 1988; Whittington et al. 2000). The cell is unable to grow at the inorganic nutrient concentrations (nitrate or phosphate) in surface waters (whether organic nutrient concentrations are high enough to support growth is a question that future studies need to address) and the nutricline is too deep to be reached by diurnal vertical migration, even when cells descend earlier in the day due to nitrate limitation (Heaney and Eppley 1981). If the concentration of ciliates is high enough, or if nutrients are abundant due to a recent upwelling event, cells will remain in this "healthy" state. However, under normal non-upwelling conditions, or when ciliate prey concentrations drop below those required to maintain sufficient predator/prey encounters, the cell will start to become nutrient limited. At this point, the ingestion rate of the *Neoceratium* cell begins to increase (Smalley and Coats 2002; Smalley et al. 2003) and this may be sufficient to counteract the reduction in prey density; if the cell can feed on just a single ciliate this would likely be sufficient to return it to its original "healthy dividing" state. If this increased feeding rate is not sufficient to lead to the capture of prey, and higher prey densities are not encountered, the cell becomes increasingly nutrient limited. Beyond 10 days of nutrient limitation its chance of survival steadily begins to decrease, up until day 26 when it reaches zero (Aldridge et al. 2014). At any point in this period the cell may encounter and ingest a ciliate, returning it to a state where nutrient limitation is reduced or eradicated. Beyond 14 days, phosphate becomes limiting and the cell stops performing phototaxis (Heaney and Eppley 1981; Taylor et al. 1988) and begins to lose buoyancy due to reduced motility brought about by a lack of ATP. The cell begins to sink towards the nutricline, and this sinking rate increases as the cell becomes less motile. At this point, the cell is destined to reach the nutricline unless nutrients are encountered from another source (via prey or upwelled nutrients) – in which case

intracellular nutrient concentrations are restored, phototaxis resumes and the cell returns to the euphotic zone. If prey is not encountered and ingested, the cell reaches the nutricline, where sinking is impeded by density differences at the pycnocline (Blasco 1978; Whittington et al. 2000). The cell takes up nutrients at the nutricline and returns to the euphotic zone. If the nutricline is too deep, nutrient limitation will have led to the death of the cell after approximately 12 days of the cell first beginning to lose buoyancy. Total migration to the nutricline and back must not exceed 16 days – the maximum amount of time that the cell can survive being exposed to the low light irradiances found here.

It is difficult to comprehensively test the conceptual model presented in Fig. 6.1 *in situ* with current techniques. However, it is possible to predict the implications of this theory and then to observe whether those implications actually occur. For example, in a scenario where all other things are equal (nutricline depth, limiting nutrient concentrations, depth of euphotic zone etc.) areas with lower concentrations of ciliates should correspond with areas where *Neoceratium* occurs deeper in the water column: the assumption being that in locations where nutrients are not being obtained from prey ingestion, more cells will be nutrient limited and therefore have reduced motility and buoyancy. It may even be possible to put a precise number on the prey concentrations that would lead to *Neoceratium* occurring at deeper depths. In this study, based on the nitrogen requirements for *Neoceratium* and the nitrogen content of ciliates (back-calculated from protein measurements), a broad estimate for a minimum ingestion rate of 0.01-0.44 ciliates day^{-1} was calculated for *Neoceratium* to survive in OSGs – this would equate to approximate *in situ* prey concentrations of 100 to 4400 cells L^{-1}, which is a very large range. It would be useful to further constrain this estimate by a) performing a greater number of measurements on protein content (or ideally N-content) of *Neoceratium* cultured under OSG conditions, and b) by determining exactly which ciliates *Neoceratium* feed on in OSGs, and then obtaining estimates for how much protein (or N) these species contain. In order to do this, a method for accurately quantifying prey items from *in situ* samples is required. Perhaps the most likely breakthrough would be the design of fluorescence in-situ hybridisation (FISH) probes for the full range of ciliates that are encountered in the OSGs.

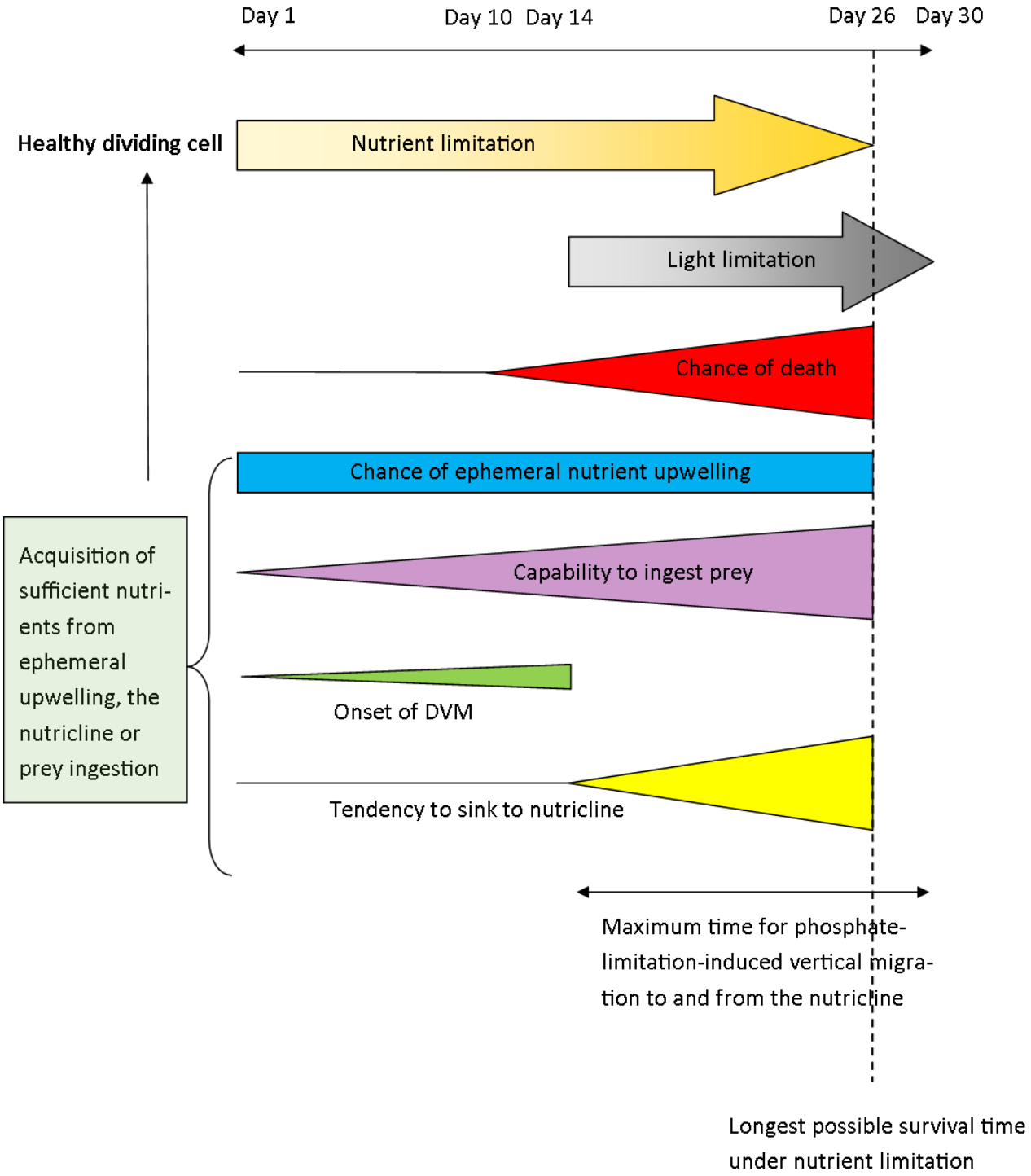

Fig. 6.1. A conceptual model, based on previous studies and data from this thesis, demonstrating the various mechanisms by which *Neoceratium* in oligotrophic subtropical gyres are likely to obtain inorganic nutrients required for survival and growth.

It appears that the key adaptation that *Neoceratium* possesses is the ability to survive long periods of time without nutrients, providing them with the time to exploit nutrients from other sources, whether those sources of nutrients are from phagotrophy, vertical migration, dissolved organic nutrients or ephemeral upwelling. Whilst phagotrophy and vertical migration have been the subject of a number of studies, the use of dissolved organic nutrients and nutrients from ephemeral upwelling need to be understood more fully. Studies suggest that *Neoceratium* can utilise both DOP and DON, but what needs investigating is whether *Neoceratium* are capable of growth at DON and DOP concentrations found in the OSGs. There is also a need to understand the role of ephemeral upwelling more fully, especially given its potential impacts on ciliate concentrations (chapter 4) – It is foreseeable that ephemeral upwelling benefits mixotrophs initially though increased inorganic nutrient concentrations, and then subsequently through increased prey concentrations. Johnson et al (2010) in one of the few long-term *in situ* studies looking at this phenomenon, using a profiling float with a sample frequency of 5 days, showed that in the North Pacific subtropical gyre episodic fluxes of nitrate (greater than 1 μM) into the euphotic zone occur with a frequency of about once per month. Studies like this are a vital step in understanding the role of ephemeral upwelling in supporting primary production in OSGs. However, its resolution (5 days) potentially leads to some upwelling events being missed. What are required are new methodologies that allow for the continuous monitoring of *in situ* nutrient concentrations, along with the response of the phytoplankton community (e.g. biomass and community composition) to these nutrient influxes.

Appendices

Appendix 1: Seasonal abundance patterns of *Neoceratium* (genus) in the North Atlantic Ocean standard CPR zones that were combined into 5 larger zones (Zones 1-5). Below the figure, a table shows the results from a Kruskal-Wallis one-way ANOVA on ranks performed on the standard CPR areas combined into each zone.

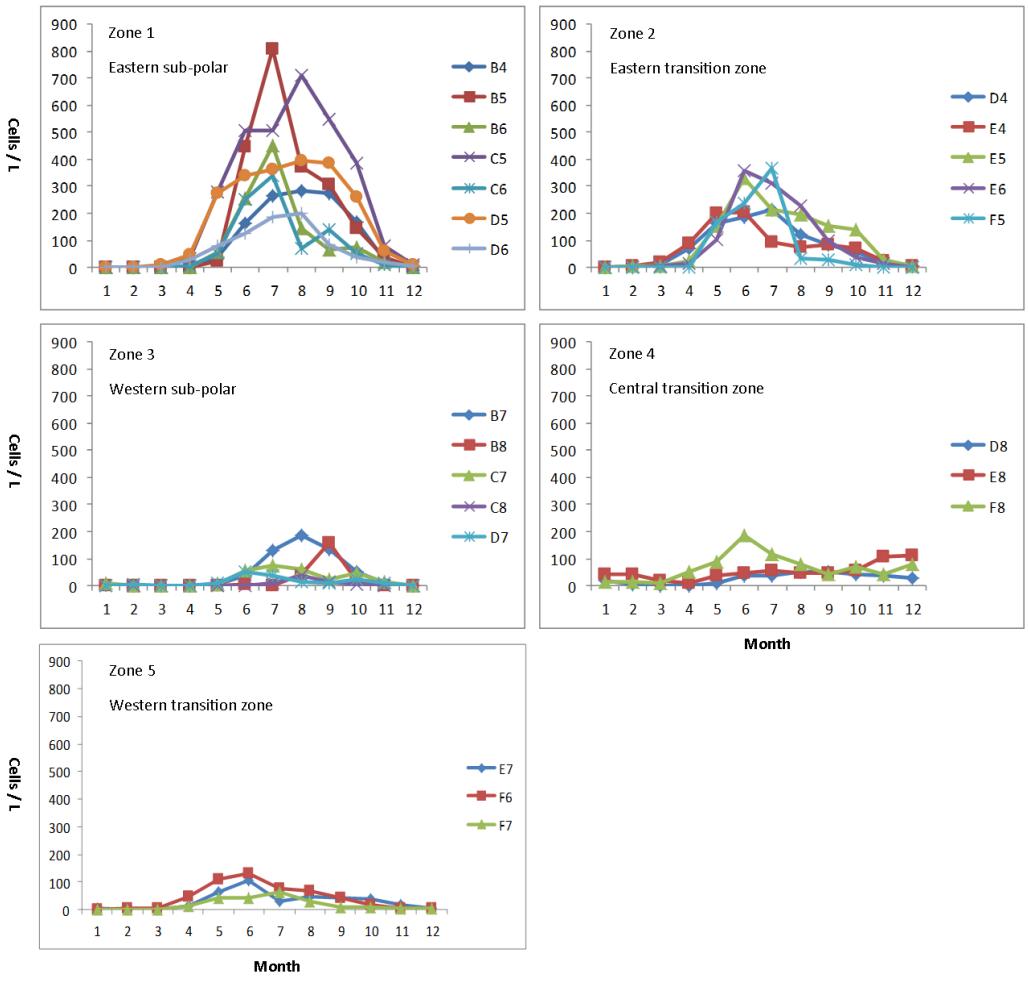

Zone Number	Degrees of Freedom	P value	Significant difference
1	6	0.42	No
2	4	0.64	No
3	4	0.11	No
4	2	0.02	Yes
5	2	0.22	No

Appendix 2: Table showing the differences in experimental design between mixotrophy experiments.

Prey	**Reason for choice of prey**	***Neoceratium* spp. tested**	**Initial nutrients**	**Evidence of mixotrophy**
R. marina	-Right size for ingestion -Easy to observe as has orange fluorescence	*N. hexacanthum* *N. candelabrum*	NUSW	No
M. rubrum	-Ingested in previous studies (see table 4.2) -Easy to observe as has orange fluorescence	*N. tripos*	K/75	No
Flourescent microbeads	-Right size for potential ingestion via flagellar pocket -Used in previous studies with some success (e.g. Zhang et al. 2011) -Easy to observe as have bright green fluorescence	*N. hexacanthum* *N. candelabrum* *N. horridum*	NAGSW	No
Synechococcus	-Suggested prey of freshwater species, C. hirundinella (Callieri et al. 2006) -Easy to observe as has orange fluorescence	*N. hexacanthum*	K/5 (-P)	No

Appendix 3: Details of cultures maintained

Species	Origin	Strain	Isolated	Media
Neoceratium candelabrum	Gulf of Villefranche, Med. Sea (point B, 0-80m)	P10B2	06/12/2007	K/5
N. hexacanthum	Gulf of Villefranche, Med. Sea (point B, 0-80m)	P37C2	09/12/2008	K/5
N. horridum	Unknown	Unkown	Unknown	K/5
N. tripos	Plymouth, Station L4, (0-20m)	NA	11/10/2012	K/5
Rhodomonas marina	Unknown	Unkown	Unkown	F/20
Isochrysis galbana	Unknown	Unknown	Unknown	F/20
Mesodinium rubrum	Denmark (from lab of Per Juel Hansen)	Unkown	Unkown	K/5
Teleaulax sp.	Denmark (from lab of Per Juel Hansen)	Unkown	Unkown	K/5
Synechococcus	Unknown	Unknown	Unknown	K/5

Appendix 4: Vertical distributions of *N. tripos* cells at different times of the day, from day 4, 7, 10, 13, 17 and 21. Grey columns represent periods in the dark; white columns represent periods in the light.

Day 4

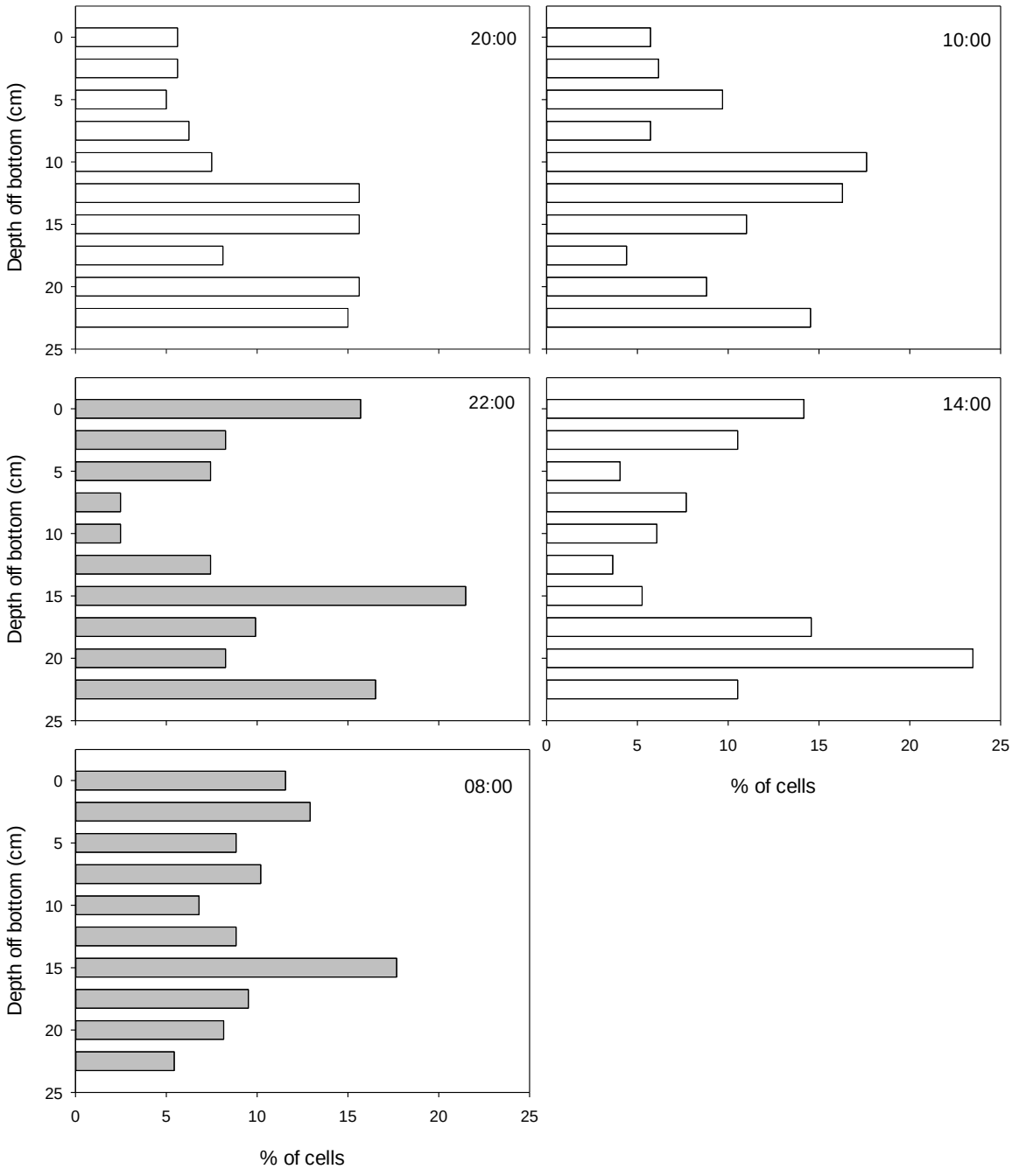

Day 7

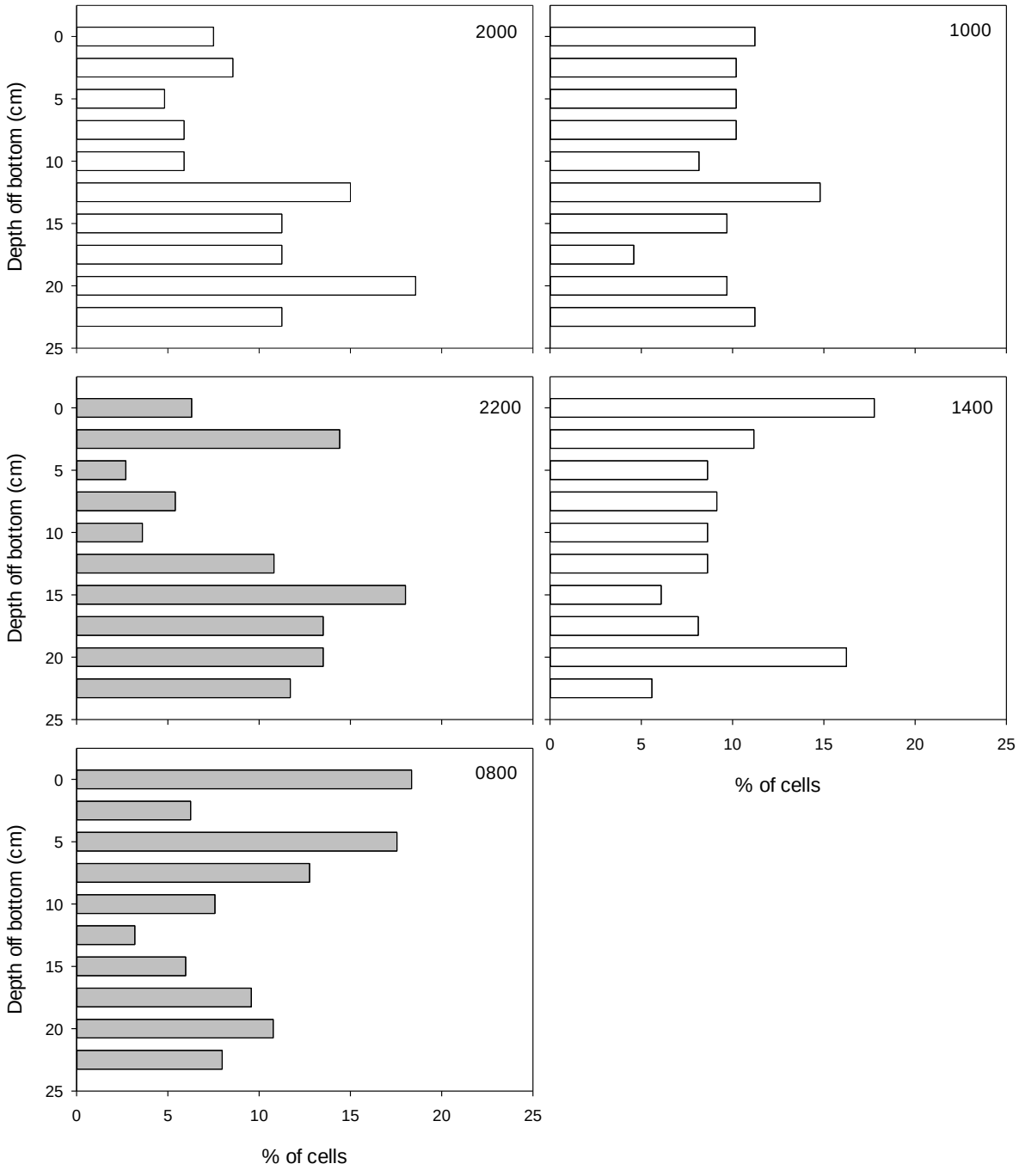
2000
1000
2200
1400
0800
Depth off bottom (cm)
0
5
10
15
20
25
% of cells

Day 10

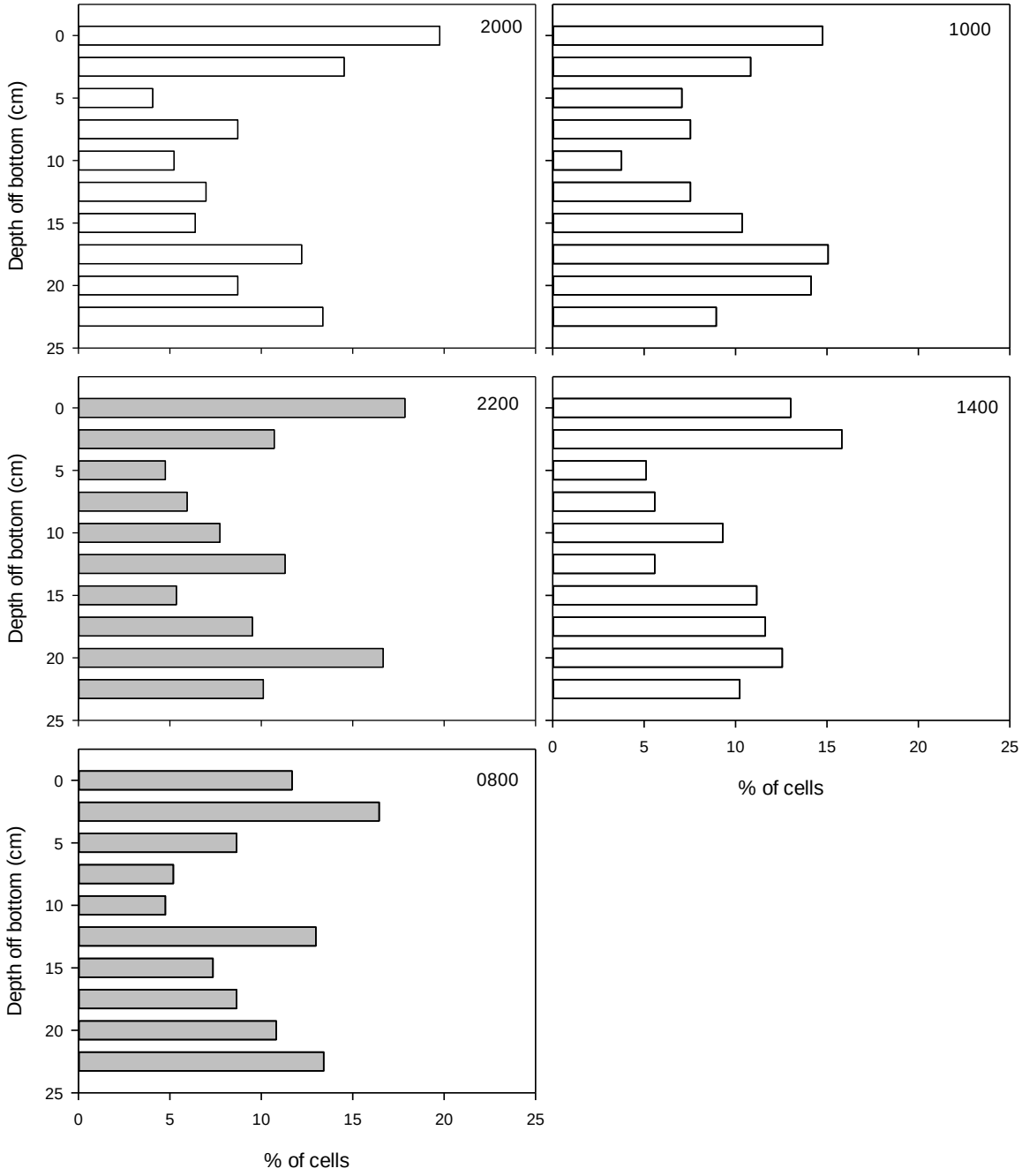
2000
1000
2200
1400
0800
Depth off bottom (cm)
0
5
10
15
20
25
% of cells

Day 13

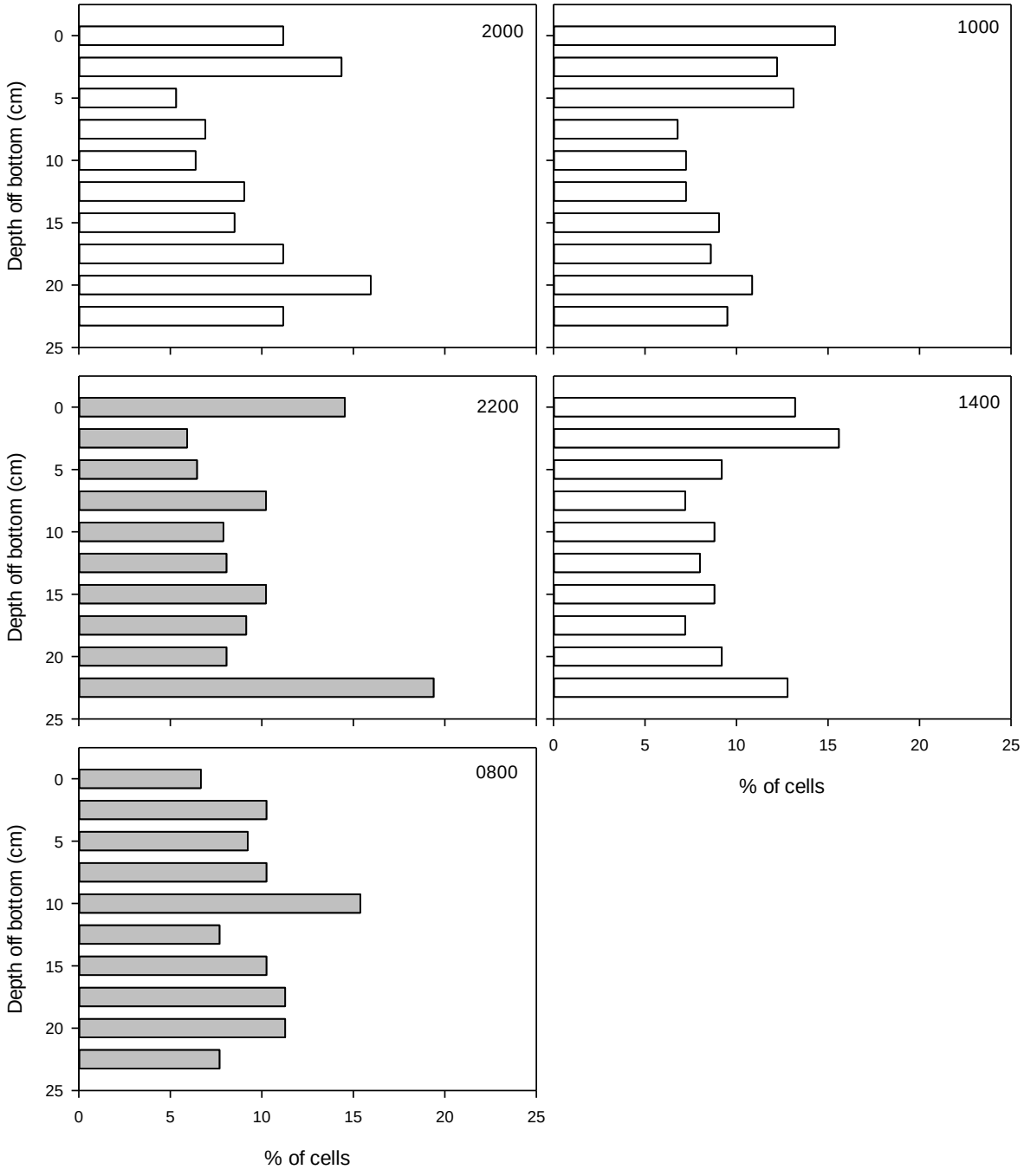
2000
1000
2200
1400
0800
Depth off bottom (cm)
0
5
10
15
20
25
% of cells

Day 17

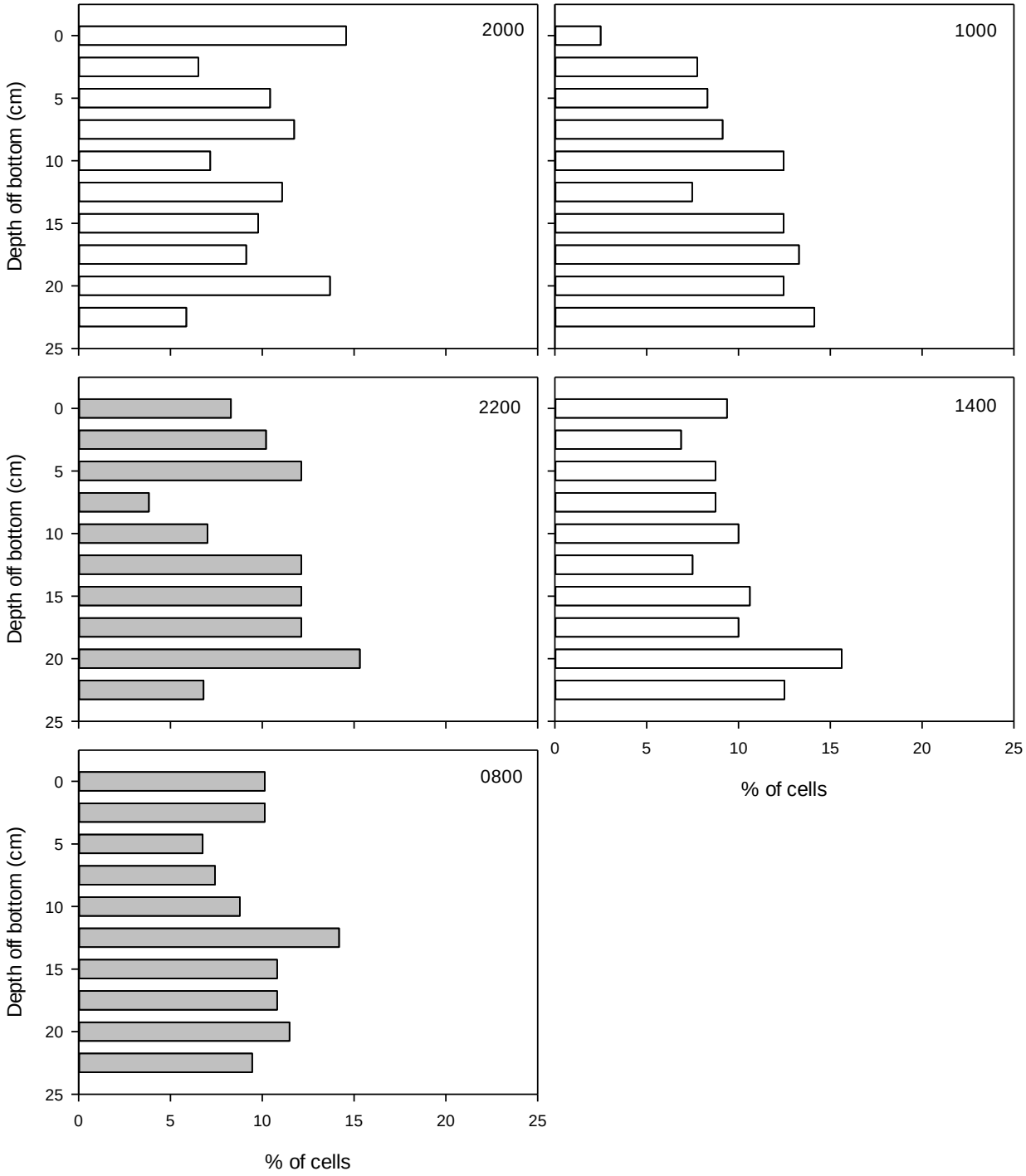
2000
1000
2200
1400
0800
Depth off bottom (cm)
0
5
10
15
20
25
% of cells

Day 21

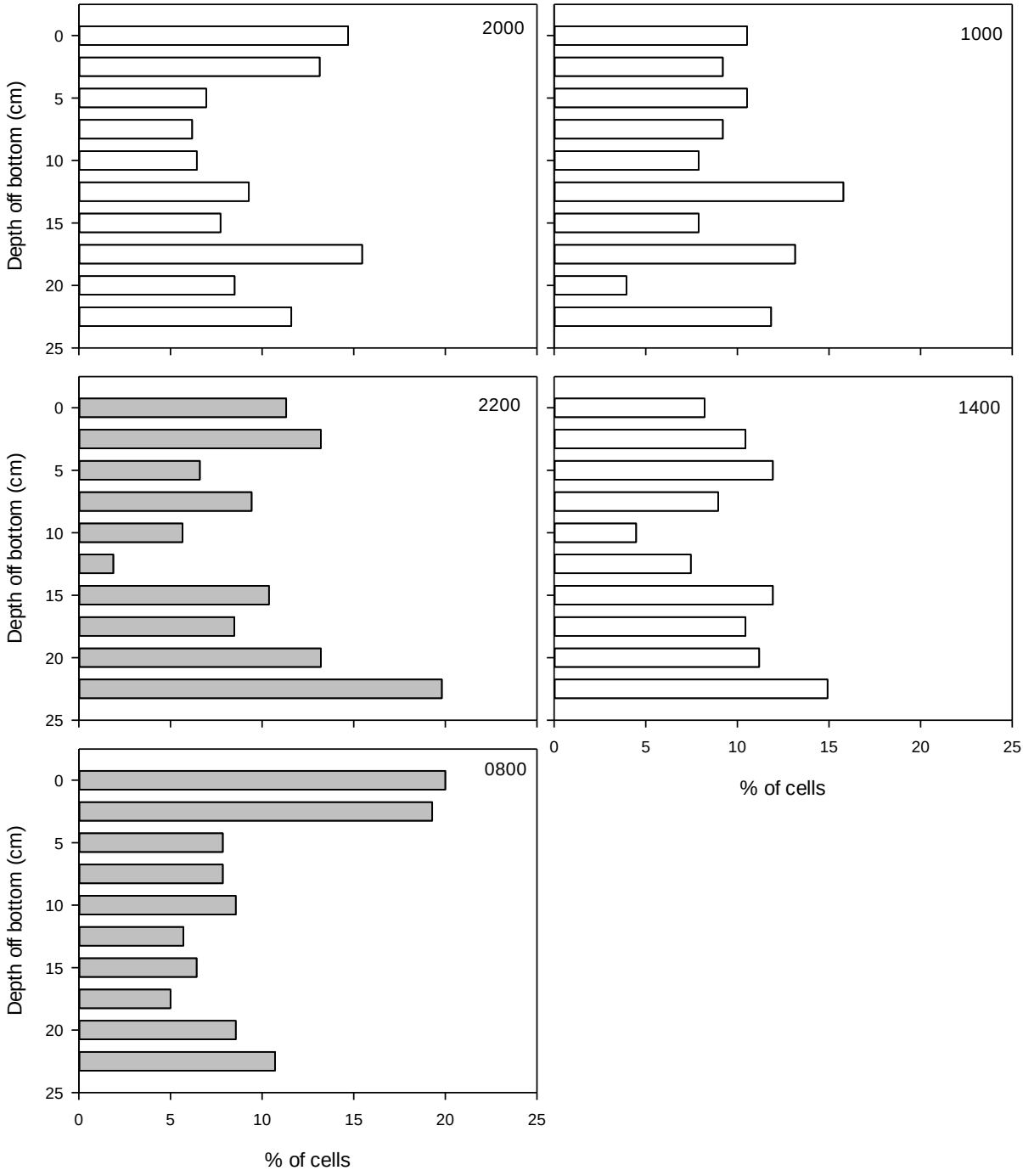
2000
1000
2200
1400
0800
Depth off bottom (cm)
0
5
10
15
20
25
% of cells

Appendix 5: Changes in the sinking rate distributions of immotile *N. tripos* cells with increasing PO_4^{3-} limitation between day 1 and 21.

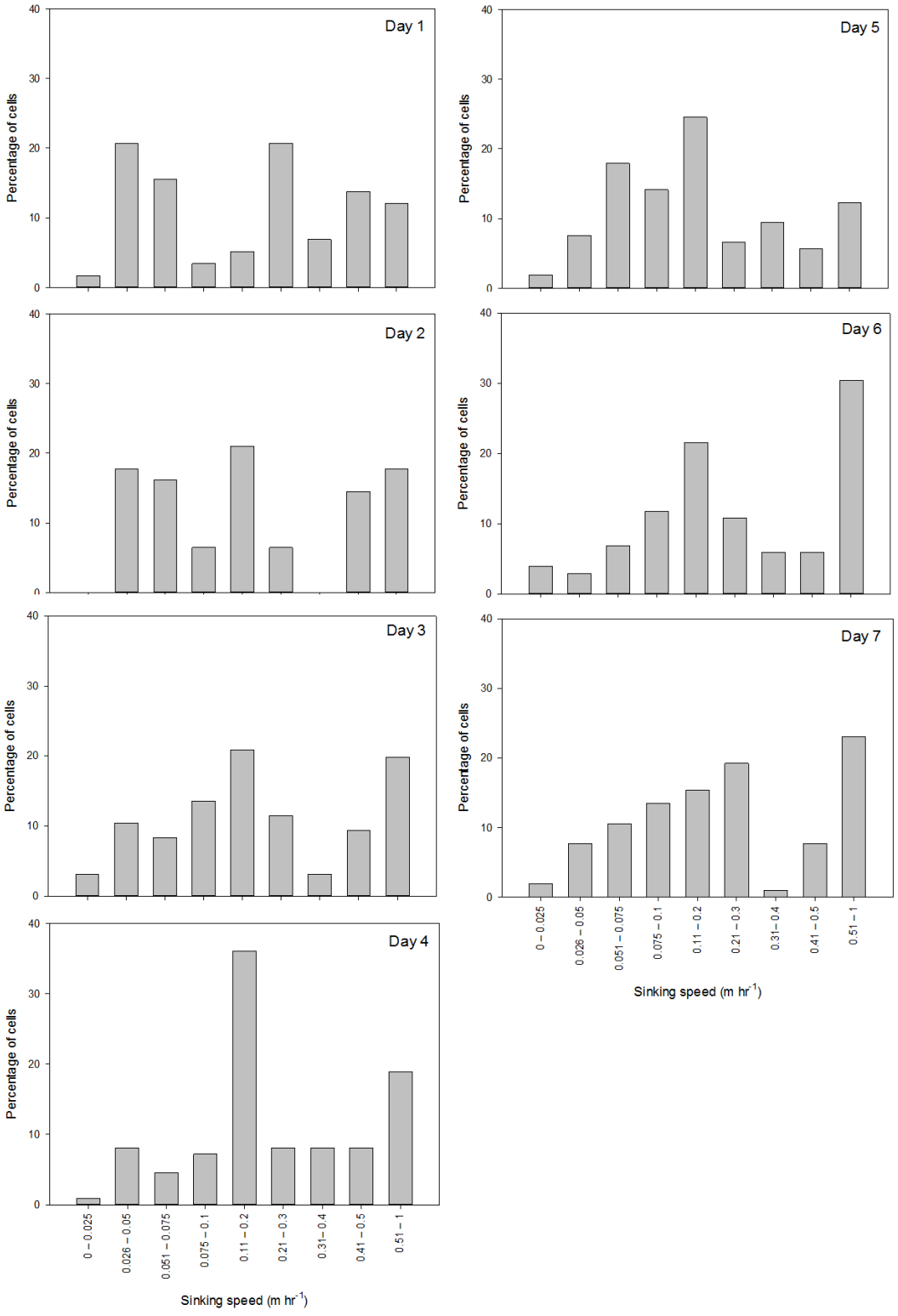

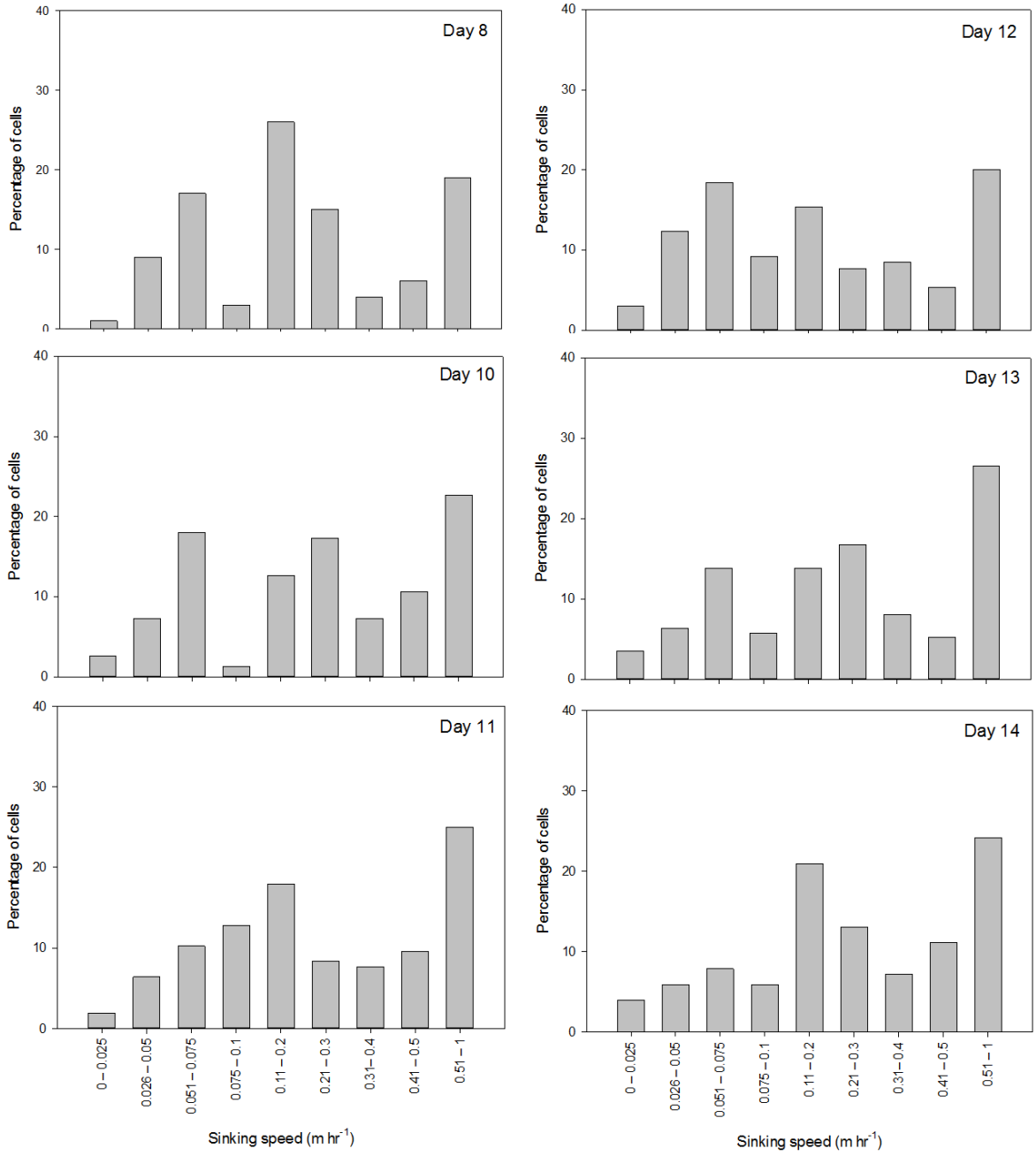
Day 8
Day 12
Day 10
Day 13
Day 11
Day 14
Percentage of cells
0
10
20
30
40
0 – 0.025
0.026 – 0.05
0.051 – 0.075
0.075 – 0.1
0.11 – 0.2
0.21 – 0.3
0.31– 0.4
0.41 – 0.5
0.51 – 1
Sinking speed (m hr-1)

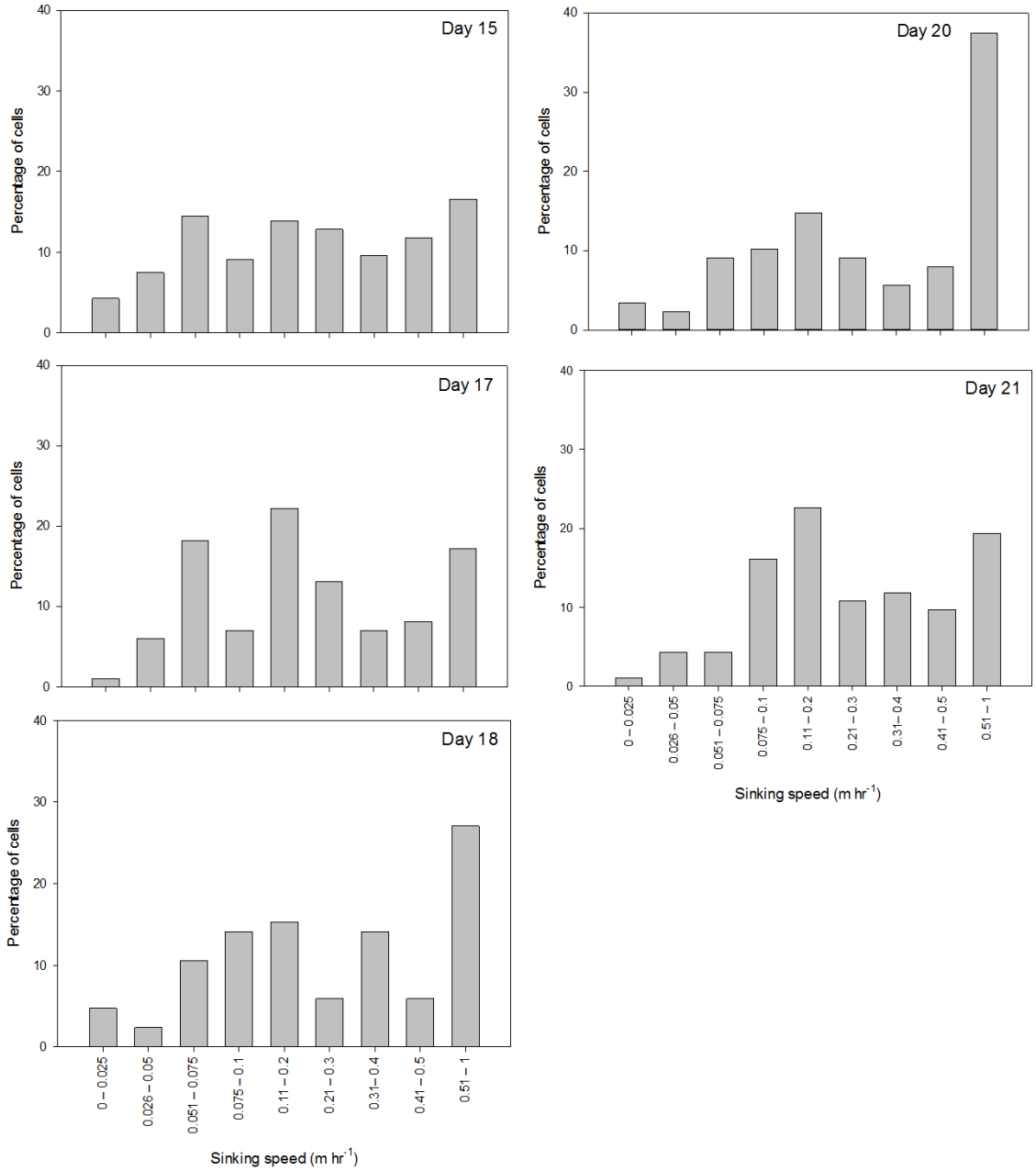
Day 15
Day 20
Day 17
Day 21
Day 18
Percentage of cells
0
10
20
30
40
0 – 0.025
0.026 – 0.05
0.051 – 0.075
0.075 – 0.1
0.11 – 0.2
0.21 – 0.3
0.31– 0.4
0.41 – 0.5
0.51 – 1
Sinking speed (m hr-1)

Appendix 6: Changes in the sinking rate distributions of motile *N. tripos* cells with increasing PO_4^{3-} limitation between day 1 and 21.

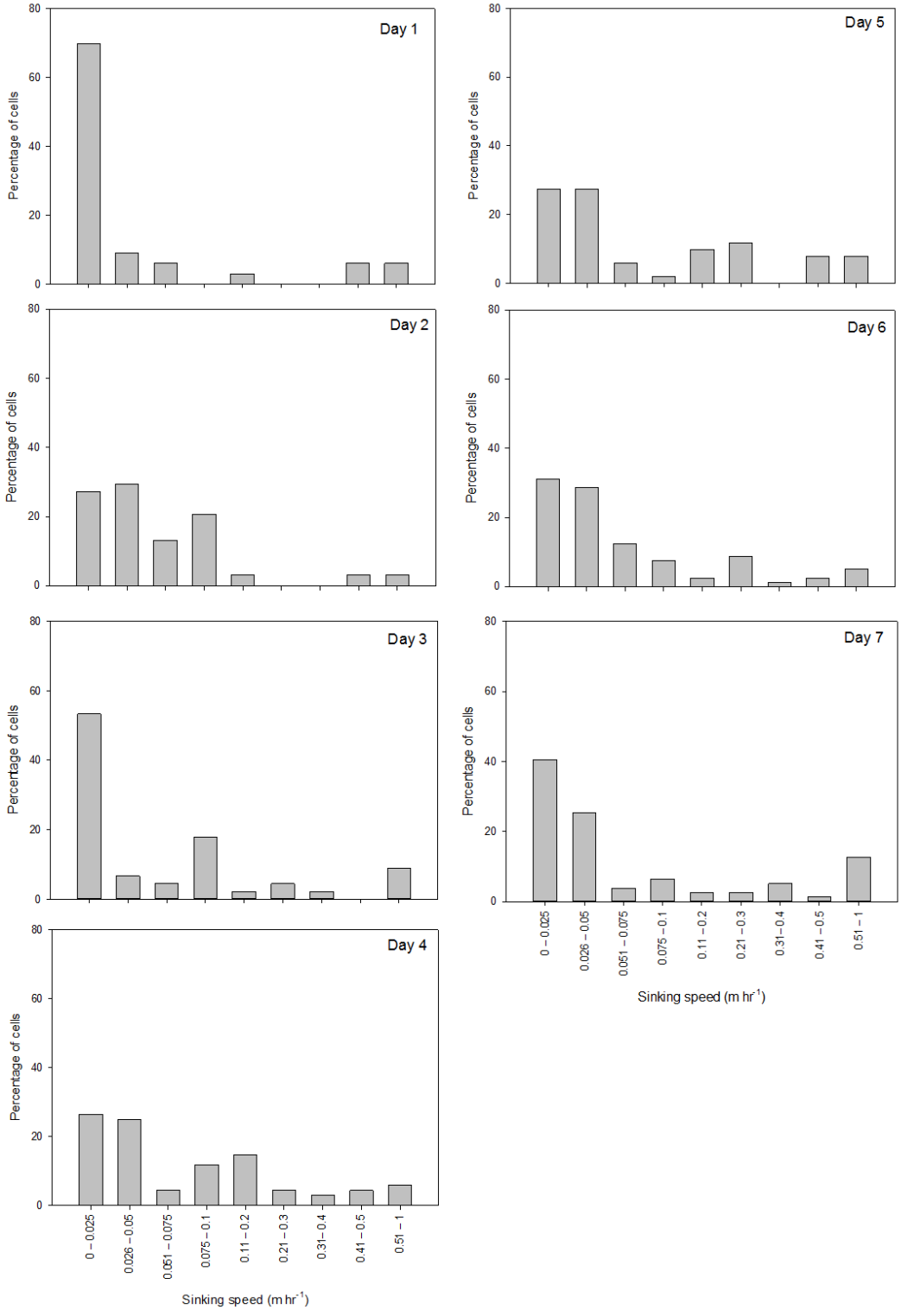

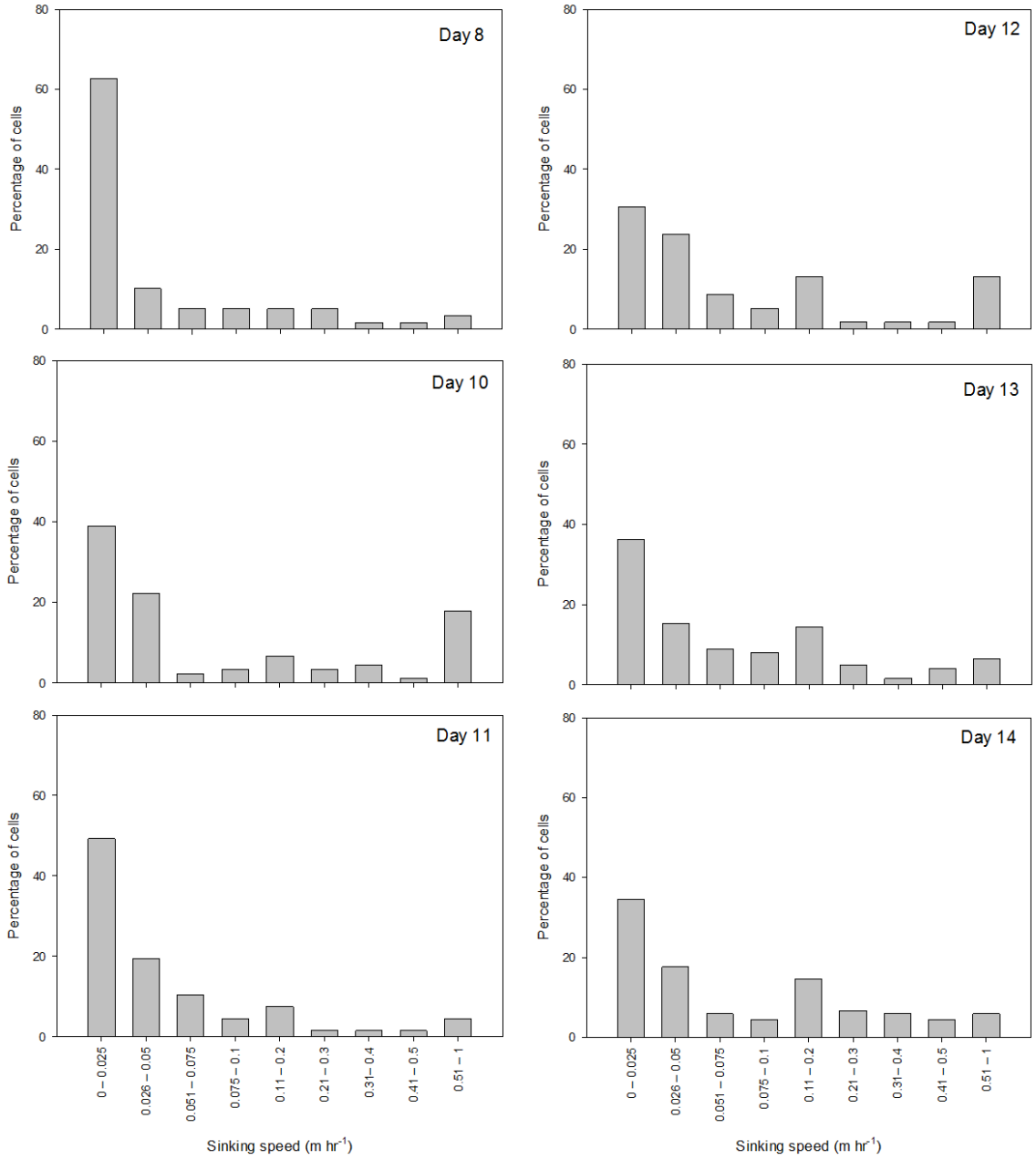
Day 8
Day 12
Day 10
Day 13
Day 11
Day 14
Percentage of cells
0
20
40
60
80
0 – 0.025
0.026 – 0.05
0.051 – 0.075
0.075 – 0.1
0.11 – 0.2
0.21 – 0.3
0.31– 0.4
0.41 – 0.5
0.51 – 1
Sinking speed (m hr-1)

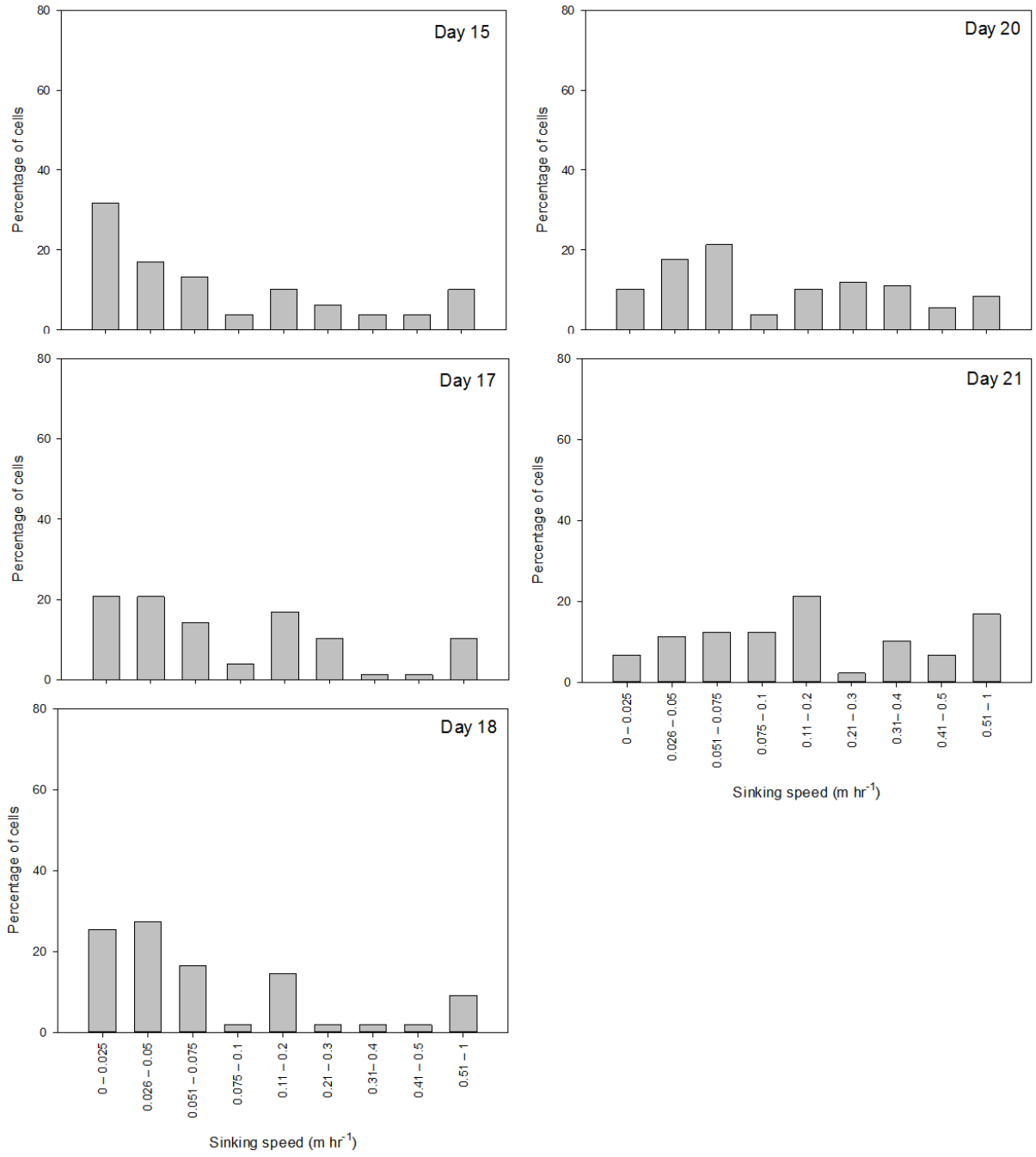
Day 15
Day 20
Day 17
Day 21
Day 18
Percentage of cells
0
20
40
60
80
0 – 0.025
0.026 – 0.05
0.051 – 0.075
0.075 – 0.1
0.11 – 0.2
0.21 – 0.3
0.31– 0.4
0.41 – 0.5
0.51 – 1
Sinking speed (m hr-1)

List of References

Aksnes, D. L., and D. K. Egge. 1991. A theoretical model for nutrient uptake in phytoplankton. Mar. Ecol. Ser. **70**: 65–72.

Aldridge, D., D. A. Purdie, and M. V. Zubkov. 2014. Growth and survival of *Neoceratium hexacanthum* and *Neoceratium candelabrum* under simulated nutrient-depleted conditions. J. Plankton Res. **36 (2):** 439–449.

Allen, C. B., J. Kanda, and E. A. Laws. 1996. New production and photosynthetic rates within and outside a cyclonic mesoscale eddy in the North Pacific subtropical gyre. Deep Sea Res. Part I Oceanogr. Res. Pap. **43**: 917–936.

Anderson, R. 2005. Algal Culturing Techniques, Academic Press Inc.

Anderson, T., and D. O. Hessen. 1995. Carbon or nitrogen limitation in marine copepods? J. Plank. Res. **17**: 317–331.

Baek, S. H., S. Shimode, M. S. Han, and T. Kikuchi. 2008a. Growth of dinoflagellates, *Ceratium furca* and *Ceratium fusus* in Sagami Bay, Japan: The role of nutrients. Harmful Algae **7**: 729–739.

Baek, S. H., S. Shimode, M.-S. Han, and T. Kikuchi. 2008b. Growth of dinoflagellates, *Ceratium furca* and *Ceratium fusus* in Sagami Bay, Japan: The role of nutrients. Harmful Algae **7**: 729–739.

Baek, S. H., S. Shimode, and T. Kikuchi. 2007. Reproductive ecology of the dominant dinoflagellate, *Ceratium fusus*, in coastal area of Sagami Bay, Japan. J. Oceanogr. **63**: 35–45.

Baek, S. H., S. Shimode, and T. Kikuchi. 2008c. Growth of dinoflagellates, *Ceratium furca* and *Ceratium fusus* in Sagami Bay, Japan: The role of temperature, light intensity and photoperiod. Harmful Algae **7**: 163–173.

Baek, S. H., S. Shimode, K. Shin, M.-S. Han, and T. Kikuchi. 2009. Growth of dinoflagellates, *Ceratium furca* and *Ceratium fusus* in Sagami Bay, Japan: The role of vertical migration and cell division. Harmful Algae **8**: 843–856.

Batten, S., R. Clark, J. Flinkman, G. Hays, E. John, A. W. John, T. Jonas, J. Lindley, D. Stevens, and A. Walne. 2003. CPR sampling: the technical background, materials and methods, consistency and comparability. Prog. Oceanogr. **58**: 193–215.

Beers, J. R., F. M. H. Reid, and G. L. Stewart. 1982. Seasonal abundance of the microplankton population in the North Pacific central gyre. Deep. Res. Part I Oceanogr. Res. Pap. **29**: 227–245.

Bhattacharya, D., H. S. Yoon, and J. D. Hackett. 2004. Photosynthetic eukaryotes unite: endosymbiosis connects the dots. Bioessays **26**: 50–60.

Blasco, D. 1978. Observations on the diel migration of marine dinoflagellates off the Baja California coast. Mar. Biol. **46**: 41–47.

Bockstahler, K. R., and D. W. Coats. 1993a. Grazing of the mixotrophic dinoflagellate *Gymnodinium sanguineum* on ciliate populations of Chesapeake Bay. Mar. Biol. **116**: 477–487.

Bockstahler, K. R., and D. W. Coats. 1993b. Spatial and temporal aspects of mixotrophy in Chesapeake Bay dinoflagellates. J. Eukaryot. Microbiol. **40**: 49–60.

Brewer, P. G., and J. P. Riley. 1965. The automatic determination of nitrate in sea water. Deep Sea Res. Oceanogr. Abstr. **12**: 765–772.

Bronk, D. A., J. H. See, P. Bradley, and L. Killberg. 2007. DON as a source of bioavailable nitrogen for phytoplankton. Biogeosciences **4**: 283–296.

Cachon, M., J. Cachon, J. Cosson, C. Greuet, and P. Huitorel. 1991. Dinoflagellate flagella adopt various conformations in response to different needs. Biol. Cell **71**: 175–182.

Cachon, M., C. Greuet, J. Cosson, and P. Huitorel. 1992. Analysis of the mechanism of dinoflagellate flagella contraction-relaxation cycle. Biol. Cell **76**: 33–42.

Callieri, C., E. Caravati, G. Morabito, and A. Oggioni. 2006. The unicellular freshwater cyanobacterium *Synechococcus* and mixotrophic flagellates: evidence for a functional association in an oligotrophic, subalpine lake. Freshw. Biol. **51**: 263–273.

Cembella, A. D., N. J. Antia, and P. J. Harrison. 1984. The utilization of inorganic and organic phosphorus-compounds as nutrients by eukaryotic microalgae - a multidisciplinary perspective .1. Crit. Rev. Microbiol. **10**: 317–391.

Chang, F. H., and M. McClean. 1997. Growth responses of *Alexandrium minutum* (Dinophyceae) as a function of three different nitrogen sources and irradiance. New Zeal. J. Mar. Freshw. Res. **31**: 1–7.

Chang, J., and E. J. Carpenter. 1994. Inclusion bodies in several species of *Ceratium* Schrank (Dinophyceae) from the Caribbean Sea examined with DNA-specific staining. J. Plankton Res. **16**: 197–202.

Chisholm, S. W. 1992. Phytoplankton size, p. 213–237. *In* P.G. Falkowski and A.D. Woodhead [eds.], Primary Productivity and Biogeochemical Cycles in the Sea. Plenum Press.

Cho, B. C., and F. Azam. 1988. Major role of bacteria in biogeochemical fluxes in the ocean's interior. Nature **332**: 441–443.

Colebrook, J. M. 1982. Continuous plankton records: seasonal variations in the distribution and abundance of plankton in the North Atlantic Ocean and the North Sea. J. Plankton Res. **4**: 435–462.

Collos, Y. 1986. Time-lag algal growth dynamics: biological constraints on primary production in aquatic environments. Mar. Ecol. Ser. **33**: 193–206.

Crawford, D. W. 1992. Metabolic cost of motility in planktonic protists: Theoretical considerations on size scaling and swimming speed speed. Microb. Ecol. **24**: 1–10.

Cullen, J. J., and S. G. Horrigan. 1981. Effects of nitrate on the diurnal vertical migration, carbon to nitrogen ratio, and the photosynthetic capacity of the dinoflagellate *Gymnodinium splendens*. Mar. Biol. **62**: 81–89.

Cuvelier, M. L., A. E. Allen, A. Monier, J. P. McCrow, M. Messié, S. G. Tringe, T. Woyke, R. M. Welsh, T. Ishoey, J.-H. Lee, B. J. Binder, C. L. DuPont, M. Latasa, C. Guigand, K. R. Buck, J. Hilton, M. Thiagarajan, E. Caler, B. Read, R. S. Lasken, F. P. Chavez, and A. Z. Worden. 2010. Targeted metagenomics and ecology of globally important uncultured eukaryotic phytoplankton. Proc. Natl. Acad. Sci. U. S. A. **107**: 14679–84.

Denman, K. L., and A. E. Gargett. 1983. Time and space scales of vertical mixing and advection of phytoplankton in the upper ocean. Limnol. Oceanogr. **28**: 801–815.

DiTullio, G. R., and E. A. Laws. 1991. Impact of an atmospheric-oceanic disturbance on phytoplankton community dynamics in the North Pacific Central Gyre. Deep Sea Res. Part I Oceanogr. Res. Pap. **38**: 1305–1329.

Dodge, J. D., and R. M. Crawford. 1970. The morphology and fine structure of *Ceratium hirundinella* (Dinophycae). J. Phycol. **6**: 137–149.

Dodge, J. D., and H. G. Marshall. 1994. Biogeographic analysis of the armored planktonic dinoflagellate *Ceratium* in the North Atlantic and adjacent seas. J. Phycol. **30**: 905–922.

Dodson, A. N., and W. H. Thomas. 1977. Marine phytoplankton growth and survival under simulated upwelling and oligotrophic conditions. J. Exp. Mar. Bio. Ecol. **26**: 153–161.

Edwards, M., D. G. Johns, S. C. Leterme, E. Svendsen, and A. J. Richardson, 2006. Regional climate change and harmful algal blooms in the northeast Atlantic. Limnol. Oceanogr. **51**: 820–829.

Epp, R. W., and W. M. Lewis. 1984. Cost and speed of locomotion for rotifers. Oecologia **61**: 289–292.

Eppley, R. W., O. Holm-Hansen, and J. D. H. Strickland. 1968. Some observation on the vertical migration of dinoflagellates. J. Phycol. **4**: 333–340.

Falkowski, P. G., Z. Dubinsky, and K. Wyman. 1985. Growth-irradaiance relationships in phytoplankton. Limnol. Oceanogr. **30**: 311–321.

Falkowski, P. G., M. E. Katz, A. H. Knoll, A. Quigg, J. A. Raven, O. Schofield, and F. J. R. Taylor. 2004. The evolution of modern eukaryotic phytoplankton. Science **305**: 354–360.

Falkowski, P. G., and T. G. Owens. 1978. Effects of light intensity on photosynthesis and dark respiration in six species of marine phytoplankton. Mar. Biol. **45**: 289–295.

Falkowski, P. G., D. Ziemann, Z. Kolber, and P. K. Bienfang. 1991. Role of eddy pumping in enhancing primary production in the ocean. Nature **352**: 55–58.

Figueroa, R. I., K. Rengefors, I. Bravo, and S. Bensch. 2010. From homothally to heterothally: Mating preferences and genetic variation within clones of the dinoflagellate *Gymnodinium catenatum*. Deep. Res. Part II Topical Stud. Oceanogr. **57**: 190–198.

Finkel, Z. V., J. Beardall, K. J. Flynn, A. Quigg, T. A. V. Rees, and J. A. Raven. 2009. Phytoplankton in a changing world: cell size and elemental stoichiometry. J. Plankton Res. **32**: 119–137.

Flynn, K. J., and A. Mitra. 2009. Building the “perfect beast”: modelling mixotrophic plankton. **31**: 965–992.

Fowler, J., and L. Cohen. 1991. Practical statistics for field biology. John Wiley & Sons, Chichester, 227 pp.

Fuhrman, J. A., T. D. Sleeter, C. A. Carlson, and L. M. Proctor. 1989. Dominance of bacterial biomass in the Sargasso Sea and its ecological implications. Mar. Ecol. Ser. **57**: 207–217.

Garrett, C., and W. Munk. 1972. Oceanic mixing by breaking internal waves. Deep Sea Res. Oceanogr. Abstr. **19**: 823–832.

Girault, M., H. Arakawa, and F. Hashihama. 2012. Phosphorus stress of microphytoplankton community in the western subtropical North Pacific. J. Plankton Res. fbs076–.

Gómez, F., D. Moreira, and P. López-García, (2010) *Neoceratium* gen. nov., a new genus for all marine species currently assigned to *Ceratium* (Dinophyceae). Protist, ***161***: 35–54.

Gonzalez, N., R. Anadon, B. Mourino, E. Fernandez, B. Sinha, J. Escanez, and D. De Armas. 2001. The metabolic balance of the planktonic community in the North Atlantic Subtropical Gyre: the role of mesoscale instabilities. Limnol. Oceanogr. **46**: 946–952.

Graham, H. W. 1941. An oceanographic consideration of the dinoflagellate genus *Ceratium*. Ecol. Monogr. **11**: 99–116.

Graham, H. W., and N. Bronikovsky. 1944. The genus *Ceratium* in the Pacific and North Atlantic Oceans. Carnegie Inst. Washingt. Publ. **565**: 1–209.

Graham, L. E., and L. W. Wilcox. 2000. Algae, Prentice-Hall.

Gregg, M. C., T. B. Sanford, and D. P. Winkel. 2003. Reduced mixing from the breaking of internal waves in equatorial waters. Nature **422**: 513–5.

Hansen, P. J. 2011. The Role of photosynthesis and food uptake for the growth of marine mixotrophic dinoflagellates. J. Eukaryot. Microbiol. **58**: 203–214.

Hansen, P. J., and A. J. Calado. 1999. Phagotrophic mechanisms and prey selection in free-living dinoflagellates. J. Eukaryot. Microbiol. **46**: 382–389.

Hansen, P. J., and T. Fenchel. 2006. The bloom-forming ciliate *Mesodinium rubrum* harbours a single permanent endosymbiont. Mar. Biol. Res. **2**: 169–177.

Hartmann, M., C. Grob, D. J. Scanlan, A. P. Martin, P. H. Burkill, and M. V Zubkov. 2011. Comparison of phosphate uptake rates by the smallest plastidic and aplastidic protists in the North Atlantic subtropical gyre. FEMS Microbiol. Ecol. **78**: 327–335.

Hartmann, M., C. Grob, G. A. Tarran, A. P. Martin, P. H. Burkill, D. J. Scanlan, and M. V Zubkov. 2012. Mixotrophic basis of Atlantic oligotrophic ecosystems. Proc. Natl. Acad. Sci. U. S. A. **109**: 5756–5760.

Hayhome, B. A., D. J. Whitten, K. R. Harkins, and L. A. Pfiester. 1987. Intraspecific variation in the dinoflagellate *Peridium volzii*. J. Phycol. **23**: 573–580.

Hays, G. C., and A. J. Warner. 1993. Consistency of towing speed and sampling depth for the Ccntinuous plankton recorder. J. Mar. Biol. Assoc. United Kingdom **73**: 967.

Heaney, S. I., and R. W. Eppley. 1981. Light, temperature and nitrogen as interacting factor affecting diel vertical migration of dinoflagellates in culture. J. Plankton Res. **3**: 331–344.

Heaney, S. I., and T. I. Furnass. 1980. Laboratory models of diel vertical migration in the dinoflagellate *Ceratium hirundinella*. Freshw. Biol. **10**: 163–170.

Henson, S. A., J. P. Dunne, and J. L. Sarmiento. 2009. Decadal variability in North Atlantic phytoplankton blooms. J. Geophys. Res. **114**: C04013.

Hofender, H. 1930. Uber die animalische Ernahrung von Ceratiumhirundinella O.F. Muller and uber die Rolle des Kernes bei dieser Zellfunktion. Arch. Protistenk **71**: 1–32.

Jacobson, D. M., and D. M. Anderson. 1996. Widespread phagocytosis of ciliates and other protists by marine mixotrophic and heterotrophic thecate dinoflagellates. J. Phycol. **32**: 279–285.

James, W. F., W. D. Taylor, and J. W. Barko. 1992. Production and vertical migration of *Ceratium hirundinella* in relation to phosphorus availability in Eau Galle Reservoir, Wisconsin. Can. J. Fish. Aquat. Sci. **49**: 694–700.

Jeong, H. J., J. Y. Park, J. H. Nho, M. O. Park, J. H. Ha, K. A. Seong, C. Jeng, C. N. Seong, K. Y. Lee, and W. H. Yih. 2005a. Feeding by red-tide dinoflagellates on the cyanobacterium *Synechococcus*. Aquat. Microb. Ecol. **41**: 131–143.

Jeong, H. J., K. A. Seong, Y. Du Yoo, T. H. Kim, N. S. Kang, S. Kim, J. Y. Park, J. S. Kim, G. H. Kim, and J. Y. Song. 2008. Feeding and grazing impact by small marine heterotrophic dinoflagellates on heterotrophic bacteria. J. Eukaryot. Microbiol. **55**: 271–288.

Jeong, H. J., Y. Du Yoo, J. Y. Park, J. Y. Song, S. T. Kim, S. H. Lee, K. Y. Kim, and W. H. Yih. 2005b. Feeding by phototrophic red-tide dinoflagellates: five species newly revealed and six species previously known to be mixotrophic. Aquat. Microb. Ecol. **40**: 133–150.

Jochum, M., P. Malanotte-Rizzoli, and A. Busalacchi. 2004. Tropical instability waves in the Atlantic Ocean. Ocean Model. **7**: 145–163.

Johnson, K. S., S.C. Riser, and D.M. Karl. 2010. Nitrate supply from deep to near surface waters of the North Pacific subtropical gyre. Nature **465:** 1062–1065.

Karl, D. M. 1999. A Sea of Change: Biogeochemical Variability in the North Pacific Subtropical Gyre. Earth Sci. **2**: 181–214.

Karl, D. M. 2002. Nutrient dynamics in the deep blue sea. Trends Microbiol. **10**: 410–418.

Karl, D. M., J. R. Christian, J. E. Dore, D. V. Hebel, R. M. Letelier, L. M. Tupas, and C. D. Winn. 1996. Seasonal and interannual variability in primary production and particle flux at Station ALOHA. Deep Sea Res. Part II Top. Stud. Oceanogr. **43**: 539–568.

Keller, M. D., R. C. Selvin, W. Claus, and R. R. L. Guillard. 1987. Media for the culture of oceanic ultraphytoplankton. J. Phycol. **23**: 633–638.

Kiefer, D. A., R. J. Olson, and O. Holmhansen. 1976. Another look at nitrite and chlorophyll maxima in central North Pacific. Deep. Res. **23**: 1199–1208.

Kirkwood, D. . 1989. Simultaneous determination of selected nutrients in seawater. ICES C. **29**: 12.

Kolber, Z., and P. G. Falkowski. 1993. Use of active fluorescence to estimate photosynthesis *in-situ*. Limnol. Oceanogr. **38**: 1646–1665.

Kolber, Z. S., O. Prasil, and P. G. Falkowski. 1998. Measurements of variable chlorophyll fluorescence using fast repetition rate techniques: defining methodology and experimental protocols. Biochim. Biophys. Acta-Bioenergetics **1367**: 88–106.

Kolber, Z., J. Zehr, and P. Falkowski. 1988. Effects of growth irradiance and nitrogen limitation on photosynthetic energy conversion in photosystem II. Plant Physiol. **88**: 923–929.

Langdon, C. 1987. On the causes of interspecific differences in the growth-irradiance relationship for phytoplankton. Part I. A comparative study of the growth-irradiance relationship of three marine phytoplankton species: *Skeletonema costatum*, *Olithodiscus luteus* and *Gonyaulax tamarensis*. J. Plankton Res. **9**: 459–482.

Leadbeater, B., and J. D. Dodge. 1967. An electron microscope study of dinoflagellate flagella. J. Gen. Microbiol. **46**: 305–314.

Lebour, M. V. 1925. The dinoflagellates of northern seas, Plymouth Marine Biological Association.

Lee, R. E. 1989. Phycology, Cambride University Press.

Lehman, J. T., and D. Scavia. 1982. Microscale patchiness of nutrients in plankton communities. Science (80-.). **216**: 729–730.

Leong, S. C. Y., and S. Taguchi. 2004. Response of the dinoflagellate *Alexandrium tamarense* to a range of nitrogen sources and concentrations: growth rate, chemical carbon and nitrogen, and pigments. Hydrobiologia **515**: 215–224.

Lepère, C., D. Vaulot, and D. J. Scanlan. 2009. Photosynthetic picoeukaryote community structure in the South East Pacific Ocean encompassing the most oligotrophic waters on Earth. Environ. Microbiol. **11**: 3105–17.

Letelier, R. M., D. M. Karl, M. R. Abbott, P. Flament, M. H. Freilich, R. Lukas, and P. T. Strub. 2000. Role of late winter mesoscale events in the biogeochemical variability of the upper water column of the North Pacific Subtropical Gyre.

Li, A. S., D. K. Stoecker, and J. E. Adolf. 1999. Feeding, pigmentation, photosynthesis and growth of the mixotrophic dinoflagellate *Gyrodinium galatheanum*. Aquat. Microb. Ecol. **19**: 163–176.

Li, A. S., D. K. Stoecker, and D. W. Coats. 2000. Mixotrophy in *Gyrodinium galatheanum* (Dinophyceae): Grazing responses to light intensity and inorganic nutrients. J. Phycol. **36**: 33–45.

Li, A. S., D. K. Stoecker, D. W. Coats, and E. J. Adam. 1996. Ingestion of fluorescently labeled and phycoerythrin-containing prey by mixotrophic dinoflagellates. Aquat. Microb. Ecol. **10**: 139–147.

Longhurst, A., S. Sathyendranath, T. Platt, C. Caverhill. 1995. An estimate of global primary production in the ocean from satellite radiometer data. J Plankton Res. **17**:1245–1271.

Mackey, K. R. M., C. E. Mioni, J. P. Ryan, and A. Paytan. 2012. Phosphorus cycling in the red tide incubator region of Monterey Bay in response to upwelling. Front. Microbiol. **3**: 33.

Marañón, E., P. Cermeño, D. C. López-Sandoval, T. Rodríguez-Ramos, C. Sobrino, M. Huete-Ortega, J. M. Blanco, and J. Rodríguez. 2013. Unimodal size scaling of phytoplankton growth and the size dependence of nutrient uptake and use. Ecol. Lett. **16**: 371–9.

Maranon, E., P. M. Holligan, M. Varela, B. Mourino, and A. J. Bale. 2000. Basin-scale variability of phytoplankton biomass, production and growth in the Atlantic Ocean. Deep. Res. Part I Oceanographic Res. Pap. **47**: 825–857.

Marra, J. 2004. The compensation irradiance for phytoplankton in nature. Geophys. Res. Lett. **31**: L06305.

Maruyama, T. 1981. Motion of the longitudinal flagellum in *Ceratium tripos* (dinoflagellida) - a retractile flagellar motion. J. Protozool. **28**: 328–336.

Maruyama, T. 1982. Fine-structure of the longitudinal flagellum in *Ceratium tripos*, a marine dinoflagellate. J. Cell Sci. **58**: 109–123.

Mather, R. L., S. E. Reynolds, G. A. Wolff, R. G. Williams, S. Torres-Valdes, E. M. S. Woodward, A. Landolfi, X. Pan, R. Sanders, and E. P. Achterberg. 2008. Phosphorus cycling in the North and South Atlantic Ocean subtropical gyres. Nat. Geosci. **1**: 439–443.

Matrai, P. A. 1986. The distribution of the dinoflagellate *Ceratium* in relation to environmental factors along 28 N in the eastern North Pacific. J. Plankton Res. **8**: 105–118.

McClain, C. R., S. R. Signorini, and J. R. Christian. 2004. Subtropical gyre variability observed by ocean-color satellites. Deep Sea Res. Part II Top. Stud. Oceanogr. **51**: 281–301.

McGillicuddy, D. J., and A. R. Robinson. 1997. Eddy-induced nutrient supply and new production in the Sargasso Sea. Deep Sea Res. Part I Oceanogr. Res. Pap. **44**: 1427–1450.

McGillicuddy, D. J., A. R. Robinson, D. A. Siegel, H. W. Jannasch, R. Johnson, T. D. Dickey, J. McNeil, A. F. Michaels, and A. H. Knap.

1998. Influence of mesoscale eddies on new production in the Sargasso Sea. Nature **394**: 263–266.

McGowan, J. A., and T. L. Hayward. 1978. Mixing and oceanic productivity. Deep Sea Res. **25**: 771–793.

McQuatters-Gollop, A., D. E. Raitsos, M. Edwards, and M. Attrill. 2007. Spatial patterns of diatom and dinoflagellate seasonal cycles in the NE Atlantic Ocean. Mar. Ecol. **339**: 301–306.

Miyasaka, I., K. Nanba, K. Furuya, Y. Nimura, and A. Azuma. 2004. Functional roles of the transverse and longitudinal flagella in the swimming motility of *Prorocentrum minimum* (Dinophyceae). J. Exp. Biol. **207**: 3055–3066.

Montresor, M., S. Sgrosso, G. Procaccini, and W. Kooistra. 2003. Intraspecific diversity in *Scrippsiella trochoidea* (Dinophyceae): evidence for cryptic species. Phycologia **42**: 56–70.

Montresor, M., and C. R. Tomas. 1988. Growth and probable gamete formation in the marine dinoflagelate *Ceratium schrankii*. J. Phycol. **24**: 495–502.

Moore, C. M., M. I. Lucas, R. Sanders, and R. Davidson. 2005. Basin-scale variability of phytoplankton bio-optical characteristics in relation to bloom state and community structure in the Northeast Atlantic. Deep. Res. Part I-Oceanographic Res. Pap. **52**: 401–419.

Moore, C. M., M. M. Mills, K. R. Arrigo, I. Berman-Frank, L. Bopp, P. W. Boyd, E. D. Galbraith, R. J. Geider, C. Guieu, S. L. Jaccard, T. D. Jickells, J. La Roche, T. M. Lenton, N. M. Mahowald, E. Marañón, I. Marinov, J. K. Moore, T. Nakatsuka, A. Oschlies, M. A. Saito, T. F. Thingstad, A. Tsuda, and O. Ulloa. 2013. Processes and patterns of oceanic nutrient limitation. Nat. Geosci. **6**: 701–710.

Moore, C. M., D. J. Suggett, A. E. Hickman, Y. N. Kim, J. F. Tweddle, J. Sharples, R. J. Geider, and P. M. Holligan. 2006. Phytoplankton photoacclimation and photoadaptation in response to environmental gradients in a shelf sea. Limnol. Oceanogr. **51**: 936–949.

Van Mooy, B. A. S., H. F. Fredricks, B. E. Pedler, S. T. Dyhrman, D. M. Karl, M. Koblizek, M. W. Lomas, T. J. Mincer, L. R. Moore, T. Moutin, M. S. Rappe, and E. A. Webb. 2009. Phytoplankton in the ocean use non-phosphorus lipids in response to phosphorus scarcity. Nature **458**: 69–72.

Morel, A., H. Claustre, and B. Gentili. 2010. The most oligotrophic subtropical zones of the global ocean: similarities and differences in

terms of chlorophyll and yellow substance. Biogeosciences **7**: 3139–3151.

Müller, O. F. 1786. *Animalcula Infusoria Fluviatilia et Marina: Quae Detexit, Systematice Descripsit et ad Vivum Delineari Curavit*. Copenhagen, Denmark,

Myers, J. H. 1978. Sex-ratio adjustment under food stress - maximization of quality or numbers of offspring. Am. Nat. **112**: 381–388.

Nielsen, T. G. 1991. Contribution of zooplankton grazing to the decline of a *Ceratium* bloom. Limnol. Oceanogr. **36**: 1091–1106.

Norris, D. R. 1969. Possible phagotrophic feeding in *Ceratium lunula* Schimper. Limnol. Oceanogr. **14**: 448–449.

Ochoa, N., and O. Gómez. 1987. Dinoflagellates as indicators of water masses during El Niño, 1982–1983. J. Geophys. Res. Oceans. **92**: 14355–14367.

Paasche, E., I. Bryceson, and K. Tangen. 1984. Interspecific variation in dark nitrogen uptake by dinoflagellates. J. Phycol. **20**: 394–401.

Perez, V., E. Fernandez, E. Maranon, X. A. G. Moran, and M. V Zubkov. 2006. Vertical distribution of phytoplankton biomass, production and growth in the Atlantic subtropical gyres. Deep. Res. Part I Oceanographic Res. Pap. **53**: 1616–1634.

Pfiester, L. A. 1984. Sexual reproduction, D.L. Spector [ed.]. Academic Press, Inc.

Qasim, S. Z., P. M. A. Bhattath, and V. P. Devassy. 1973. Growth kinetics and nutrient requirements of 2 tropical marine phytoplankters. Mar. Biol. **21**: 299–304.

Quevedo, M. 2003. The protistan microzooplankton community in the oligotrophicnorth-eastern Atlantic: large and mesoscale patterns. J. Plankton Res. **25**: 551–563.

Raine, R., M. White, and J. D. Dodge. 2002. The summer distribution of net plankton dinoflagellates and their relation to water movements in the NE Atlantic Ocean, west of Ireland. J. Plankton Res. 24: 1131–1147.

Richardson, A. J., A. W. Walne, A. W. G. John, T. D. Jonas, J. A. Lindley, D. W. Sims, D. Stevens, and M. Witt. 2006. Using continuous plankton recorder data. Prog. Oceanogr. **68**: 27–74.

Sanders, R., and T. Jickells. 2000. Total organic nutrients in Drake Passage. Deep. Res. Part I Oceanographic Res. Pap. **47**: 997–1014.

Seong, K. A., H. J. Jeong, S. Kim, G. H. Kim, and J. H. Kang. 2006. Bacterivory by co-occurring red-tide algae, heterotrophic nanoflagellates, and ciliates. Mar. Ecol. Ser. **322**: 85–97.

Shim, J., T. A. Klochova, J. W. Han, G. H. Kim, Y. D. Yoo, and H. J. Jeong. 2011. Comparative proteomics of the mixotrophic dinoflagellate *Prorocentrum micans* growing in different trophic modes. Algae **26(1)**: 87–96.

Siegel, D. A., S. C. Doney, and J. A. Yoder. 2002. The North Atlantic spring phytoplankton bloom and Sverdrup's critical depth hypothesis. Science **296**: 730–733.

Siegel, D. A., D. J. McGillicuddy, and E. A. Fields. 1999. Mesoscale eddies, satellite altimetry, and new production in the Sargasso Sea. J. Geophys. Res. **104**: 13359.

Sieracki, C. K., M. E. Sieracki, and C. S. Yentsch. 1998. An imaging-in-flow system for automated analysis of marine microplankton. Mar. Ecol. Prog. Ser. **168**: 285–296.

Smalley, G. W., and D. W. Coats. 2002. Ecology of the red-tide dinoflagellate *Ceratium furca*: Distribution, mixotrophy, and grazing impact on ciliate populations of Chesapeake Bay. J. Eukaryot. Microbiol. **49**: 63–73.

Smalley, G. W., D. W. Coats, and E. J. Adam. 1999. A new method using fluorescent microspheres to determine grazing on ciliates by the mixotrophic dinoflagellate *Ceratium furca*. Aquat. Microb. Ecol. **17**: 167–179.

Smalley, G. W., D. W. Coats, and D. K. Stoecker. 2003. Feeding in the mixotrophic dinoflagellate *Ceratium furca* is influenced by intracellular nutrient concentrations. Mar. Ecol. Ser. **262**: 137–151.

Smalley, G. W., D. W. Coats, and D. K. Stoecker. 2012. Influence of inorganic nutrients, irradiance, and time of day on food uptake by the mixotrophic dinoflagellate *Neoceratium furca*. Aquat. Microb. Ecol. **68**: 29–41.

Smith, P., R. Krohn, G. Hermanson, A. Mallia, F. Gartner, M. Provenzano, E. Fujimoto, N. Goeke, B. Olson, and D. Klenk. 1985. Measurement of protein using bicinchoninic acid. Anal. Biochem. **150**: 76–85.

Sournia, A. 1967. Le genre *Ceratium* (péridinien planctonique) dans le Canal de Mozambique: Contribution à une révision mondiale. *Vie Milieu A*, **18**: 375–499.

Sournia, A. 1982. Is there a shade flora in the marine plankton? J. Plankton Res. **4**: 391–399.

Stickney, H. L., R. R. Hood, and D. K. Stoecker. 2000. The impact of mixotrophy on planktonic marine ecosystems. Ecol. Modell. **125**: 203–230.

Stoecker, D. K. 1988. Are marine planktonic ciliates suspension feeders? J. Protozool. **35**: 252-255.

Stoecker, D. K. 1998. Conceptual models of mixotrophy in planktonic protists and some ecological and evolutionary implications. Eur. J. Protistol. **34**: 281–290.

Stoecker, D. K. 1999. Mixotrophy among dinoflagellates. J. Eukaryot. Microbiol. **46**: 397–401.

Stoecker, D. K., A. S. Li, D. W. Coats, D. E. Gustafson, and M. K. Nannen. 1997. Mixotrophy in the dinoflagellate *Prorocentrum minimum*. Mar. Ecol. Ser. **152**: 1–12.

von Stosch, H. A. 1964. Zum Problem der sexuellen Fortpllanzung in der Peridineengattung *Ceratium*. Helgolander Wissenschaftliche Meeresuntersuchungen **10**: 140–152.

von Stosch, H. A. 1972. La signification cytologique de la “cyclose nucleaire” dans le cycle de vie des dinoflagelles. Bull. Soc. Bot. Fr., Mem. 201–212.

Striebel, M., S. Bartholme, R. Zernecke, C. Steinlein, F. Haupt, S. Diehl, and H. Stibor. 2009. Carbon sequestration and stoichiometry of motile and nonmotile green algae. Limnol. Oceanogr. **54**: 1746–1752.

Suggett, D. J., C. M. Moore, A. E. Hickman, and R. J. Geider. 2009. Interpretation of fast repetition rate (FRR) fluorescence: signatures of phytoplankton community structure versus physiological state. Mar. Ecol. Ser. **376**: 1–19.

Suggett, D. J., K. Oxborough, N. R. Baker, H. L. MacIntyre, T. M. Kana, and R. J. Geider. 2003. Fast repetition rate and pulse amplitude modulation chlorophyll a fluorescence measurements for assessment of photosynthetic electron transport in marine phytoplankton. Eur. J. Phycol. **38**: 371–384.

Takahashi, M., and P. K. Bienfang. 1983. Size structure of phytoplankton biomass and photosynthesis in subtropical Hawaiian waters. Mar. Biol. **76**: 203–211.

Taylor, W. D., J. W. Barko, and W. F. James. 1988. Contrasting diel patterns of vertical migration in the dinoflagellate *Ceratium hirundinella* in relation to phosphorus supply in a north temperate reservoir. Can. J. Fish. Aquat. Sci. **45**: 1093–1098.

Tunin-Ley, A., and R. Lemée. 2013. The genus *Neoceratium* (planktonic dinoflagellates) as a potential indicator of ocean warming. Microorganisms. **1: 58-70.**

Tunin-Ley, A., J.-P. Labat, S. Gasparini, S. Mousseau, and R. Lemee. 2007. Annual cycle and diversity of species and infraspecific taxa of *Ceratium* (Dinophyceae) in the Ligurian Sea, northwest Mediterranean. J. Phycol. **43**: 1149–1163.

Venrick, E. L. 1979. Lateral extent and characteristics of the North Pacific central environment at 35-degrees-N. Deep. Res. Part a-Oceanographic Res. Pap. **26**: 1153–1178.

Venrick, E. L. 1982. Phytoplankton in an Oligotrophic Ocean: Observations and Questions. Ecol. Monogr. **52**: 129–154.

Venrick, E. L., J. A. McGowan, and A. W. Mantyla. 1973. Deep maxima of photosynthetic chlorophyll in Pacific Ocean. Fish. Bull. **71**: 41–52.

Villareal, T. A., and F. Lipschultz. 1995. Internal nitrate concentrations in single cells of large phytoplankton from the Sargasso Sea. J. Phycol. **31**: 689–696.

Watanabe, M., K. Kohata, and M. Kunugi. 1988. Phosphate accumulation and metabolism by *Heterosigma akashiwo* (raphidophycae) during diel vertical migration in a stratified microcosm. J. Phycol. **24**: 22–28.

Weiler, C. S. 1980. Population structure and in situ division rates of *Ceratium* in oligotrophic waters of the North Pacific central gyre. Limnol. Oceanogr. **25**: 610–619.

Weiler, C. S., and S. W. Chisholm. 1976. Phased cell division in natural populations of marine dinoflagellates from shipboard cultures. J. Exp. Mar. Bio. Ecol. **25**: 239–247.

Weiler, C. S., and R. W. Eppley. 1979. Temporal pattern of division in the dinoflagellate genus *Ceratium* and its application to the determination of growth rate. J. Exp. Mar. Bio. Ecol. **39**: 1–24.

Weiler, C. S., and D. M. Karl. 1979. Diel changes in phased-dividing cultures of *Ceratium furca* (dinophyceae): nucleotide triphosphates, adenylate energy charge, cell carbon, and patterns of vertical migration. J. Phycol. **15**: 384–391.

Whittington, J., B. Sherman, D. Green, and R. L. Oliver. 2000. Growth of *Ceratium hirundinella* in a subtropical Australian reservoir: the role of vertical migration. J. Plankton Res. **22**: 1025–1045.

Williams, R. G., and M. J. Follows. 1998. The Ekman transfer of nutrients and maintenance of new production over the North Atlantic. Deep Sea Res. Part I Oceanogr. Res. Pap. **45**: 461–489.

Wilson, C., and X. Qiu. 2008. Global distribution of summer chlorophyll blooms in the oligotrophic gyres. Prog. Oceanogr. **78**: 107–134.

Winn, C. D., L. Campbell, J. R. Christian, R. M. Letelier, D. V. Hebel, J. E. Dore, L. Fujieki, and D. M. Karl. 1995. Seasonal variability in the phytoplankton community of the North Pacific Subtropical Gyre. Global Biogeochem. Cycles **9**: 605.

Wolda, H., and J. Marek. 1994. Measuring variation in abundance, the problem with zeros. Eur. J. Entomol. **91**: 145–161.

Wu, J. F., W. Sunda, E. A. Boyle, and D. M. Karl. 2000. Phosphate depletion in the western North Atlantic Ocean. Science. **289**: 759–762.

Zhang, Q., R. Yu, J. Song, T. Yan, Y. Wang, and M. Zhou. 2011. Will harmful dinoflagellate *Karenia mikimotoi* grow phagotrophically? Chinese J. Oceanol. Limnol. **29**: 849–859.

Zingmark, R. G. 1970. Sexual reproduction in dinoflagellate *Noctiluca miliaris*. J. Phycol. **6**: 122–.

Zubkov, M. V, M. A. Sleigh, G. A. Tarran, P. H. Burkill, and R. J. . Leakey. 1998. Picoplanktonic community structure on an Atlantic transect from 50°N to 50°S. Deep Sea Res. Part I Oceanogr. Res. Pap. **45**: 1339–1355.

Zubkov, M. V., I. Mary, E. M. S. Woodward, P. E. Warwick, B. M. Fuchs, D. J. Scanlan, and P. H. Burkill. 2007. Microbial control of phosphate in the nutrient-depleted North Atlantic subtropical gyre. Environ. Microbiol. **9**: 2079–2089.

Zubkov, M. V., and M. A. Sleigh. 1996. Bacterivory by the ciliate *Euplotes* in different states of hunger. FEMS Microbiol. Ecol. **20**: 137–147.

Zubkov, M. V., and M. A. Sleigh. 2000. Comparison of Growth Efficiencies of Protozoa Growing on Bacteria Deposited on Surfaces and in Suspension. J. Eukaryot. Microbiol. **47**: 62–69.

Zubkov, M. V., M. A. Sleigh, P. H. Burkill, and R. J. G. Leakey. 2000. Picoplankton community structure on the Atlantic Meridional Transect: a comparison between seasons. Prog. Oceanogr. **45**: 369–386.

Zubkov, M. V., and G. A. Tarran. 2008. High bacterivory by the smallest phytoplankton in the North Atlantic Ocean. Nature **455**: 224–226.